Proceedings of ISAMA 2009

Eighth Interdisciplinary Conference of The International Society of the Arts, Mathematics, and Architecture

University at Albany, Albany, New York

June 22-25, 2009

Conference Organization Chair

Nathaniel Friedman (University at Albany, Albany, New York)

Publication Chair

Ergun Akleman (Texas A&M University, College Station, Texas)

Communication Chair

John M. Sullivan (Technische Universitat Berlin, Berlin, Germany)

Proceeding Editors

Ergun Akleman (Texas A&M University, College Station, Texas)

Nathaniel Friedman (University at Albany, Albany, New York)

Preface

It is hard to believe the first art/math conference AM 92 was held here at the University at Albany seventeen years ago. Where does the time go?? This is already the eighth ISAMA conference since the founding of ISAMA in 1998. Looking back over the years, I have to thank all the people that helped co-organize conferences, in particular Carlo Sequin, Javier Barrallo, Dietmar Guderian, John Sullivan, Jose Martinez-Aroza, Juan Antonio Maldonado, Reza Sarhangi, Steve Luecking, Ergun Akleman, Vinod Srinivasan, Alfred Peris, and Joan Peiro. I especially want to thank John Sullivan and Ergun Akleman for all their work in making our publication Hyperseeing a success. The art/math movement has now been recognized by the MAA = Mathematical Association of America and the AMS = American Mathematical Society. I want to thank Robert Fathauer for organizing the many exhibits at the joint math meetings of the MAA and AMS, as well as the exhibits at the Bridges Conferences, which have produced a first-class series of Proceedings due to the many years of work of Reza Sarhangi, as well as Carlo Sequin, George Hart and Craig Kaplan. There are also the Math and Design conferences organized by Vera Spinadel, the Nexus conferences relating mathematics and architecture and the Nexus Network Journal organized and edited by Kim Williams, and the various Hungarian Symmetry Conferences organized by our friends in Budapest. Most of all, thank you so much to all the conference participants over the years. You made the conferences.

Next year Nexus 2010 will be in Porto, Portugal, June 13-15, followed by ISAMA 2010 in Paris, France, June 21-25, co-organized with Claude Bruter. Now all you wine-lovers have something to look forward to. After all that great wine and seafood in Porto, pour yourself on a train to Paris to continue the party!

In conclusion, I would like to thank the University at Albany (UA) for hosting ISAMA 2009. UA deserves a lot of credit for all the help they have provided in launching and continuing the art/math movement.

Nat Friedman

ISAMA 2009 Organizing Committee

Ergun Akleman (Texas A&M University, College Station, Texas, USA)
Javier Barrallo (The University of the Basque Country, San Sebastian, Spain)
Nathaniel Friedman(University at Albany, Albany, New York, USA)
Stephen Luecking (DePaul University, Chicago, Illinois, USA)
John Sullivan (Technische Universitat Berlin, Berlin, Germany)

Table of Contents

Page #	Authors	*Paper Title*
1-4	Robert Bosch	*Knothole Sculptures*
5-12	Gary Greenfield	*On Variation Within Swarm Paintings*
13-19	James Mallos	*How to Weave a Basket of Arbitrary Shape*
21-28	Susan Happersett	*Algorithms, Art, and Aesthetics*
29-36	Robert Kauffman	*Fish Tile Animation: Anatomy of an Animated Tessellation*
37-41	Yang Liu	*From Sona Drawings to Contemporary Art*
43-50	Y. Liu and G. Toussaint	*A New Method for Classifying Fret and Meander Patterns.*
51-56	Robert Spann	*Algorithmic Art Based on Completely Chaotic Rational Functions*
57-62	Steve Luecking	*Collapsed Orbs: Astroidal Sculptures from the Breakdown of the Sphere*
63-64	CJ Fearnley	*Foldable Great Circle Geometries*
65-68	Benigna Chilla	*Intaglio Monoprints: Lines Patterns, Line Surfaces*
69-73	Doug Dunham	*Transforming "Circle Limit III" Patterns - First Steps*
75-82	Claude Bruter	*The Boy Surface as Architecture and Sculpture*
83-90	Doug Peden	*Period In Progress*
91-94	Donna Lish	*Beading in the Stream of Consciousness*
95-102	George Hart	*Comet!*
103-112	Stephanie Strickland	*Slippingglimpse: Making and Reading a Born-Digital Poem*
113-117	James Mallos	*Unit-Weave the Cubic Polyhedra*
118-120	Garousi Mehrdad	*Fractal tesselation*
122-128	G. Mehrdad & S. M. Mansoor	*Aesthetics in Creating Fractal Images*
130-135	Nat Friedman	*Moebius bands, Braids and Knots*
136-140	R. Fathauer & N. Friedman	*Slot Canyons: Form, Space, Light & Color*

Knothole Sculptures

Robert Bosch
Oberlin College
Oberlin, OH 44074
bobb@cs.oberlin.edu

Abstract

We use variants of the Traveling Salesman Problem to create two-piece sculptures that resemble wooden knots and knotholes.

Knothole Sculptures

We begin with a drawing of a mathematical knot or link. We convert it into a stipple drawing, a collection of dots. We think of these dots as the cities of a Traveling Salesman Problem (TSP), in which a salesman based in one city must visit each of the other cities exactly once before returning home, while minimizing total distance traveled. We solve the TSP, obtaining a salesman's optimal tour, a simple closed curve. (Since the total distance traveled by the salesman is the sum of the lengths of the edges -- line segments -- that make up his tour, and since each edge length is computed using the Euclidean distance formula, the TSP is a geometric TSP. Optimal tours for geometric TSPs do not have edge crossings [1].) Thus the resulting curve is a Jordan curve and decomposes the plane into an inside region and an outside region.

We then copy this curve onto a sheet of acrylic or metal and cut along it with a laser or water jet cutter. By doing this, we separate the material into two pieces: an inside piece and an outside piece. We call the resulting object a *knothole sculpture* for the following reasons: it came from a mathematical knot (or link), it looks like a mathematical knot (or link), its inside piece resembles a wooden knot or knot hole, and its outside piece resembles the part of a wooden board that remains when a wooden knot is removed.

Figure 1: (a) a drawing of a two-component link, (b) a 500-city TSP stipple drawing of the link, (c) the salesman's optimal tour, (d) a picture of the knothole (in white) and board (in gray) formed from the optimal tour, (e) a picture of the knothole and board formed from a well-behaved tour.

Figures 1 (a), (b), (c) illustrate the process, and Figure 1 (d) and (e) demonstrate that the optimal tour does not necessarily generate a knothole sculpture that does justice to the original drawing. In this example, the TSP's 500 cities define four city-free regions, marked A through D. The knothole sculpture formed from the optimal tour places regions A and B in the knothole (the inside of the tour) and regions C and D in the board (the outside of the tour). This sculpture does not resemble the original drawing! The second knothole sculpture, formed from an alternate "well-behaved" tour, is much better. Because it places regions B and D in the knothole and regions A and C in the board, it more closely resembles the original drawing. Like the original drawing, it has 180^{o} rotational symmetry, at least when viewed from a distance.

To obtain optimal tours, like the one displayed in Figures 1 (c) and (d), we use Concorde [1, 4], the best package for solving large-scale TSPs to optimality. Unfortunately, Concorde does not solve TSPs that have side constraints. And to obtain well-behaved tours like the one in Figure 1(e), we definitely need side constraints: we need to force the salesman to wind his way through the cities in such a way that certain pairs of user-selected, city-free regions will end up on the same side of his tour, while others end up on opposite sides. For the Figure 1 example, we wanted regions A and C to be on the same side of the tour, regions B and D to be on the same side of the tour, regions A and B on opposite sides of the tour, and regions C and D to be on opposite sides of the tour.

Figure 2. Four knothole sculptures made from laser-cut acrylic. Each is approximately 3" in diameter and is made from 0.125" acrylics (an ivory knothole and a black board)

To obtain well-behaved tours, we use ILOG's CPLEX [6] integer programming solver to solve what turns out to be a simple modification of the Dantzig-Fulkerson-Johnson integer programming formulation of the TSP [5]. (The DFJ IP formulation is at the heart of Concorde). We make only small changes to the DFJ formulation, adding one binary variable and one linear equation for each side constraint of the form described above. For details, see [2].

Often we start with a symmetric drawing of a knot or link, and we want to preserve the symmetry. To do this we create a symmetric stipple drawing, using a simple modification of MacQueen's method [8]. To force the salesman's tour to be symmetric, we add additional side constraints to our integer programming formulation.

Figure 2 displays a collection of laser-cut knothole sculptures. Each one is approximately 3" in diameter and is made from 0.125" acrylics (an ivory knothole and a black board). Each of these sculptures has three-fold rotational symmetry. Actually the top right and bottom right sculptures have even more symmetry than is immediately apparent: their stipple drawings TSPs have six-fold rotational symmetry, which leads to certain geometric figures appearing three times in the knothole and three times in the board. (For example, a certain section of the top right sculpture looks very much like the head of a snake. This snake head appears three times in the knot hole and three times in the black board.)

Figure 3 displays two knothole sculptures made from water-jet-cut metals. The design is the same as the one used for the top right sculpture in Figure 2. For additional examples of how the TSP can be used to create pieces of visual artwork, see [3] and [7].

Figure 3. Two versions of a knothole sculpture made from water-jet-cut metals. Each is approximately 6" in diameter. In the top version, both pieces are 0.25" thick, the knothole is stainless steel, and the board is brass. In the bottom version, both pieces are stainless steel, the knothole is 0.25" thick and the board is 0.125" thick.

References

[1] David L. Applegate, Robert E. Bixby, Vasek Chvatal, and William Cook. *The Traveling Salesman Problem: A Computational Study*. Princeton University Press, 2006.

[2] Robert Bosch, Connecting the dots: the ins and outs of TSP art. In *Bridges Leewarden; mathematical connections in art, music, and science*, pages 235-242. 2008.

[3] Robert Bosch and Adrianne Herman. Continuous line drawing via the Traveling Salesman Problem. *Operations Research Letters*, 32(4): 302-303, 2004.

[4] Concorde TSP Solver. www.tsp.gatech.edu/concorde/index.html.

[5] G. Dantzig, R. Fulkerson, and S. Johnson. Solution of a large-scale traveling-salesman problem. Operations Research, 2:393-410, 1954.

[6] ILOG CPLEX. High-performance software for mathematical programming and Optimization. www.ilog.com/products/cplex/

[7] Craig S. Kaplan and Robert Bosch. TSP art. In *Renaissance Banff: Bridges 2005: mathematical art, music, and science*, pages 301-308, 2005.

[8] J. MacQueen. Some methods for classification and analysis of multivariate observations. In *Proc. Fifth Berkeley Symposium on Mathematical Statistics and Probability, I*, pages 281-297. 1967.

On Variation within Swarm Paintings

Gary R. Greenfield
Department of Mathematics & Computer Science
University of Richmond
Richmond, VA 23173, USA
E-mail: ggreenfi@richmond.edu

Abstract

Swarm paintings are algorithmic artworks that are created by simulating swarm behavior using a large number of virtual agents that roam on a toroidal grid (or in three dimensional space) and disperse virtual paint according to their pre-programmed behaviors. One of the limitations to this art form is the sameness to the swarm paintings that result. In this paper we consider mechanisms for introducing greater image variation and diversity within the swarm painting conceptual framework..

Introduction

To the best of our knowledge, swarm paintings trace their origins to the ant colony simulation experiments of Ramos [10] [11]who investigated the use of ant colony simulations for image processing purposes. This early work of Ramos eventually led to the physically embodied collective robotics paintings of Moura [8] [9] (see Figure 1 and Figure 2). Interestingly, image processing and non-photorealistic rendering continue to be application domains for ant colony simulation research (see for example Ramos [12] or O'Reilly et al. [13]).

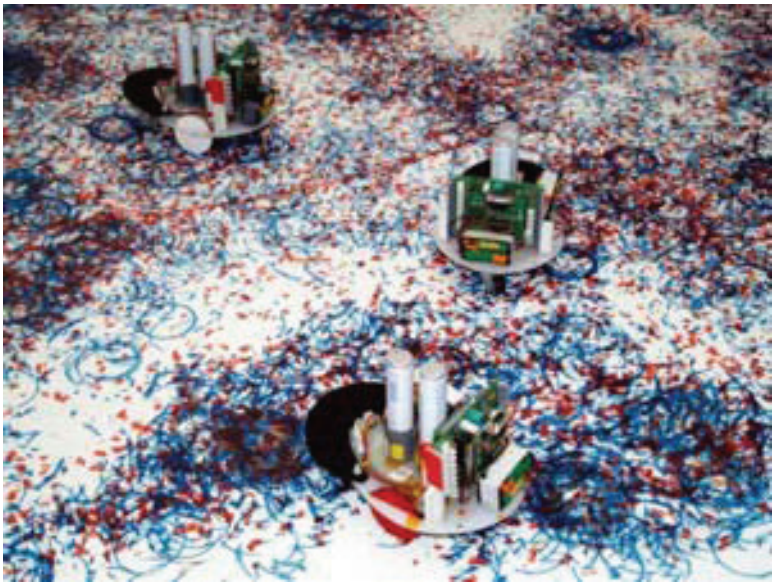

Figure 1: *Close of up of Moura's physically embodied robots engaged in collective robotics painting.*

Figure 2: *Gallery hung example of one of Moura's finished collective robotics painting.*

A group led by Monmarché [2] appears to be the first to have used the term “ant painting" to describe abstract images made by *virtual* ants that roam over a toroidal canvas. In their model a small number (4-6) of virtual ants paint by depositing one color while searching for a different color, thus color serves as the “scent". Moreover, their image generation scheme is interactive because a technique known as user-guided aesthetics is implemented so that the user can evolve ant paintings. Greenfield [4] considered non-interactive methods for evolving ant paintings using a similar model, but again using only a small number (8-12) of virtual ants. Figure 3 shows an example of each type of ant painting.

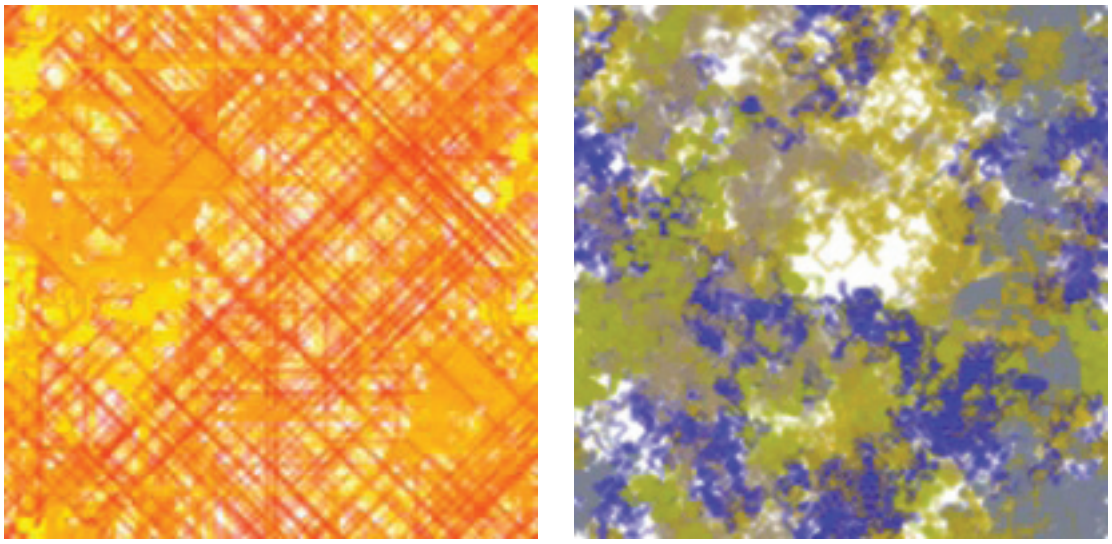

Figure 3: *Left: An ant painting reproduced using the Momarché et al. model from data found in [2]. Right: An example of an ant painting produced using a related model developed by Greenfield [4]. In both cases color acts as the scent.*

Subsequently, Urbano [15] considered an ant painting model where each individual cell in the *environment* exuded virtual scent - the attractant - until it was visited by an ant. By diffusing and evaporating this exuded scent; by using two competing species with large numbers (25-250) of ants; and by marking each cell according to which species of ant reached it first, Urbano's technique yielded ant paintings that were ``finished" once there were no more unvisited cells left to exude scent. Greenfield [3] [4] improved upon this model by also allowing the ants themselves to exude virtual scents, and by having

their behaviors controlled by treating these scents as attractants and repellents. Figure 4 shows an example of each type of ant painting. Jacob et al. have explored 2D swarm painting models based on simulating large colonies of bacteria [6] as well as 3D swarm paintings based on simulating flocks of birds [7]. Annunziato et al. [1] have exhibited artificial life inspired installation artworks using large numbers of virtual agents.

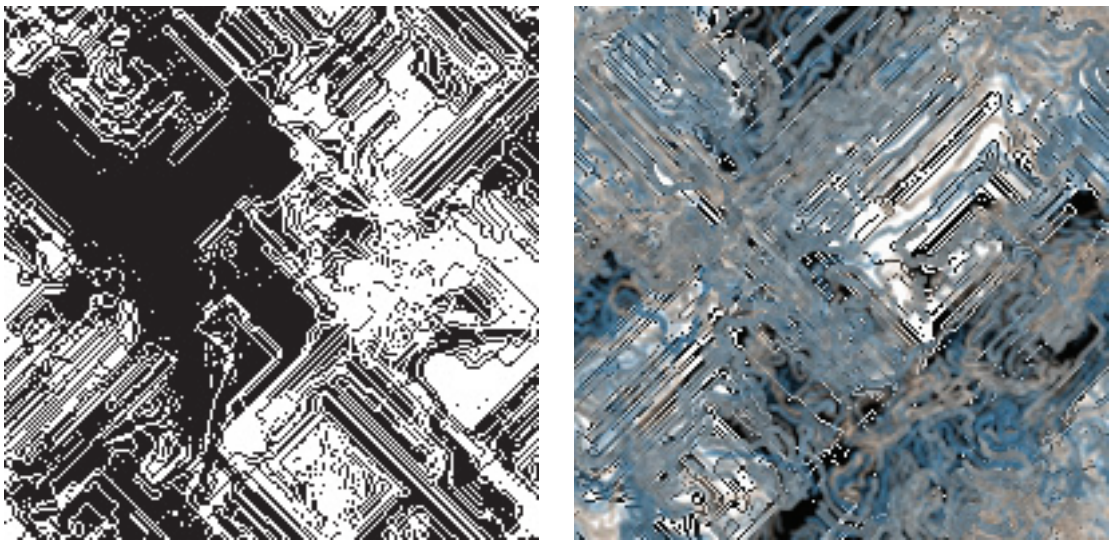

Figure 4: *Left: An ant painting in the style of Urbano[15] where randomly placed ants roam and mark each cell of a 200 x 200 toroidal grid on the basis of which one of two species of ants reaches it first. Cells in the grid attract ants by exuding scent. Right: An ant painting after Greenfield [3] where virtual scent dispersed by the ants induces "overpainting" on an Urbano style ant underpainting.*

We should also point out that both Urbano and Moura appeal to the concept of *stigmergy* to help explain why their respective physical and virtual software controlled entities are able to exhibit creative or artistic tendencies. Stigmergy [14] refers to the situation where the behavior of agents in swarms is controlled wholly by external, environmental factors.

Starting from the observation that all of the ant painting models that we are aware of yield images that have a sameness to them, in this paper we consider the use of global attributes as a design source for introducing image variation and diversity within the ant painting conceptual framework.

Our virtual ants

The model for a virtual ant that we use here is an amalgam of the scent-by-color model of Monarché [2] and the scent-by-virtual-pheromone model of Greenfield [5]. Each virtual ant maintains a location and a compass heading. At each time step it senses the three cells immediately in front of it in order to ascertain their color luminances and the concentrations of each of the two ant produced pheromones. It then deposits color in the cell it currently occupies and advances between 1 and 4 cells in a direction determined by one of the three sensed cells. Ants have both individual attributes and species attributes. Individual attributes are caste, color to deposit, color to follow, and number of cells traversed at each time step. Species attributes are the available colors to choose from, the scent detection thresholds, the probability of following color scent if it is detected, the probability of following (or avoiding) a virtual

scent if one is detected, and the probabilities for which direction (forward, left, or right) to follow when no scent is detected or scent is being ignored. Which species attributes will actually come in to play is determined by the caste the ant belongs to. In other words, the critical individual attribute is the ant's caste designation because that wholly determines its behavior.

For the ant paintings shown here we have designed and implemented three castes, i.e., behaviors. The *explorer* caste tries to find unvisited cells. Thus, if there are unvisited cells in its current field of vision they will determine its direction, but if none are present it will rely on the directional probabilities to make that choice. The *color* caste is sensitive to detection of either the deposited color or the sought color. If the deposited color is sensed then the ant tries to avoid it. If the following color is sensed then (almost always) the ant will follow it. Similarly, the *pheromone* caste is sensitive to the presence of virtual scent. As indicated above, one of the scents is a following scent; the other is a repelling scent.

The environmental parameters that are needed to be able to simulate ant behavior are the number of colors a species will be permitted to work with (6), the amounts of virtual scent dispersed per ant at each time step (fixed, but different for each of the two scents), the virtual scent evaporation rate (3\%), and the virtual scent diffusion rate (7\%). The ant painting examples below were all obtained using a 256 x 256 toroidal grid of cells.

Adding global attributes to the model

To introduce variation and diversity to ant paintings, we now consider the inclusion of four global attributes that will affect the nature of a painting once the caste attributes and individual attributes are fixed. Since ants are stochastic in the sense that under certain conditions their behavior is based on probabilities, in order to make ant paintings reproducible each painting must be assigned an integer seed s that can be used to initialize the pseudorandom number generator. Unlike Urbano [15], our ant paintings are extremely sensitive to the number of time steps, so we let t be the number of steps allocated for depositing color. The number of ants n obviously affects the character of an ant painting. The key attribute we introduce is the ``footprint size'' f of a painting. When color is deposited, f determines the width of a strip of cells oriented consistent with the ant's current heading that will be colored.

Although it is outside our present scope, ant paintings are not particularly sensitive to the seed s, so it bears repeating that its inclusion is only for the sake of reproducibility. For the examples below, we restrict t to be a multiple of 5, with $25 \leq t \leq 225$; we restrict n to be a multiple of 5, with $20 \leq n \leq 80$; and we require $2 \leq f \leq 12$.

Variation exhibited by the model

We wish to emphasize that unlike the ant paintings in Figure 3 and Figure 4 all the ant paintings we present below use the same initial placement configuration for the virtual ants. More precisely, rather than initially placing the ants at pseudorandom locations on the grid, we always cluster the virtual ants into five equally sized groups, with one group placed at the center of our canvas, and the other four groups placed at the centers of each of the four quadrants. Further, we use consistent initial heading orientations for all the ants within each cluster.

Here, it is not possible to systematically explore the variation induced by our three levels of attributes. Thus as an experiment, we pseudorandomly generated 70 ant paintings. In Figure 5 we present nine examples we culled to showcase the variation and diversity our model supports. By pseudorandomly

generate, we mean first a set of six colors is pseudorandomly generated subject to the constraint $16 \leq R,G,B \leq 240$; next a set of species attributes is pseudorandomly generated; then values for s, t, n, f are pseudorandomly generated; and finally for each of the n virtual ants required a set of individual attributes is pseudorandomly generated.

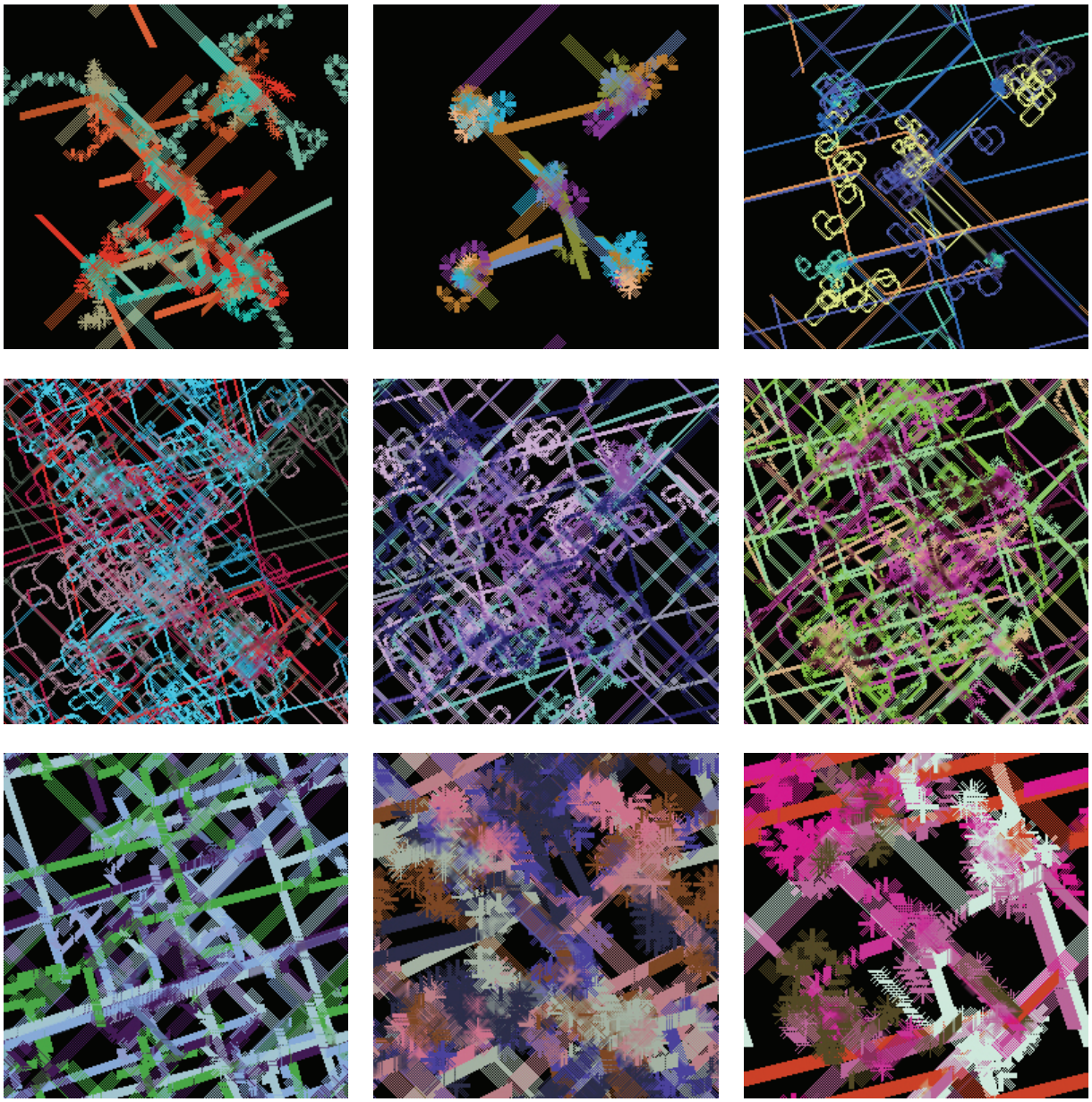

Figure 5: *Nine examples selected from a group of 70 pseudorandomly generated ant paintings using our model that illustrate the image variation and diversity that the model supports.*

The ZDD series of ant paintings

Of course, even though the hand of the artist may be self-evident in the design and implementation of the algorithms, in the case of algorithmic artworks simply relying on the technique of pseudorandomly

generating images does not make a very strong case for labeling the product as “art". Thus, in this section we attempt to harness the potential of our ant painting model in such a way that the images are produced with artistic intent. The ZDD series of ant paintings were conceived of as a collection of “bi" ant paintings. Here we use the word “bi" in two ways as follows.

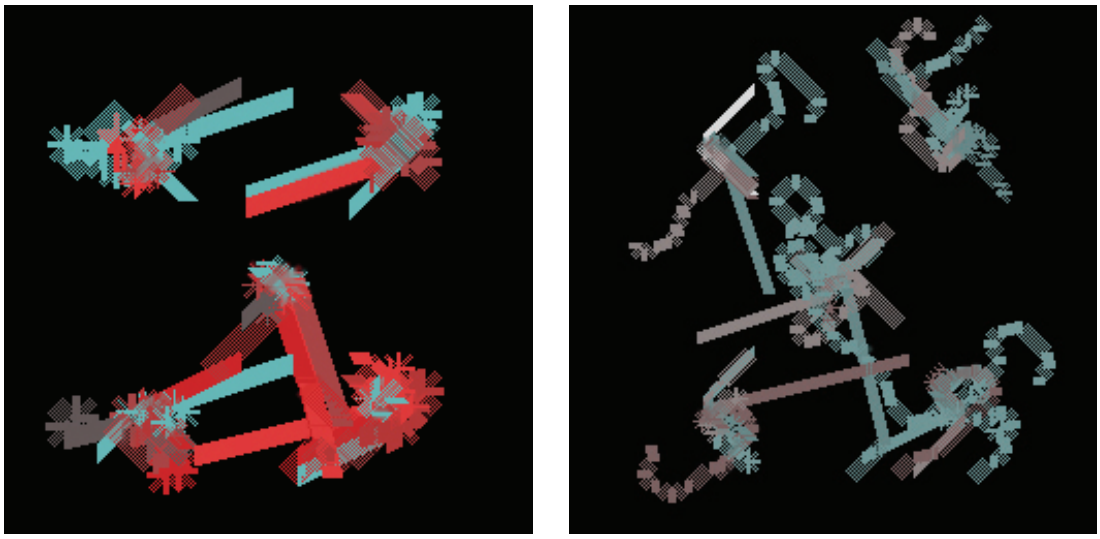

Figure 6: *Two images from the ZDD series in the cyan and red color scheme. Note that the occurrence of white in the image of the right resulted from the situation where all three color components coincidentally assumed the same value, in this case 218.*

It is a cliché to point out that the choice of (pseudo)coloring schemes in algorithmic art dominates the viewer's response to the artwork. Images in the ZDD series are bi-colored, or technically *duotone*, because the six colors used in each coloring scheme are always constrained so that for each color, two components are the same. Moreover, the same two components must agree across all six colors. This implies the scheme must be either R+G, B or G+B, R, or B+R, G i.e. yellow and blue, or cyan and red, or magenta and green. This deadens the emotional impact of the images. Images in the ZDD series are bi-composite because they are obtained by trying to “fit" the composition to two different target images. This gives what might be described as a sense of tension and release, or perhaps yin and yang, to the images. The technical details of how this fitting takes place is beyond the scope of this paper. In summary then, the artistic intent underlying the ZDD series of ant paintings is to produce a series of “bi-polar" images vis-á-vis the definition ``having two poles, as the earth". Figure 6 shows two examples using the cyan and red color scheme. Figure 7 and Figure 8 give further examples rounding out the use of the color schemes.

Conclusions and an open problem

We have described a new framework for producing ant paintings by introducing a limited number of global attributes to a previous model we considered in order to increase the range of image variation and the potential for image diversity. A general shortcoming to ant paintings is the lack of scalability. That is, the inability to increase the resolution of a given ant painting. Our examples were all done using a 256 x 256 toroidal grid. Increasing the size of the grid slows image generation. Further, using the same data, it does not preserve image fidelity. It remains an open problem to devise an attribute formulation that preserves salient compositional structures when the resolution of the underlying grid is increased.

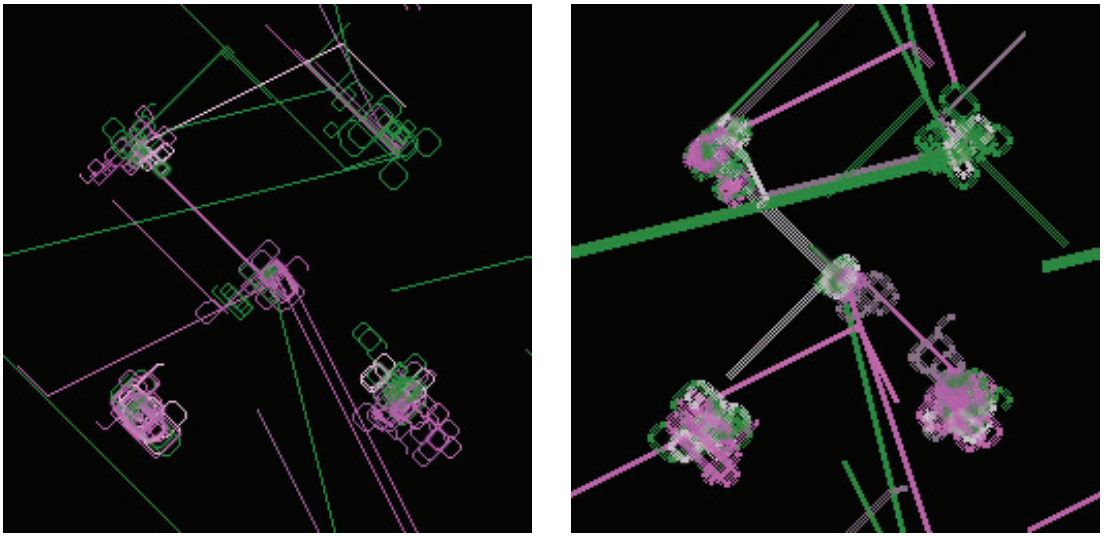

Figure 7: *Two images from the ZDD series in the magenta and green color scheme. Effects due to the use of global attributes are emphasized by these examples.*

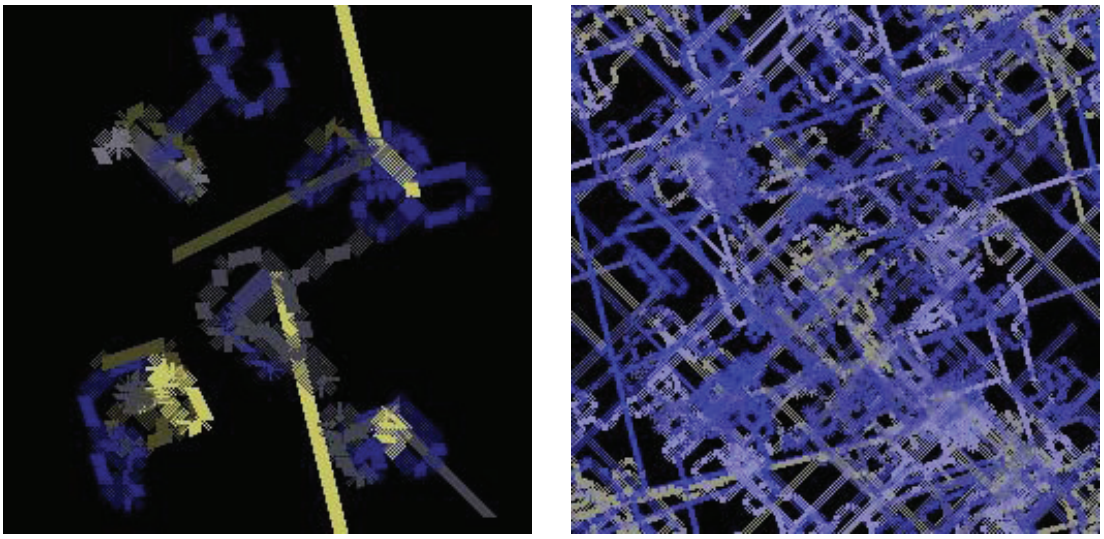

Figure 8: *Two images from the ZDD series in the yellow and blue color scheme.*

Acknowledgment

This work was supported in part by the 2008-2009 University of Richmond Arts & Sciences enhanced sabbatical program. I would like to thank Penousal Machado of the University of Coimbra for hosting the Fall portion of my sabbatical and for his insights and contributions to this work. I would also like to thank a source of artistic inspiration who wishes to remain anonymous.

References

[1] Annunziato, M., Pierucci, P., Relazioni emergenti: experiments with the art of emergence, *Leonardo*, vol. 35, no. 2, 2002, pp. 147-152.

[2] Aupetit, S., Bordeau, V., Monmarché, N., Slimane, M., Venturini, G.: Interactive evolution of ant paintings, *2003 Congress on Evolutionary Computation Proceedings* (eds. B. McKay et al.), IEEE Press, vol. 2, 2003, pp. 1376-1383.

[3] Greenfield, G., Ant paintings using a multiple pheromone model, *BRIDGES 2006 Conference Proceedings* (eds. R. Sarhangi and J. Sharp), 2006, pp. 319-326.

[4] Greenfield, G., Evolutionary methods for ant colony paintings, *Applications of Evolutionary Computing, EvoWorkshops 2005 Proceedings*, Springer-Verlag Lecture Notes in Computer Science, LNCS 3449 (eds. F. Rotlauf et al), 2005, pp. 478-487.

[5] Greenfield, G., On evolving multi-pheromone ant paintings, *2006 IEEE World Congress on Computational Intelligence*, Vancouver, BC, Canada, IEEE Press, WCCI06 Conference Proceedings, (DVD-ROM ISBN: 0-7803-9489-5), 2006, pp. 7425-7431.

[6] Hoar, R., Penner, J., Jacob, C., Transcription and evolution of a virtual bacteria culture, {\em 2003 Congress on Evolutionary Computation Proceedings}, IEEE Press, 2003, 54--61.

[7] Jacob, C., Hushlak, G., Boyd, J., Sayles, M., Nuytten, P., Pilat, M., Swarmart: Interactive art from swarm intelligence, *Leonardo*, vol. 40, no. 3, 2007, pp. 248-254.

[8] Moura, L., Pereira, H., *Man + Robots: Symbiotic Art*, Institut d'Art Contemporain, Lyon/Villeurbanne, France, 2004.

[9] Moura, L., Ramos, V., Swarm paintings - nonhuman art, *Architopia: Book, Art, Architecture, and Science* (eds. J. Maubant et al.), Institut d'Art Contemporain, Lyon/Villeurbanne, France, 2002, pp. 5-24.

[10] Ramos, V., Almeida, F., Artificial ant colonies in digital image habitats - a mass behaviour effect study on pattern recognition, *Proceedings of ANTS'2000 - 2nd International Workshop on Ant Algorithms: From Ant Colonies to Artificial Ants* (eds. M. Dorigo et al.), Brussels, Belgium, 2000, pp. 113-116.

[11] Ramos, V., Merelo, J., Self-organized stigmergic document maps: environment as a mechanism for context learning, *AEB´2002, First Spanish Conference on Evolutionary and Bio-Inspired Algorithms* (eds. E. Alba et al.), Mérida, Spain, 2002, pp. 284-293.

[12] Ramos, V., Self-organizing the abstract: canvas as a swarm habitat for collective memory, perception and cooperative distributed creativity, *First Art & Science Symposium, Models to Know Reality* (eds. J. Rekalde et al.), Bilbao, Spain, 2003, p. 59.

[13] Semet, Y., O'Reilly, U., Durand, F., An interactive artificial ant approach to non-photorealistic rendering, *Genetic and Evolutionary COmputation - GECCO 2004*, (eds. K. Deb et al.), Springer-Verlag Lecture Notes in Computer Science, LNCS 3102, 2004, pp. 188-200.

[14] Theraulaz, G., Bonabeau, E., A brief history of stigmergy, *Artifical Life*, vol. 5, no. 2, 1999, pp. 97-116.

[15] Urbano, P., Playing in the pheromone playground: experiences in swarm painting, *Applications of Evolutionary Computing, EvoWorkshops 2005 Proceedings*, Springer-Verlag Lecture Notes in Computer Science, LNCS 3449 (eds. F. Rothlauf et al.), 2005, pp. 478-487.

How to Weave a Basket of Arbitrary Shape

James Mallos
3101 Parker Avenue
Silver Spring, MD, 20902, USA
E-mail: jbmallos@gmail.com

Abstract

The problem of designing a triaxial weave for a given surface can be shown to be equivalent to the problem of triangulating the surface. As surface triangulation has been extensively studied by computer scientists and widely utilized in computer graphics, the possibilities of basket making today are vastly increased. Almost any 3-D shape we might see rendered on a computer screen can be woven as a basket, indeed, the computer may have already done the work of designing the weave before it rendered the image. I present a method to convert a triangle mesh into patterns for weavers that can be woven into a basket of the desired shape.

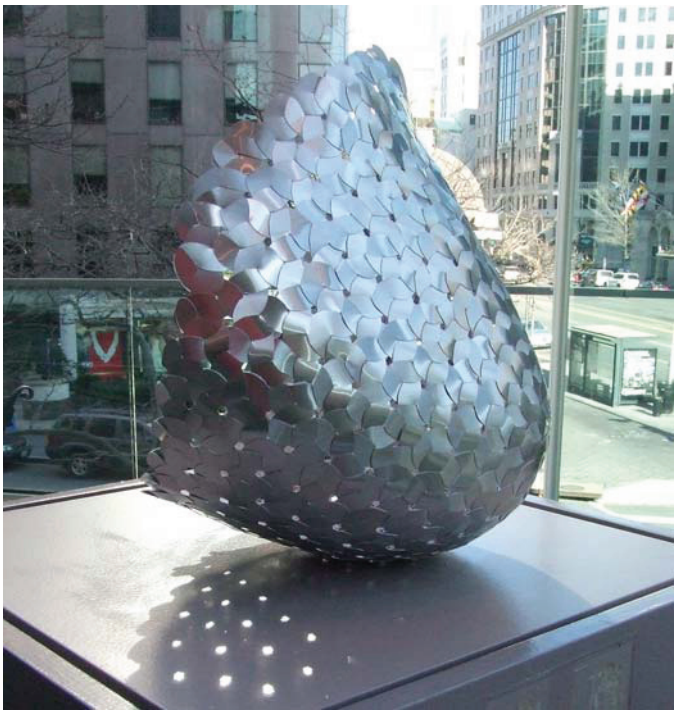

Figure 1. James Mallos, *Olivier's Fingertip.*

Introduction

A need in common among architects, sculptors, and industrial designers is a way to build curved shapes. Of the many ways now available, one of the oldest, basket weaving, is sometimes the best. Baskets are strong, resilient, and light; and basket weaving does not require part-specific tooling, so it dovetails well with modern concepts of flexible manufacturing. In most cases the shape the designer would like to make is defined in a computer file that is either already a triangle mesh or is readily converted into one, so the

remaining problems are how to convert a triangle mesh into patterns for custom-cut weavers, and how to correctly place the weavers in the weaving. Akleman, Xing, and Chen [1] have offered a proof that any manifold mesh can be woven. What this practically means to the basket maker is the surprising result that *any* surface can be woven in *any* pattern. Here I offer a visual demonstration for only the simplest weave and the most widely used mesh.

Weaving and Triangulation

"Triangulation is the division of a surface or plane polygon into a set of triangles, usually with the restriction that each triangle side is entirely shared by two adjacent triangles." [2] A topologist's use of triangulation is to decompose a surface into a number of pieces, each homeomorphic to a plane triangle, in order to create an atlas of the surface that captures its topology. For a computer scientist, triangulation is a way to build up an approximation of a surface using a mesh of planar triangles. These two different takes on triangulation are of course interrelated. Topology handles the hard part. Once a topologically complex surface has been divided into triangular pieces it is relatively easy to subdivide further, into smaller and smaller sub-triangles, to obtain as close an approximation of the surface as necessary.

The wide applicability of surface triangulation is firmly established by a theorem due to Rado[3]: *"Every compact surface admits a triangulation."* Since a *non*-compact surface [4] would seem to require infinite human effort to build—even if built of mathematical constructs—Rado's Theorem guarantees that any surface within the sensible purview of human ambition can be triangulated.

Weaving is closely related to triangulation: triaxial weaving can be described as a triangle decoration. This is a simple version of the technique used to design Celtic knots [5-7]. On the left in Figure 2 is a plain, undecorated triangle, on the right is a triangle decorated with an illustration of the three-way crossing in a triaxial weave. One must imagine that both the triangle and the decoration on it are stretchable; in particular, that they can be stretched to precisely overlie any other triangle however it might differ in size or proportions.

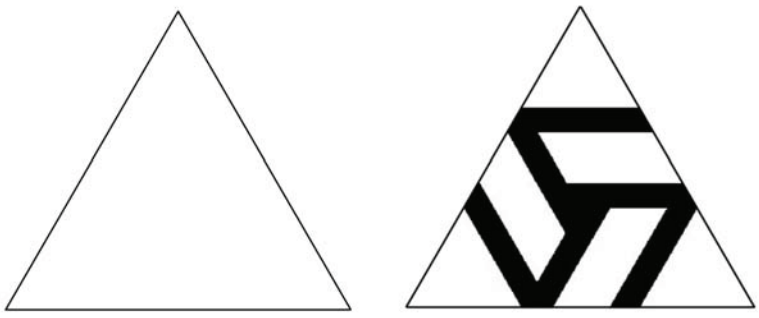

Figure 2. A plain triangle and the same triangle decorated with a triaxial weave crossing.

Having in hand such a stretchable triangle, we can proceed to decorate any triangle mesh by individually covering each triangle in the mesh with a suitably-stretched version of the decorated triangle. An example of such a decorated mesh is shown in Figure 3. On the left is a rendering of the plain triangle mesh, on the right, the same mesh with every triangle decorated. (The 3D models for the figures in this paper, as well as for *Olivier's Fingertip,* are courtesy of IMATI, INRIA, and TECHNION by the AIM@SHAPE Shape Repository.) Close inspection of Figure 3 will show that the decorated triangles trace out weaver paths

having the over-and-under pattern of real weaving. This *discovered* arrangement of weavers was implicit in the triangle mesh. Designing a triaxial weave on a surface and triangulating the surface are just different representations of the same problem.

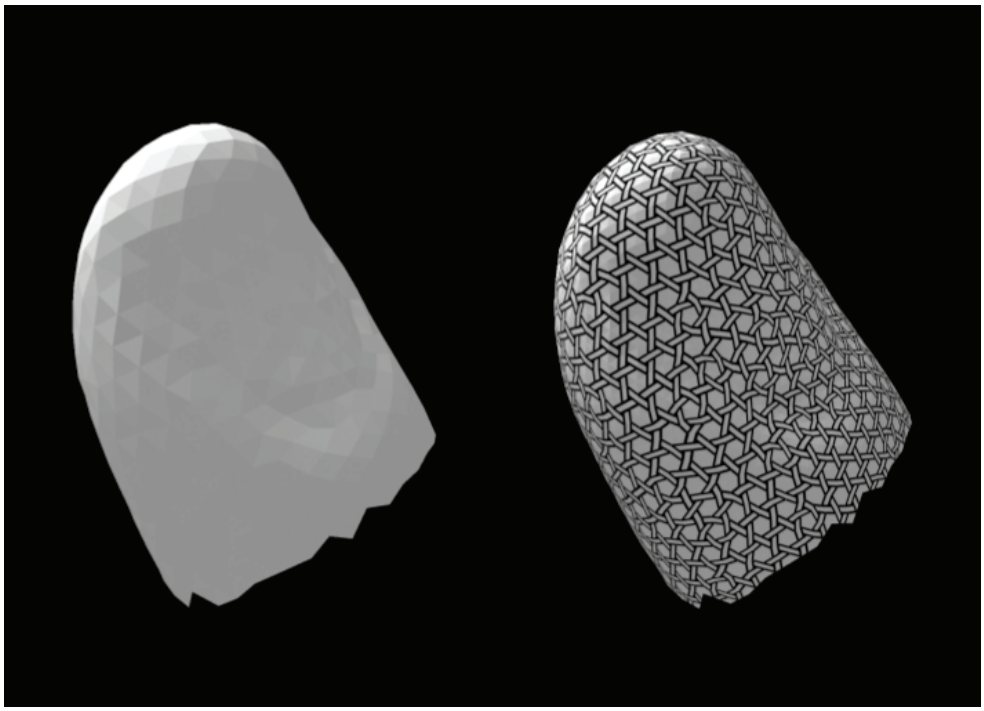

Figure 3. A plain triangle mesh, and the same mesh with the triangles decorated.

Weaving and Chirality

Weave crossings look the same viewed from either side of the work. That is, they do not look 'flipped over' or 'mirrored' when seen from the back. For this reason it is strictly necessary to decorate both faces of every triangle in the mesh with the identical decoration to properly illustrate the weaving. Since we simply decorate *both* faces of *every* triangle in the same way, there is no difficulty in dealing with a non-orientable surface such as a Mobius strip or Klein bottle. To design a weave pattern on a non-orientable surface, one simply chooses a triangulation (one is guaranteed to exist by Rado's Theorem) and decorates both sides of every triangle with the same crossover pattern. (Of course, the self-intersections of the surface will still require some ingenuity—Morgan [8] has woven a Klein bottle that re-enters itself through a single weave opening!)

Snelson [9] describes the chirality of weaving in his patent on 3-D weaving. Every thread in a piece of woven fabric forms the boundary between two fabric openings. The threads that border the same opening lie in a helical arrangement around it. The opening can therefore be assigned a handedness in accordance with the usual rules for classifying screws and helices. In Figure 4, each opening has been labelled 'R' or 'L' according to its handedness. As can be seen in the figure, a woven thread forms the boundary between openings of opposite handedness. In biaxial weaving the openings on either side of the thread are squares, but in triaxial weaving triangular openings alternate with hexagonal openings in a way that leaves all the

triangular openings with one handedness, and all the hexagonal openings with the other. The upshot is that there is essentially only one way to weave biaxially, but there are two chirally distinct ways to weave triaxially. This causes no problem when decorating a triangle mesh. One simply has a choice of decoration: a pattern like that in Figure 2 (which yields left-handed triangles) or its enantiomorph (which would yield right-handed triangles.)

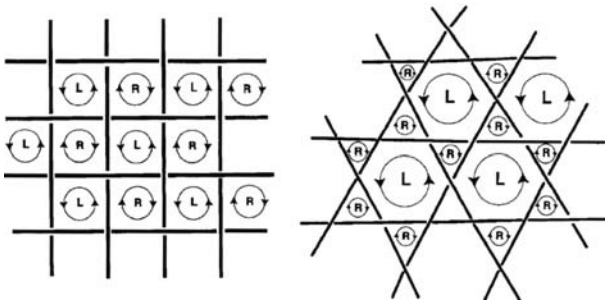

Figure 4. Chirality of the fundamental biaxial and triaxial weaves (from Snelson).

From Mesh to Weavers

I have written a piece of software called WeaverMaker that generates a pdf of weaver templates given a suitable .OFF (Object File Format) file describing the surface to be woven. The software assumes that the mesh consists entirely of triangles and does not have any mesh pathologies such as edges shared by more than two triangles. At this writing, the software is not capable of dealing with the problem of segmenting long weavers into splice-able lengths, or dealing with any weavers that form closed loops in the work. Its application is therefore limited to working with meshes with a modest number of triangles and generous free boundary (the place where weavers conveniently come to an end.) WeaverMaker is written in the Processing language, its source is available for download [10].

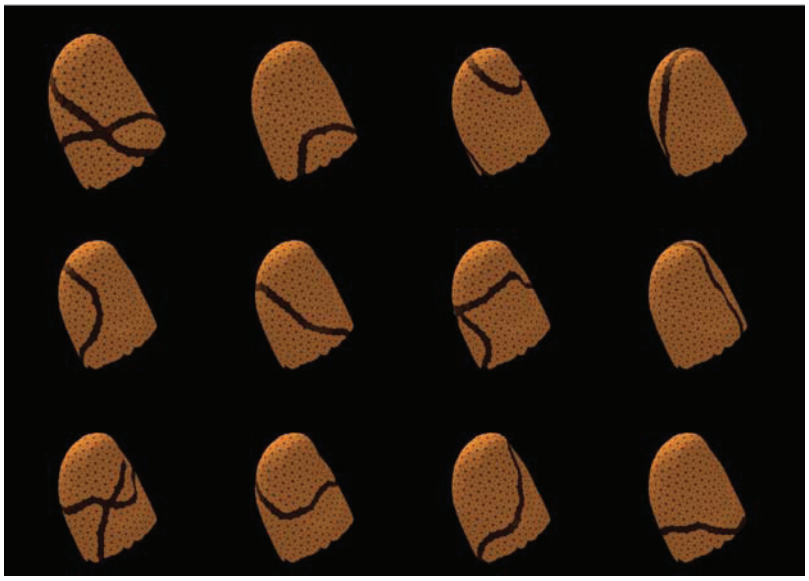

Figure 5. The weavers discovered in a triangle mesh have looping paths and some self-crossings.

A key suggestion in dealing with a triangle mesh is to index data structures by triangle vertices, not by vertices of the mesh per se. This may seem redundant—why store five or six vertices when you can store one?—but the triangle vertices, I call them *trivexes*, have just the right information. Each forms a natural pair with the trivex sharing the opposing edge (these pairings store all the connectivity information of the mesh) and each identifies with a particular weaver (i.e., the one that passes through their triangle parallel to the opposing edge.)

My software assigns to each trivex a weaver number by going to the lexically earliest trivex that does not yet have one, giving it the next weaver number, and then tracing that weaver from end to end in both directions assigning that number to every trivex encountered on the way; then it repeats this step until every trivex is assigned to its weaver and the total number of weavers is known.

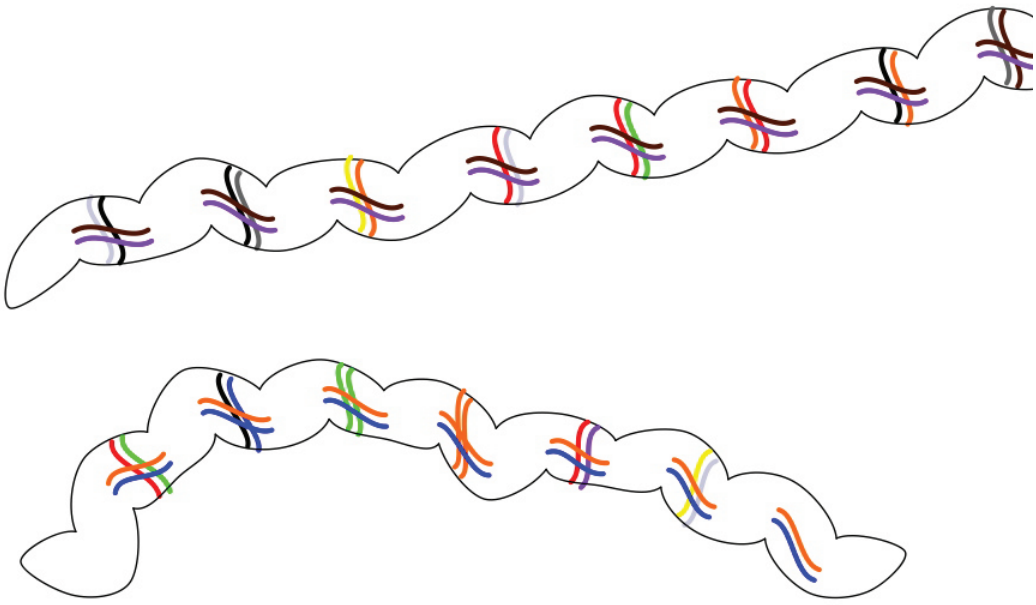

Figure 6. Typical weaver patterns as output by WeaverMaker.

The pdf file created by WeaverMaker prints out on letter-sized sheets which are spliced together to make a rather space-consuming array of paper templates. These are then roughly cut-out and pasted by hand in a closely-spaced arrangement on a sheet of the material to be woven. In the case of *Olivier's Fingertip* the material is thin aluminum sheet. After roughly cutting out the aluminum weavers, I use a triangular punch to cut the deep concavities in the profiles (the location of these deep concavities is the only dimension-critical part,) then I make the easy left-turning cuts while looking at the template, then flip the work over , and working blind, make the remaining cuts in the same left-turning direction.

Weaving

I start the weaving at a centrally located crossing (Figure 7) and work outward. The weavers are marked both with their own two-color code and the two-color code of the weavers that will cross in front. This proves to be more information than necessary: once a weaver is started in the work, it can only go one

way. The outward bellying of the weaver shapes between crossings lets every threeway crossing lock in place as soon as it is completed. The weaving would require much more skill if the weavers did not cooperate in this way.

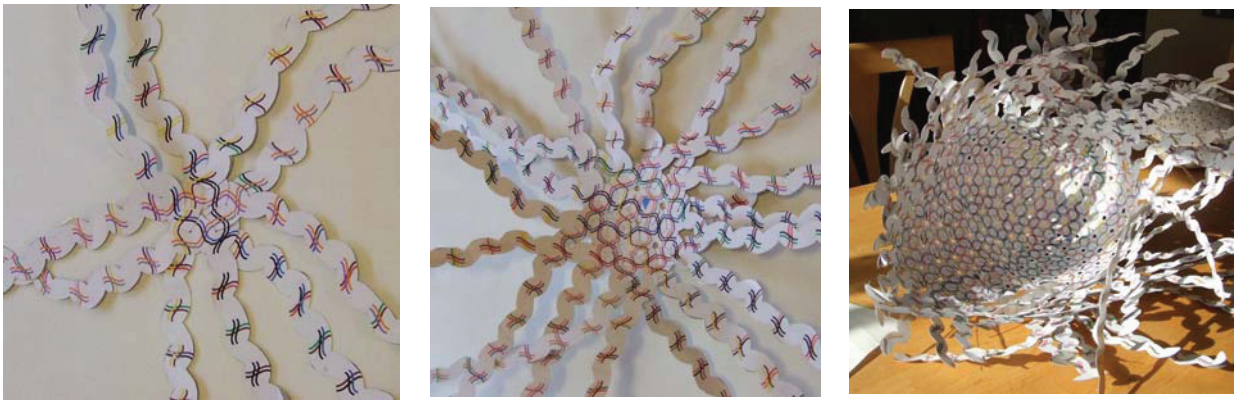

Figure 7. Stages in the weaving of *Olivier's Fingertip*.

Acknowledgement

The author is grateful for the beautiful, high-quality triangle meshes generously posted online by L'Institut National de Recherche en Informatique et en Automatique and its collaborating institutions. My work would not have been undertaken without their inspiration.

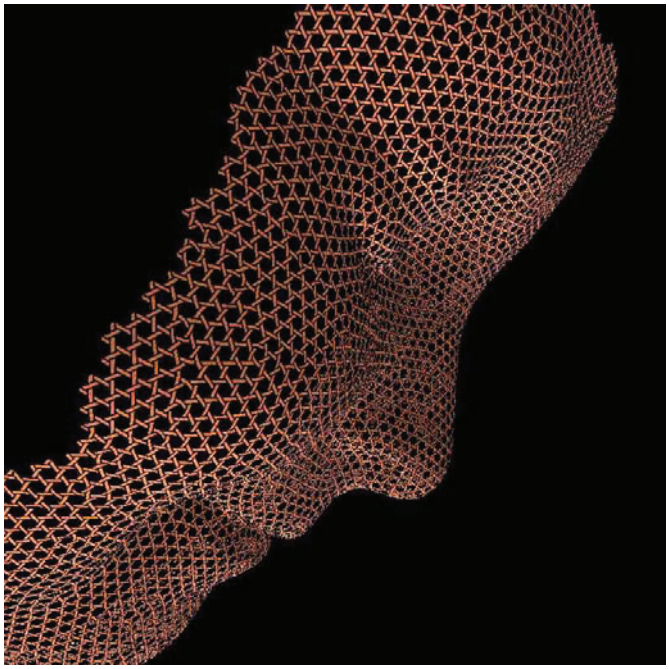

Figure 8. James Mallos, *Project for Girl's Face after Pampaloni*.

References

[1] Akleman, E., Chen, J., Xing, Q., and, J. Gross "Cyclic Plain-Weaving on Polygonal Mesh Surfaces with Graph Rotation Systems" Proceedings of ACM Siggraph'2009, Accepted, August 2009.

[2] Weisstein, E. W., "Triangulation." From MathWorld--A Wolfram Web Resource. http://mathworld.wolfram.com/Triangulation.html

[3] Francis, G. K. and Weeks, J. R., "Conway's ZIP Proof." Amer. Math. Monthly 106, 393-399, 1999.

[4] O'Neill, B., Elementary Differential Geometry, Second Edition, 178-9, 1997.

[5] Mercat, C., "Les entrelacs des enluminures celtes", Dossier Pour La Science, no. 15, 1997.

[6] Kaplan, M., Praun, E., and Cohen, E., "Pattern Oriented Remeshing For Celtic Decoration", Proceedings of Pacific Graphics 2004, 199-206, 2004.

[7] Kaplan, M., and Cohen, E., "Computer Generated Celtic Design", Proceedings of the Eurographics Symposium on Rendering 2003, 9-19, 2003.

[8] Morgan, S., "Work by Shiela Morgan." http://www.kleinbottle.net/Morgan/index.htm

[9] Snelson, K., U.S. Patent 6,739,937.

[10] Mallos, J., "WeaverMaker," http://www.alice-on-mars.com/downloads

Algorithms, Art and Aesthetics

Susan Happersett
Jersey City, NJ
fibonaccisusan@yahoo.com
www.happersett.com

Throughout history artists have been influenced by external societal factors. I intend to argue that there is a correlation between early conceptual art of the 1960's and mathematical algorithms, and that this correlation extends to conceptual art in the later 20th and 21st centuries.

As seen in the public conscious, there was a prevalence of algorithmic thinking in society that was initiated by the birth of computer science. The April 2nd 1965 Issue of Time Magazine featured a cartoon of a computer and the caption: "*The Computer in Society*"[1]. This cartoon computer was surrounded on top with a huge human looking brain. It had many arms: To answer the phone, to feed itself key punch cards, and to type on a sort of typewriter printer. The humans in the cartoon were gathered under the computer to offer it more punch cards and to read the long looping paper tapes spilling out of the printer. The concept of computerization was at the front of the public conscious in 1965, and this cartoon depicts this phenomenon with both humor and anxiety. The acceptance of these developments in technology into the cultural discourse was historically parallel with the introduction of Conceptual Art of the mid to late 1960's. The artists creating conceptual art were influenced by the mathematical ideas that were part of the contemporary dialogue.

Art and Mathematics both enable humans to understand the natural world by uncovering patterns and structures. By studying 20th century art, I find that the foundations of conceptual art offer excellent examples of algorithmically based art. Sol Lewitt gave us one of the most concise definitions of Conceptual Art in 1967:

> "In Conceptual Art the idea or concept is the most important aspect of the work….. All planning and decisions are made beforehand and executed in a perfunctory affair. The idea is the machine that makes the art."[2]

At the same time, Sol Lewitt was writing his paragraphs and sentences on conceptual art, society was thrown into the realm of algorithmic thinking and working due to the age of computerization. Computers were everywhere in the public consciousness, and the idea of algorithmic thinking was becoming part of the cultural dialogue, people were encountering computers in the work place, and the relationship between humans and computers was being examined in popular culture. For a definition of mathematical algorithm I turn to David Berlinski. In his book *The Advent of Algorithm* he states:

> "An algorithm is a finite procedure, written in a fixed symbolic vocabulary, governed by precise instructions, intelligence, or perspicuity, and that sooner or later comes to an end"[3].

An algorithm is finite, which means it has a natural, logical end, and it is precise, which means that the algorithm is unambiguous and every execution of the algorithm renders the same output, given the same input. The building blocks of the algorithm are primitive operations, which

include mathematical operations and logical evaluations. These primitive operations are executed in a specified sequence. Sets of primitive operations can be repeated until a specified end-condition exists. Finally, sets of primitive operations can be conditionally executed, only when a certain condition exists. With these building blocks of primitive operations, sequence, iteration and condition, algorithms of any level of complexity can be constructed.

Comparing the definition of algorithm with the early writings of conceptual art, we can see that the two fields are closely related. Like an algorithm, conceptual art begins with a set of rules that governs the process of art making. Once these predetermined decisions have been made and the process is put into motion, no external factors are allowed to interfere with the final outcome. According to Sol Lewitt, the execution is "perfunctory"[4].

When trying to examine the beauty and grace of mathematical algorithms, it is advantageous to view mathematics from a distant plane, from outside the mathematical system. To see algorithms in a wider context, I need to briefly introduce the topic of meta-mathematics. Meta-mathematics is the study of mathematics as a complete system. I like to think of meta-mathematics in this way: All mathematical processes are taking place inside a snow globe, and the meta-mathematician is standing outside of the snow globe looking in. Using the ideas and language of mathematics, the meta-mathematician tries to explain and prove what is going on inside the glass sphere. During the 20th and 21st Centuries, there has been a lot of interest in meta- mathematics. In the 1930's, Kurt Gödel introduced two of the most important theorems in the meta-mathematics, his First and Second Incompleteness Theorems.

These theorems suggest that that it is impossible to prove every aspect of mathematical arithmetic rules within the complete and closed system of mathematics. This was a significant issue because for decades mathematicians had been unable to establish a complete mathematical system where everything could be understood and either proved or disproved within the realm of the system, but many paradoxes were uncovered. One of the best examples of these paradoxes is Russell's Paradox discovered by Bertrand Russell around 1901:

A set S is a normal set if S is not a member of itself. Let N be the set of all normal sets S. Thus S is in N if and only if S is not in S. The trouble starts if we let S = N. Then we have N is in N if and only if N is not in N. Even if we assume there are no non-normal sets, we get in trouble by defining N.

By illuminating these limitations Gödel freed mathematicians from previous constraints to look beyond the established boundaries of the subject matter.

Alan Turing took these theorems of incompleteness and the impossibility of the idea of systemic provability and elaborated on the topic by introducing computability and un-computability. His Turing Machine is a theoretical computer that can execute algorithms. Turing was able take the innovations of meta-mathematics and apply them to algorithms in the introduction of his theoretical Turing Machine. This machine consists of a set of instructions that is a formal representation of an algorithm, a "head", that executes these instructions and produces output and an endless tape that receives the output produced by the head.

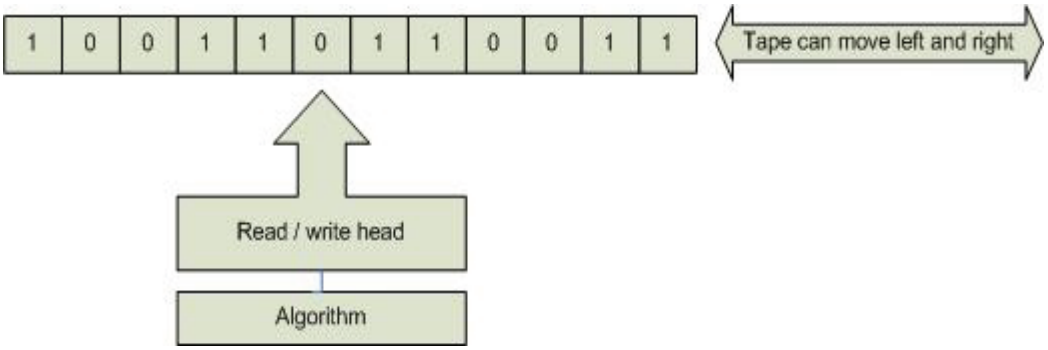

Figure 1 - *Turing Machine schematic*

The first reference for the use of the term "computer" was as a job title for people who did manual arithmetic calculations to support business, scientific and military applications. The occupation of solving large and complex calculations was the work of human computers. The use of people as computers had been an important part of academia and industry for ages. During WWII groups of people - mostly women - worked together, solving huge arithmetic computations for the government. The problems were broken down and each human computer was given one small part of the calculations to solve. It took many human computer hours to find solutions that take only a few minutes for modern electronic computers. Electronic computers are a more recent development. It was not until 1943 when the Colossus was built in the UK and 1946 when the ENIAC was built in the USA that there were productive large scale electronic computer systems functioning. It is easy to forget that modern computers are fundamentally using the same processes as the people employed as human computers, taking a complicated problem and dividing it into separate tasks and executing an order of operation with specific steps reflecting the structure of the algorithm to reach a final outcome. Both types of computers are using mathematical algorithms.

Now that I have examined some of the basic ideas of Meta-Mathematics and algorithms, I will show how conceptual artist Hanne Darboven used algorithms in her art. Darboven's work *Konstruktion* was developed around 1968. It involved the mathematical process of adding the numbers of a specific date and denoting the operation with the letter "K". She then hand wrote lists of these derived equations on multiple pages. Darboven used dates in the European format (day/month/year). The digits of the year were taken separately, but the day and month were used as a whole:

$$29/12/96 = 29+12+9+6=56K$$ [5]

The output is created by taking the date as input and transforming it into an output as the one above through a series of arithmetical and text operations. It must be noted however that Hanne Darboven did not consider her work mathematical. In 1973 she was quoted by Lucy Lippard in *ArtForum*:

> "I only use numbers because it is a way of writing without describing…. It has nothing to do with mathematics. Nothing. I choose numbers because they are so constant. Confined and artistic. Numbers are probably the only real discovery of mankind."[6]

Despite her disclaimer it might be appropriate to refer to Hanne Darboven's work as meta-mathematical. She is definitely using an algorithm to make the decision of what to write and she is using the mathematical tool of addition, creating an arithmetic algorithmic process. Using her predetermined rule all computations are decided before she starts to write her equations. She

takes her input, the numerical date and proceeds to do an ordered set of operations on that data and then she writes the process down in digits and mathematical symbols. Her process looks a lot like an implementation of the Turing Machine. Each date has a terminating set of operations performed on it, then the result is written down, because a list of dates is ultimately never ending (each day there is more input) this output or tape of script has the possibility of going on forever. In *Konstruktion* Hanna Darboven created an aesthetic experience that explores the possibilities infinitely. She is using an algorithmic process to discover the beauty of a mathematical idea by working from outside the system of mathematics, which to me seems to fit comfortably into the definition of Meta-mathematics.

My own work has been influenced by early conceptual art. The use of an algorithm to generate art is my link between mathematics and drawing. Each drawing is initiated by making a scaled sketch of the grid in a large bound drawing pad, which I refer to as my plan book. All of the mathematical decisions for each drawing are worked out in this plan book. I use concepts such as sequences, series, and fractals to generate my work. When the plan is complete and to my satisfaction, I execute the plan and create the corresponding drawing. There is a clear parallel between my drawing process and Charles Babbage's un-built Analytical Engine. The Analytical Engine consists of input, storage, mill and output:

> "A key feature was the separation of the store, which held the numbers during computation and the mill, which performed the arithmetic operations. The input and output were encoded on punch cards, as was the control device which controlled the program." [7]

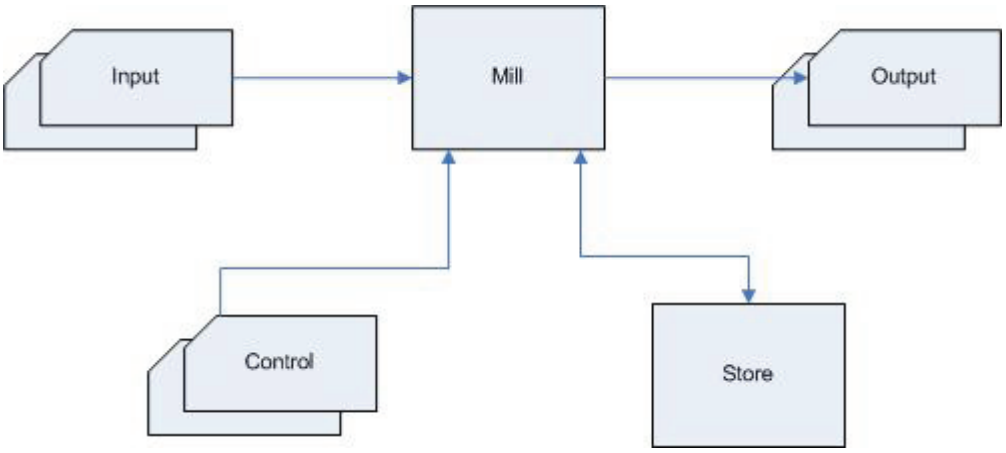

Figure 2 - *Babbage Analytical Engine schematic*

Using this model, mathematical sequences and series are my input; my plan book is my storage and control, and my hand holding the pen is the mill generating the output or the finished drawings. I select the rules, I make the plan, and then I become the machine that produces the image.

I use algorithmic processes to generate my drawings, but it is important to note that the subject matter of my work is also mathematical. It is my personal belief that there is an aesthetic component to mathematics. The grace and beauty I find in mathematics is expressed through my art. I draw inspiration from numerous mathematical sources. The drawing *Fibonacci Columns* is based on the Fibonacci sequence. This sequence starts with the numbers 1,1. Then each consecutive member of the sequence is defined by the sum of the two previous members. The first ten terms are: 1, 1, 2, 3, 5, 8, 13, 21, 34, 55... It was developed in the 13th century by the

Italian mathematician Leonardo of Pisa (Fibonacci). The actual drawing plane is divided into a grid. It is the number of marks within each square of the underlying grid that holds significance, the placement of those marks within a single cell is unplanned and not as important to me as the number of marks. When making a drawing based on the Fibonacci Sequence, the first decisions I make have to do with the number of columns on a sheet, and the ratio between the width and the height of each column. For *Fibonacci Columns* (2005) I decided to make 5 (a Fibonacci number) identical columns. Each column will have a 1 to 5 width/height ratio. Then I planned out exactly how many marks will be drawn into each grid space. In *Fibonacci Columns*, the top grid spaces of each column are occupied by one stroke, as I continue down the columns the number of strokes in each cell increases to 2, then 3, 5, 8, 13, 21 and 34, then decreasing back to 21, 13, 8, 5, 3, 2, and 1 at the bottom of the column. All of these numbers are consecutive elements of the Fibonacci sequence.

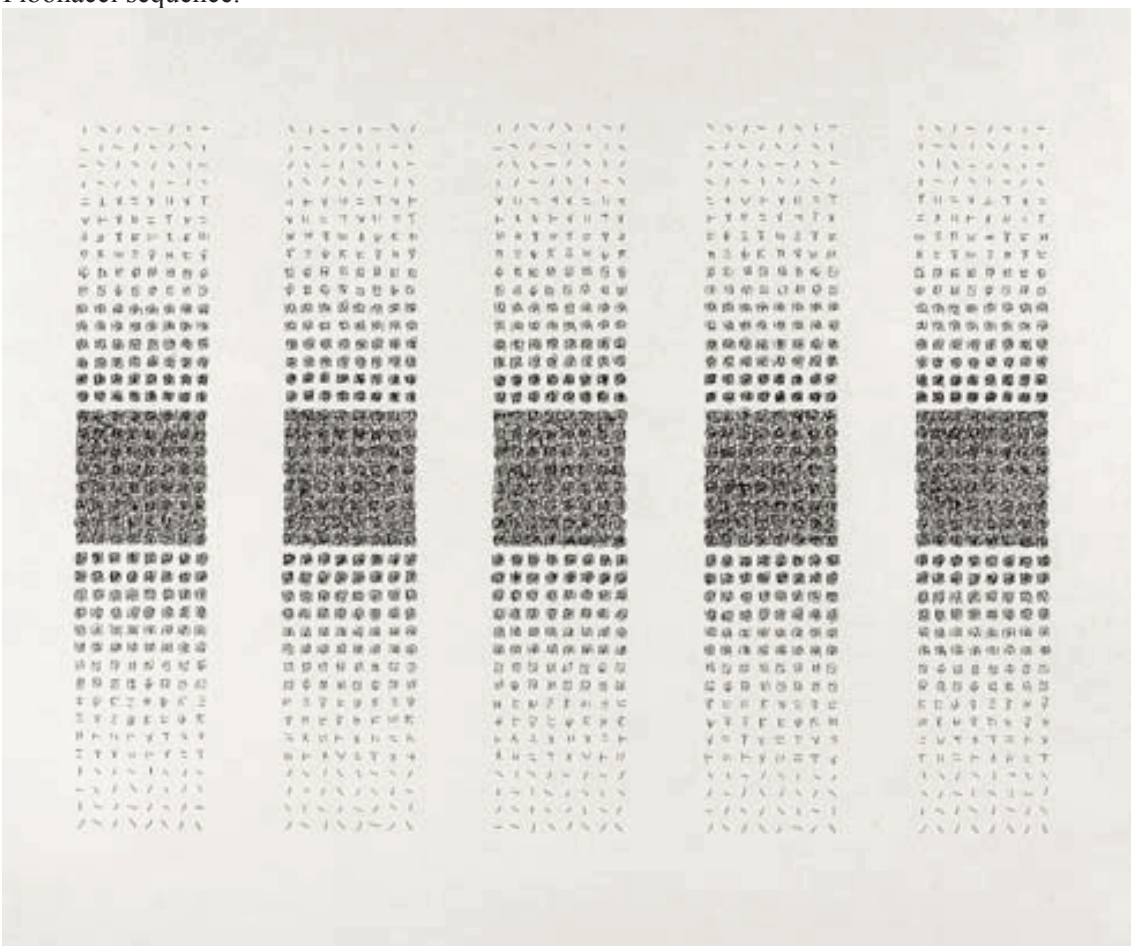

Figure 3 - *Fibonacci Columns (2005)*

Of course neither Hanna Darboven nor I are actual machines or computers. This means there is a very human element in the selection of rules and in these three examples the actual drawing is carried out by a human so there will be variations in the actual mark making. When a drawing is produced by hand, there will never be the possibility of perfect (monotonous) lines of a computer generated line drawing. But, just like the initial idea, the decision on how a conceptual work will be carried to completion is also an aesthetic decision. Is it a significant factor whether a machine or a human actually produces the final product? Are the variations created by the hand of the artist or draftsperson a positive element, or is it only a distraction in the quest for a purely conceptual art form? These questions lead us to an even more contentious question, when does an

algorithmically defined set of steps or rules generate a successful work of art? If the concept is interesting, is that enough to consider the art interesting regardless of what the final product looks like?

In an attempt to grapple with these issues about conceptual art and aesthetics, I will first discuss aesthetics away from contemporary theory and in a more historical context. I will look at Kant's "*Critique of Judgement Part I*" and try to explore how Kant would possibly answer questions about conceptual art and aesthetics.

Kant describes judgment of taste as aesthetic and subjective, not determined by cognitive understanding or logic but instead through the imagination. So the judgment of taste is based on feelings of pleasure (and displeasure, but Kant does not write much about that). This pleasure is independent of what Kant refers to as interest. This disinterest does not allow for experiencing direct sensual pleasure from the actual object, nor does it allow for the reliance on concepts for aesthetic judgment. The interest in the object would render the aesthetic experience merely agreeable or good but not beautiful. Therefore this particular pleasure does not involve desire for the actual object, but instead the delight comes from the viewer's feelings about a work of art when it is perceived through the viewer's imagination.

The premise of my own art making practice is that there are aspects of mathematics that are intrinsically beautiful. If they are expressed through an artistic sensibility, everyone should be able to see these aesthetic values of grace, balance, repetition, symmetry and the possibility of the infinite, regardless of their understanding of the actual mathematics on which the art is based. Therefore in some ways I find myself agreeing with Kant in that it is not always necessary to understand the initial concept to appreciate the final product. If we just consider the completed work of conceptual art this is not too far out of line; we can imagine how the subject could immediately see beauty without being aware of the concept. Someone looking at Hanne Darboven's *Konstruktion* could find the rhythmic repetitive nature of her handwritten numbers visually striking without knowing the algorithm she used to generate the work.

We must remember however, that it is the initial concept that drives every step of the creation of work of conceptual art so it is almost impossible to divorce the initial set of rules from the final product. This aesthetic reflective judgment according to Kant must also be universally communicable: if an object is judged to be beautiful then everyone should given the right circumstances be able to find it beautiful. In Kant's opinion judgment of taste is contemplative but is not based on the concepts, because it is subjective and not a purely cognitive judgment, therefore the actual concept used by the artist is not a permissible influence when judging the aesthetic value of the art. If an artist is able to create a set of rules using a defined decision making process carrying out those rules in a step by step manner to create a work of art and then allow the aesthetic judgment of his or her art be based on only the final product of this process, then Kantian aesthetics can be accepted at face value.

Although I feel that the final product that is presented to the subject or viewer does have the responsibility to provide the subject with the aesthetic experience similar to that described by Kant, I think it is too narrow-minded to expect the concept to lose all of its significance. Likewise, just because the initial concept seems to be of great aesthetic value, if the final product does not stir any interest or emotion in the viewer, then it is difficult to call the work of art a success. For Kant regardless of how wonderful the generating concept may be, the only thing that matters is how the subject reacts to the final product. The method of production would not matter as long as art possesses universality in its aesthetic value.

I still question if the subject needs to understand the algorithm to appreciate the product. I think that a very complex idea that is understood by a small section of the population can be used as the initial concept that through a set of generative steps can produce a work of art that has aesthetic value for the population as a whole. The concept must have merit but there is that extra human element that creates a successful work. I believe that Kant's philosophy comes closer to accepting this premise.

Kant does not allow for the concept of the object in aesthetic judgments because these judgments are subjective and concepts can require the there to exist a purpose or an end. Do all algorithmically generated works of art have a definite purpose? Due to the nature of an algorithm, each set of actions on a singular input has a defined end. If we can see the completion of this order of operation as the purpose of art then in an abstract way every conceptual work of art does have an end.

Returning back to the early parameters of conceptual art: In
Sol Lewitt's 1969 *Sentences on Conceptual Art*, sentence 9 states:

> "The concept and the idea are different. The former implies a general direction while the latter are the component. Ideas implement the concept." [8]

By delineating between the generating concept and the ideas being expressed in the final product, this sentence leaves more room for interpreting conceptual art in terms of Kantian aesthetics. The sphere of algorithmic generation can be considered on its own aesthetic merits. We can take a broader look at the more general idea of algorithmic processes from outside the specific topic or idea that is being used to generate the art. This is a similar situation to the meta-mathematicians looking at mathematics from outside the snow globe. Examining these sets of rules and steps that create intricate and at times endlessly repetitive iterations, the viewer can become overwhelmed by the infinite possibilities of these processes. Kant discusses the topic of being able to even think about something in terms of being infinite:

> "Still the mere ability even to think the given infinite without contradiction, is something that requires the presence in the human mind of a faculty that is itself supersensible." [9]

Kant's examination of humans' ability to consider the possibility of infinity opens up the whole realm of aesthetic judgments of the sublime. In order to be considered "sublime", an object or concept must possess awe-inspiring greatness and a sense of spiritual value. According to Kant, unlike the pleasure felt by the viewer when reflecting on a beautiful object, the pleasure from the sublime is indirect and is the result of a more chaotic formless object. In fact, it is not the object itself that is sublime, but it is the subject's thoughts on the object. There is a negative element to the pleasure experienced with the sublime, a sense of awe or even being momentary overwhelmed. Judgment of the sublime has cognitive elements, it requires imagination and knowledge. Kant states:

> "The beautiful in nature is a question of the form of the object, and this consists in limitations, whereas the sublime is to be found in an object even devoid of form, so far as it immediately involves, or else by its presence provokes a representation of limitlessness yet with a superadded thought of its totality" [10]

Using Kant's interpretation of how a viewer experiences the sublime, we can see how the capabilities to create processes that appear to have infinite permutations, afforded to us by algorithmic generation, can fall under the category of the sublime. The viewer struck by the

immenseness of the number of possibilities created using these systems of operations can appreciate the aesthetic qualities of the power of algorithms.

When I discuss comparing conceptual art to "mathematical algorithm" I refer to comparing the underlying processes, that is, the use of predetermined steps that are executed step by step, free from external influences that could alter the final product. I am not comparing the subject matter: the ideas being expressed in the art work may or may not be a discourse on mathematical algorithm. The effort that the artist makes to provide the rules and information to enable the works to progress without any other decision being made by the human or electronic machine is proof that algorithmic planning is an influence on their art. They are taking mathematical algorithms and giving them aesthetic expression in the context of conceptual art.

There are many similarities between the definitions and implementation of conceptual art and algorithm. Both require upfront planning and design of an unambiguous plan. Both consist of an ordered set of operations that can be performed by anyone or anything that is capable or competent of understanding and executing these operations. Finally, both are repeatable and can be performed as many times as required.

We can better understand how these similarities may have developed when we examine the social context of the media and technology of the 1960's. The 1965 *Computer and Society* issue of *Time* magazine is a perfect illustration of how people were fascinated and anxious about the new computer age and how it would affect their everyday lives. Were computers to become the masters to the human workforce where people are there to serve the computer and act on the output from those endless rolls of paper? Of course in reality it was the humans deciding on the rules and the computer was just the vehicle or tool to process the set of instructions. The computer and its process of input, set of steps, then output were a topic that people were aware of and reacting to. Although electronic computers were invented in the 1940's it was not until the mid 1960's that they were being encountered by a significant segment of the population in the workplace. Computer programming, which relied heavily on mathematical algorithms, was a new career. When the early conceptual artists were defining their new art form they chose a type of generating process that was very similar to the algorithmic procedures of computer science. Although it was not necessarily a conscious decision, the work of conceptual artists in the 1960's had a close relationship with the mathematically defined algorithms that were at the forefront of both mathematics and computer science at that time. These conceptual artists and their successors use algorithmic processes based on the generating procedures of early computer science to create their art. In other words, the design and execution of an algorithm is the core process of the conceptual artist. By using algorithms as the defining foundation of their creative process, these artists have created work that aethetisized the essence of the algorithm.

It has been forty years since Sol Lewitt wrote his Sentences and Paragraphs on Conceptual Art and a cartoon of an out-of-control computer graced the cover of a popular magazine, but artists, like me, that have been influenced by the early paradigms of conceptual art continue to use these types of algorithmic processes to generate our work.

Fish Tiling Animation: An Eye Candy Project

Robert F. Kauffmann
2401 Arden Road
Cinnaminson, NJ, 08077, USA
E-mail: mathart63@gmail.com

Abstract

A small number of artist/geometers in recent years have begun to experiment with the animation of Escher-like tilings of motifs in a plane. Under their inspiration, I have created an animated film which weaves together a collection of animated tilings entitled “Eye Candy.” This paper describes the methodology employed in the construction of one of the animated tilings that has been incorporated into the “Eye Candy” project.

Influences and Inspirations

M.C. Escher. Over the space of approximately 25 years, I have composed a number of designs based on tessellations that followed on Escher's work using iconic motifs to tile the picture plane. These works have been shown in venues in New York City and other major cities as well as being widely published electronically and in print. The examples that follow give a flavor for the work I have done in artistic tessellation previous to taking up the art of animation.

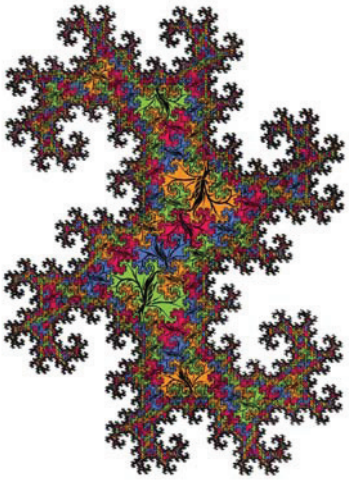

***Figure 1**: Dragon Limit I (20" x 16") handcolored serigraph.*

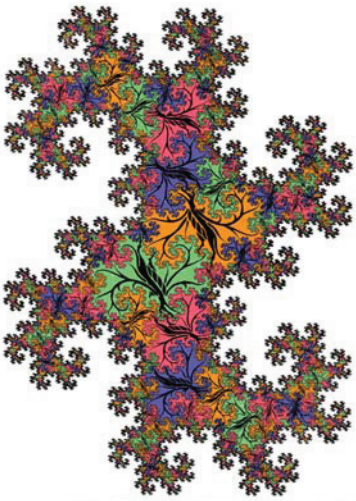

***Figure 2**: Dragon Limit III (16" x 20") handcolored serigraph*

The Dragon Limit series takes Escher's idea of approaching limits to infinity and generalizes it to include the tiling of fractal figures which approach a bounding limit which is also fractal. The fractal in this case is based on constructions by Mandelbrot of a figure called a "Twin Dragon" which he showed

could be subdivided in order to tile a plane. The *Dragon Limit* series consists of four variations arising from two different coloring schemes and two different methods of dividing the space.

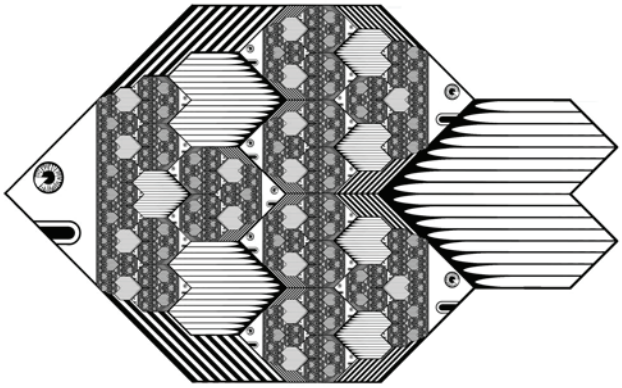

Figure 3: *Bifurcating Fish (6" x 9") serigraph*

Figure 4: *Pear Tree (18" x 12") serigraph*

Bifurcating Fish is named for its structural resemblance to a bifurcation diagram (a complicated fractal diagram used to map the behavior of certain nonlinear functions.) This design was also inspired by Escher's *Fish and Scales* [4].

Pear Tree is an exercise in transformation between negative and positive space, the branches of a tree morph into the negative space around pears growing from the negative space between the branches.

Some Tessellation Designs Created for the "Eye Candy" Film. These tessellations were developed specifically with the intent to animate them. "Eye Candy" is the latest in many animated films I have produced. Since "Eye Candy" brings together both the art of animation and the art of tessellation, it really stands as a synthesis of my life's artistic work.

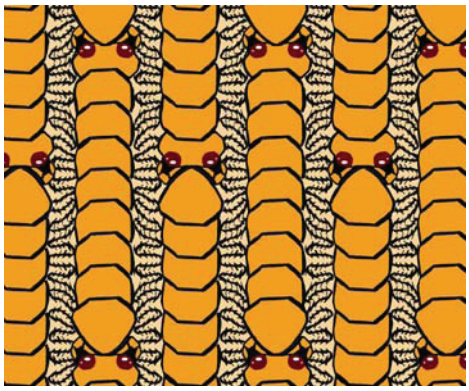

Figure 5: *Centipedes*

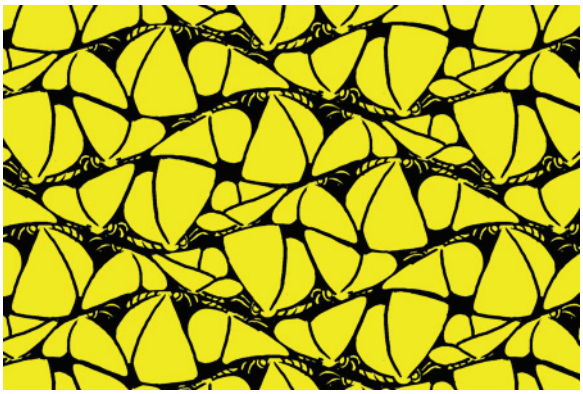

Figure 6: *Butterflies*

Figure 7: *Jamming Amoebas*

Figure 8: *Ocean Depth*

The illustration entitled *Ocean Depth* is a product of the Fish Tile Animation in four layers. This is the manner in which the animation was employed in the final film. This paper will concentrate upon the single layer animation of the fish motif.

Moser. Koloman Moser's *Trout Dance* was the work which most directly inspired the design of the Fish Tiling Animation. According to Andrew Crompton, this work was the first Escher-like tessellation (using iconic motifs, that is) ever to be published, having appeared in the magazine 'Ver Sacrum' in Vienna, in 1901--almost twenty years before Escher began his career. Crompton further observes that a number of other designs very similar to Escher's were in circulation during that era. [1]

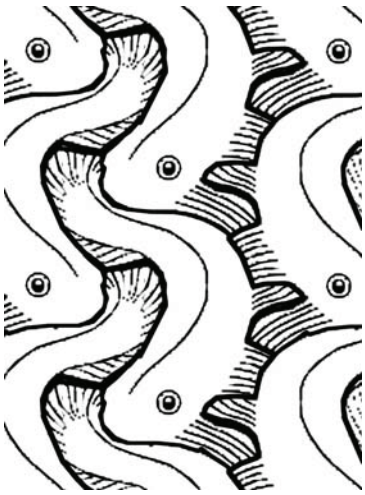

Figure 9: *Detail of Troutdance by Kolomon Moser*

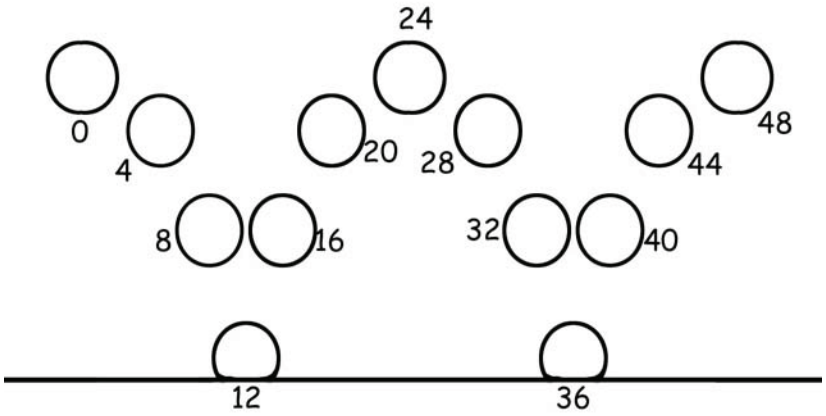

Figure 10: *Bouncing ball sequence: keyframes*

Tessellation Animators. There are a few animators in the world who have successfully produced tessellations that could be animated as cycles. The ones of which I am aware were an inspiration to me to try my own hand at integrating the art of tessellation with the craft of animation. These are Makato Nakamura, a Japanese artist whose work follows closely from Escher, Patrick Snels, a Dutch artist, and Andrew Crompton a professor of Architecture at the University of Manchester, England. Their animated tilings may be found at their websites given at the end of this paper. [1],[2],[3]

Animation

Background in Animation. Since 1990, I have been producing animated films as an independent filmmaker. Four of these films, "Animated Shorts" (1995), "The Mask of Ollock" (1999), "Food Chain Inversion" (2004), and "Song of the Moon" (2006) have garnered numerous awards and been screened in various film festivals nationwide. "Eye Candy" was completed in March, 2009, and is the latest addition to my body of work.

Some Animation Basics. At its heart, animation is the art of designing elements and their motion through space and time in frame-by-frame increments.

Keyframes. Motion of an element is first blocked out in coarsely-grained time increments—usually every fourth to tenth frame or so. The bouncing ball sequence in figure 10 has been keyframed to every fourth frame.

In-betweening. Once the overall motion of an element has been mapped out in keyframes, the in-between frames can easily be inserted. Little in the way of design decision-making goes into the construction of in-between frames. As such, traditional animation shops have historically assigned this task to inexperienced animators.[5] Figure 11 shows the bouncing ball sequence with the missing frames inserted. If this sequence is shot on 1's (1 video frame to an animation frame) the whole sequence will go by in little over one second in standard video format.

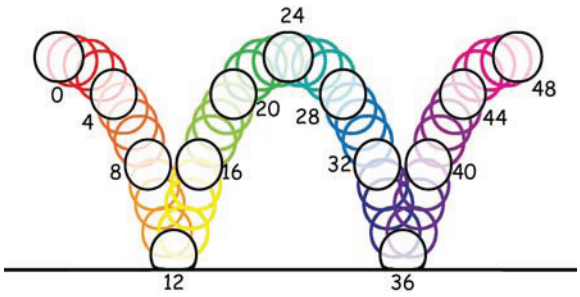

Figure 11: *Bouncing ball sequence: in-betweens*

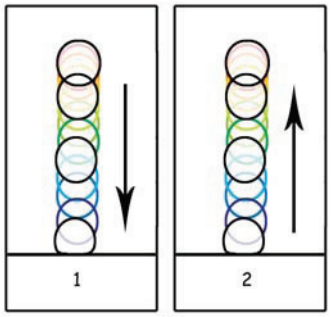

Figure 12: *Bouncing Ball Cycle*

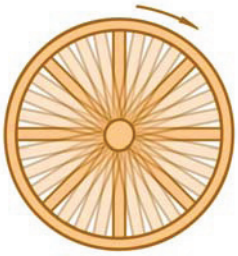

Figure 13: *Cartwheel Cycle*

Cycles. Animation is costly in terms of effort, typically requiring 10 drawings per second of video footage (shooting on 3's.) One way in which time may be filled cheaply is through the use of repeating sequences.[5] There are a number of ways in which a repeating sequence might be created; some of these are demonstrated below.

The sequence in Figure 12 shows a loop which is created using a reversible sequence. The bouncing balls downward fall can be shown in rewind, creating the illusion of a ball bouncing up and down in place. Circular motion may be exploited to create a loop as with the rotating cartwheel in Figure 13.

Note that the eightfold rotational symmetry can be further exploited to cut the number of frames required for a loop from 32 down to four.

The translational symmetry in a tiling can be put in the service of creating an animated loop. Figure 14 shows the near-tiling of bus motifs which can be animated by simply sliding the entire tiled plane a little to the right with each successive frame. This technique is one which is employed in the making of the Fish Tile Animation which is the subject of this paper

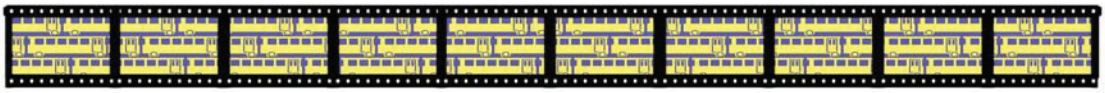

Figure 14: *Tiling Cycle*

The Fish Tile Animation

The Fish Tile Design. The Fish Tile design was developed on graph paper using layers of sine waves as both a grid and a path of movement. Figure 15 shows the completed Fish Tile design that was ultimately scanned and used to build the animation frames. The sine waves have a period of 24 units on the grid, necessitating 24 different fish to be drawn to cover one period when the frame-by-frame motion is advanced by one grid-unit per frame. The scanned-in design of Figure 15 contains all 24 fish motifs arranged on the picture plane. This one image contains all the artwork needed to produce the nearly two-minute (~2000 frame) animated sequence.

The fish motifs in the Fish Tile design, as scanned in Figure 15, are numbered from 0-23. The numbering scheme makes the progression of the animation apparent, but the fin-like elements between the fishes' bodies cannot be identified with individuals. This problem is solved by shuffling the columns of the fish in such a way as to stagger the individual fish as seen in Figure 16. The similarity of this design (Figure 16) to Moser's *Trout Dance* (Figure 10), is strikingly apparent, but this design is more amenable to animation than Moser's.

The In-betweens. The keyframes of the animated sequence can effectively be seen all in one sheet of a still such as with Figure 16, where each fish connects nose-to-tail, such that the preceding fish serves as the next keyframe. This is because the physical periodicity of the image lines up with the temporal periodicity of the animated cycle.

Note that because the interlocking fish motifs are only 18 units in length, the fish animation needs only 18 frames to complete a cycle. This can be seen in Figure 17 which shows the in-betweens from the nose of the fish. The fish motif in the adjacent path shows what the final frame of the sequence will look like 18 frames later. The choice of an 18-frame cycle used in the animation was an accident of the grid chosen for the initial layout—a choice that proved to be serviceable, if not optimal.

Tiling the In-betweens. Had a 24 frame cycle been chosen, the construction of the cycle's progression would have been simplified in that the arrangement of 24 fish motifs seen in Figure 15 could have been rearranged in a straightforward manner to create the same effect as in Figure 16 (which uses but 8 of the possible 24 motifs). The animation would have then been achieved by choosing a point of reference

from which to place fish 0 in the picture frame, then subsequent animation frames would consist of sliding over the entire tiling so that fish 1 matches the grid where fish 0 was, then fish 2, etc.

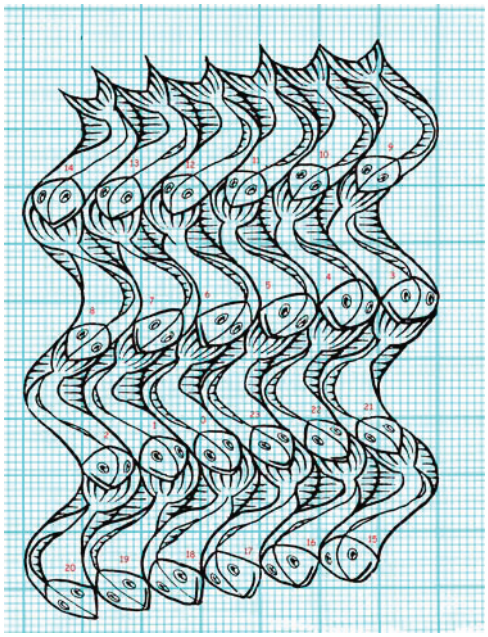

Figure 15: *Fish Tile, original*

Figure 16: *Fish Tile, modified*

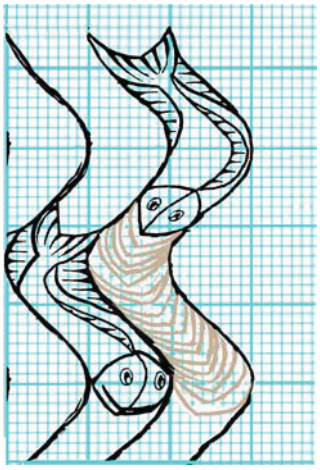

Figure 17: *Timing Diagram for Fish Tiling In-betweens*

14	13	12	11	10	9
8	7	6	5	4	3
2	1	0	23	22	21
20	19	18	17	16	15

Table 1*: motif arrangement of Figure 15*

Since the 18 unit periodicity of the required animation cycle falls short of the 24 unit periodicity of the sinusoidal path, some peculiarities are introduced. It is necessary to divide the six columns of four fish motifs into three sequential sets of double pairings. The original arrangement in Figure 15 looks like in Table 1. The three new sequence pairings are shown in Tables 2-4.

6 21 12 3 18 9 0 15	7 22 13 4 19 10 1 16	8 23 14 5 20 11 2 17	18 9 18 0 15 0 6 21 6 12 3 12 18 9 18 0 15 0
Table 2: *Frame 0 pairing*	**Table 3:** *Frame 1 pairing*	**Table 4:** *Frame 2 pairing*	***Table 5:*** *Frame 3 translation from Frame 0*

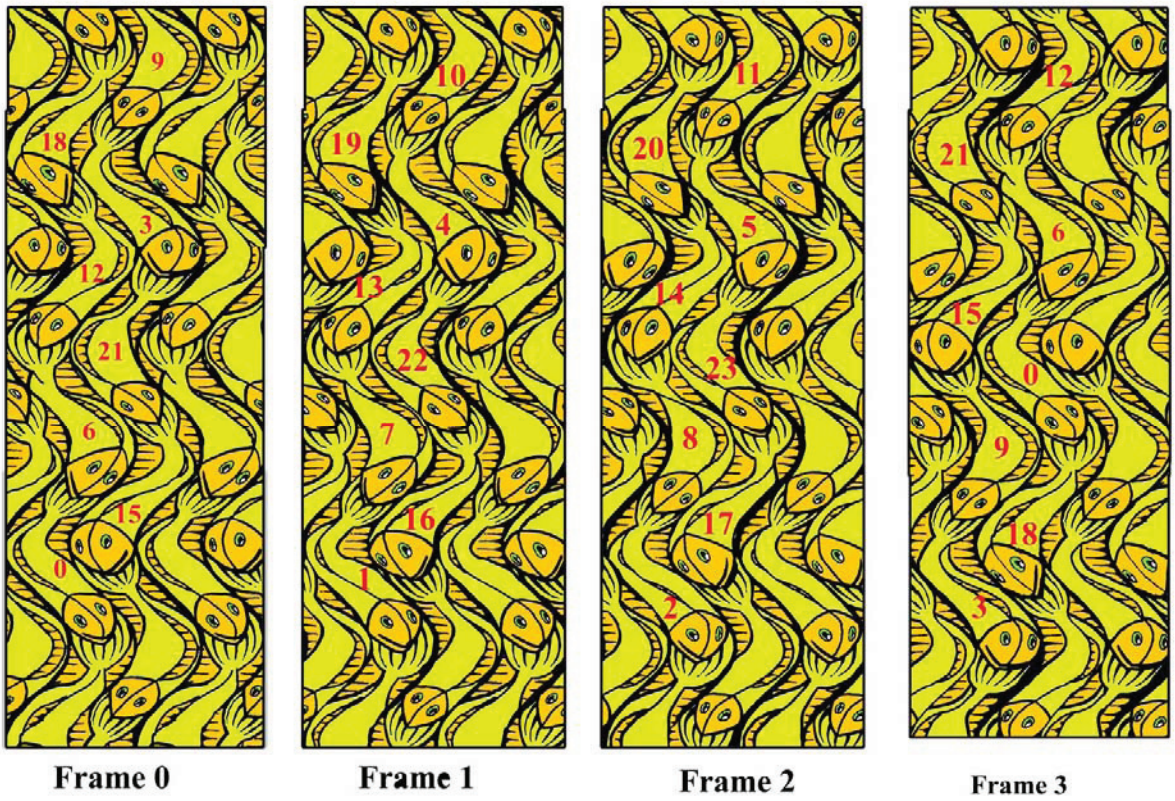

Figure 18: *Frames 0-3 with sequence pairings*

These sequences are illustrated together in Figure 18. Each patch of fish motifs is able to tile a plane completely, so a translation of the entire plane as mentioned in the previous paragraph is possible. The sequences above, from their numbering scheme, can plainly be seen to increment by one for each corresponding cell, and therefore represent a workable step-by-step animation scheme for the tiling grid. The point of registration is the lower left corner, which fish 0 occupies in Frame 0, fish 1 in Frame 1, etc.

Frames subsequent to frame 2 build on these three pairings (Tables 2-4) by shifting the entire tiling to register the fish motif to the chosen frame of reference. Frame 3 is a translation of the arrangement in Table 2 so that fish 3 occupies the place where fish 0 was. This can be seen in Table 5. Frame 3 is also pictured in Figure 18.

Figure 19: *Still from the Fish Tile Animation*

The Fish Tile Cycle. In the final version of the Fish Tile Animation, the tiling has been rotated to a 45 degree angle counterclockwise from the illustrations shown above, as shown in Figure 19. Subsequent layers beneath the top layer alternate between a 4 o'clock direction and an eight o'clock direction as seen in Figure 8.

References

[1] Andrew Crompton. *Grotesque Geometry,* University of Manchester, England, http://www.cromp.com/tess/home.html.
[2] Makato Nakamura. *Tessellation World of Makato Nakamura,* http://www.k4.dion.ne.jp/%7Emnaka/animation.html
[3] Patrick Snels. *Tessellation Database,* Patrick Snels, http://www.tessellation.info/?open=general/artistinfo.php&lang=english&style=layout&people_ID=1
[4] Robert F. Kauffmann *The Mathematical Surrealism of Robert Kauffmann, Proceedings of ISAMA'07* http://www.isama.org/hyperseeing/
[5] Susan Rubin. *Animation, The Art and the Industry,* 1984, Prentice-Hall Inc.

From *Sona* Drawings to Contemporary Art

Yang Liu
Artist
Montreal, QC, Canada
yangliu1971@gmail.com

1. Introduction

My paintings are inspired by the *sona* drawing tradition of Angola [1], as well as the *kolam* art of South India [2, 3, 5, 6], and the *sand-drawing* tradition of Vanuatu in the South Pacific [7]. This type of art typically starts by drawing a set of points, and then constructing one single curve that meanders around the points and ends where it started. Furthermore, when this process is finished, ideally each enclosed region contains exactly one point. Sometimes a region contains more than one point, sometimes a region is empty, and sometimes more than one curve is used. However, the most desirable drawings consist of a single curve, and must be drawn without ever lifting the drawing implement, and without retracing parts of the drawing already made. Hence this artwork is very geometric in nature, and for any given set of points it can be quite difficult to obtain a sona drawing that respects additional aesthetic constraints. For this reason some researchers are interested in designing algorithms that allow a computer to render the drawings as an aid to artists. Some complicated algorithms for creating sona drawings from a set of points are given in [5] and [6]. A very simple algorithm that I use in my work is given in [4]. In my contemporary artwork I incorporate sona drawings as seeds, but then I break the rules to one degree or another to see where this takes me.

The painting shown in Figure 1, entitled "*Love*" (acrylic on canvas) uses a traditional sona drawing on eight points, that signifies a man and a woman [1]. I use it as a motif to compose the Chinese character that means 'love'. The motif may be clearly seen in the upper right on the dark background. I am interested in the multicultural aspects of art, and in this piece Chinese and African concepts are brought together in a contemporary setting.

The algorithm proposed in [4] is useful for designing sona drawings that have the topological form of a tree. I became fascinated by the number of possibilities of drawing trees, under strong geometric constraints such as symmetry. In my research on trees I started with a set of points that formed a triangular lattice in the interior of a triangle. Then I searched for sona trees determined by these points that had mirror symmetry about a vertical line through the middle. I found so many different trees, that I was inspired to make the painting titled "*Tree Archive*" (acrylic on canvas) shown in Figure 2. This painting has twelve trees from the collection I found. In this case I removed the points used originally to make the drawings, and I painted their interiors. All the trees except two have symmetry about a vertical line.

Fig. 1: "*Love*" - 2008.

Fig. 2: "*Tree Archive*" - 2008.

The painting in Figure 3 titled "*Twelve*" (acrylic on canvas) contains a sona drawing in the center that signifies a young girl's first period [1]. The original drawing is more circular. I elongated the drawing in the vertical direction, removed the points, and added the two curves on the sides.

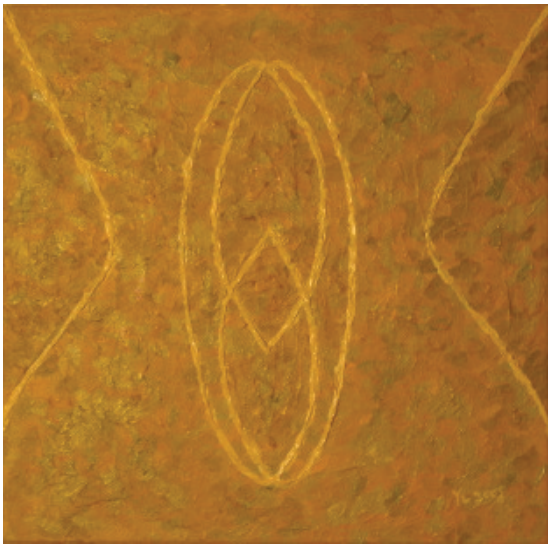

Fig. 3: "*Twelve*" - 2008.

Fig. 4: "*Thinking*" - 2008.

Fig. 5: "*Family*" - 2008.

Figure 4 is called "*Thinking*," (acrylic on canvas). It contains a sona drawing that signifies wisdom and longevity [1]. I greatly elongated the original pattern, removed the points, and added the straight lines at the top and right borders. If one looks carefully one can make out the shape of a man sitting on a rock deep in thought.

The sona drawing in the center of my painting titled "*Family*" (acrylic on canvas) shown in Figure 5, signifies three birds flying [1]. In the original drawing the three birds are all next to each other horizontally. I removed the points, skewed the birds so that they are arranged diagonally, giving a better illusion of flight, and added the remaining lines and curves.

Often, before painting on canvas, I explored ideas using software such as Adobe Illustrator. With the many tools available I could explore quite quickly what effects I could obtain by using texture, and varying other parameters, once I had input the sona drawing. This led me to explore simplicity itself. How could I find a very simple tree-like sona drawing that looked interesting to me? One example of the results of this search is the drawing shown in Figure 6 titled "*Quo Vadis*" (Illustrator). It consists of a single closed curve that varies in texture and thickness. The overall shape is that of a tree, but the topological structure is also a tree. This originally had the points, but I removed them in the interest of simplicity.

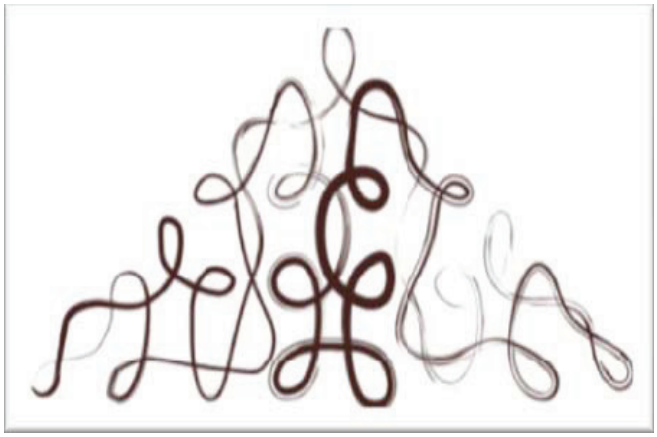

Fig. 6: "*Quo Vadis*" - 2008.

Figure 7: "*Untitled*" - 2008.

Having found an interesting tree pattern such as the one in Figure 6, I was inspired to use it in a broader context. I first tried to use just this one tree in a painting. This resulted in the piece called "*Untitled*" (acrylic on canvas) pictured in Figure 7. Here I was mainly interested in how to balance the curves of the sona drawing with straight lines.

I was also interested in combining a group of such trees to make a more complex compositions. One of the results of this research using the software program Illustrator resulted in the work I called "*Piece of Pottery*" (Illustrator) shown in Figure 8. Here all the trees are rotations and dilatations of the same tree.

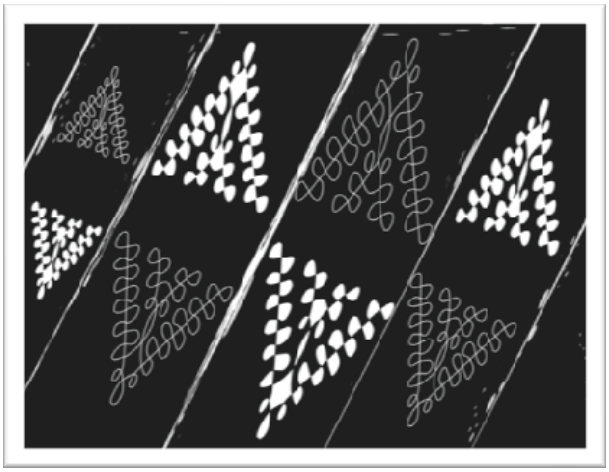

Figure 8: "*Piece of Pottery*" - 2008.

Fig. 9: "*Aquarius*" - 2009.

Although I started my research project using sona drawings as a seed for my inspiration, and wanted to be as faithful as possible to the rules and meanings of the Angolan tradition, eventually I felt the need to break free from these constraints, and yield to some of my flights of fancy. After my first SCUBA dive in Bora-Bora I was enthralled by the underwater life in the lagoon, and inspired to create "*Aquarius*" (acrylic and oil on canvas) shown in Figure 9. Here I still use lines of the sona tradition as well as Chinese calligraphy. However, I am no longer as faithful to the strict geometry that I adhered to earlier.

The last work depicted here, titled "*Mung*" (acrylic and oil on canvas) pictured in Figure 10, shows an even greater degree of freedom from my previous sona constraints. In fact there are no strict sona drawings here at all. The lines drawn are strictly Chinese characters, and my goal here was to explore color and texture more than geometry.

References

1. Gerdes, P., Sona *Geometry from Angola*, Polimetrica, Monza, Italy, 2006.
2. Nagarajan V., "Drawing Down Desires: Women, Ritual and Art in Tamil Nadu," *Forma*, Vol. 22, No. 1, 2007, pp. 127-128.
3. Nagata, S., "Digitalization and Analysis of Traditional Cycle Patterns in the World, and Their Contemporary Applications," *Forma*. Vol. 22, 2007, pp. 119-126.
4. Liu, Y. and Toussaint, G. T., "A Simple Algorithm for Constructing Perfect Monolinear *Sona* Tree Drawings, and its Application to Visual Art Education," *Conference on Artificial Intelligence, Knowledge Engineering and Data Bases* (AIKED '09), Cambridge University, United Kingdom, February 21-23, 2009.
5. Robinson, T., "Extended Pasting Scheme for Kolam Pattern Generation," *Forma*. Vol. 22, 2007, pp. 55-64.
6. Yanagisawa, K. and Nagata, S., "Fundamental Study on Design System of Kolam Pattern," *Forma*. Vol. 22, 2007, pp. 31-46.
7. Zagala, S., "Vanuatu Sand Drawing," *Museum International*. Vol. 56, No. 1-2, May 2004, pp.

32-35.

Fig. 10: "*Mung*" - 2009.

A New Method for Classifying Fret and Meander Patterns

Yang Liu
Artist
Montreal, Canada
yangliu1971@gmail.com

Godfried Toussaint
School of Computer Science
McGill University, Montreal, Canada
godfried@cs.mcgill.ca

1. Introduction

Figure 1 shows a typical fret pattern used in many cultures since antiquity, for decorating textiles such as clothing, wall hangings and carpets [9], mosaics [4], pottery [3] and architecture [5]. According to Lewis Day [3] it is a fret found frequently on ancient Greek vases. The essential feature of this fret relevant to the discussion in this paper is the *monolinear* (single curve) colored green in Figure 1, that starts on the left end, meanders up and down, and back and forth, until it reaches the right end. Day describes it as a *continuous* fret that *faces* both ways. Frets are usually drawn between two parallel lines that delimit the fret, here shown in yellow. In Amor Fenn's book on pattern design this is fret pattern No. 67, which he labels as a Chinese fret.

Fig. 1: Typical monolinear simple meander fret design [11].

Fig. 2: Simple meander fret from a Rhodes amphora on display in the Louvre Museum.

Another example of a continuous monolinear fret is shown in the photograph in Figure 2. This one comes from an amphora discovered in Rhodes dating back to 610 B.C., on display in the Louvre Museum in Paris. This fret is distinctly different from that shown in Figure 1. The latter exhibits no *chirality* (handedness); if we traverse it from left to right we travel in the same manner in both clockwise and counterclockwise orientations, in an alternating fashion. On the other hand, the curve in Figure 2 has counter-clockwise chirality. This may be observed in two ways. If we focus on the dark curve, and traverse it from left to right, then whenever we turn in a counterclockwise manner we always progress towards the center of the fret. On the other hand, when we turn in a clockwise direction we always progress towards the outside of the fret. Another way to see this is by examining the light colored background instead. All the **L**-shaped pieces making up the background start on the outsides and turn only counterclockwise. Thus, Lewis Day would say this fret does not face both ways. Both examples shown in Figures 1 and 2 belong to the class that Dunbabin calls *simple meanders* [4]. There exist many fret patterns belonging to a different class called *discontinuous* (also *broken)*, such as the fret shown in Figure 3. The reason for the name is clear, it consists of many disconnected pieces. This paper is concerned only with continuous frets and meanders.

Fig. 3: A discontinuous broken fret.

Fret patterns are also called *frieze* patterns, particularly in the mathematics literature [1]. When Lewis Day states that the fret faces both ways he is suggesting a feature for classifying frets by alluding to a type of symmetry contained in the pattern. Indeed, traditionally fret patterns have been classified for some time according to which types of symmetries they possess [1, 14]. A rather different Chinese style monolinear continuous fret that does not face both ways is illustrated in Figure 4. The crucial difference between this fret and those of Figures 1 and 2 is that this fret intersects itself at right angles creating crosses or swastikas. In spite of these self-intersections, we still refer to such frets as continuous, as long as one can trace a continuous path or cycle through the crossings. This implies that crossing points should have an even number of incident edges (almost always four).

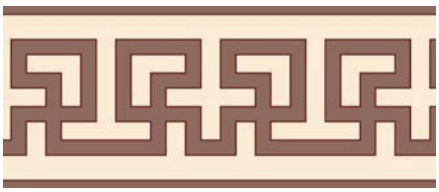

Fig. 4: A monolinear fret that faces only in one direction [11].

Fig. 5: Non-continuous fret found on a floor tile in Moorea, French Polynesia.

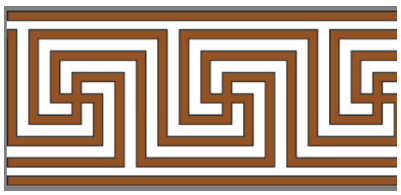

Figure 6: Bilinear Chinese fret.

Many frets are, although connected, not "continuous" for our purpose, that is, they are not determined by a single curve. In other words, they have bifurcations or crossing points that have an odd number of incident edges (usually three). An example of a non-continuous fret pattern of this type found on a floor tile in Moorea, French Polynesia is pictured in Figure 5.

Fig. 7: Bilinear knot meander pattern [2].

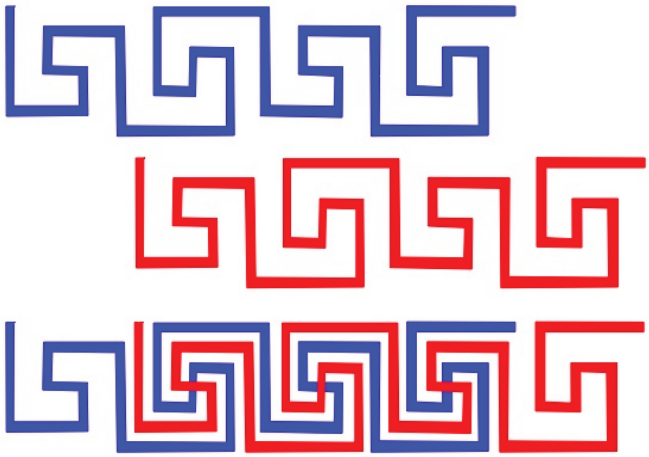

Fig. 8: The two curves that make up the fret pattern in Figure 6 are translations of each other.

In this paper we are concerned with *multilinear* frets and meanders. We use the word *fret* to describe patterns that are essentially one-dimensional, in that they have a clearly preferred direction, and may in principle continue indefinitely, as in the previous examples. They are also used as *borders* of two-dimensional regions. On the other hand, patterns that completely, or almost entirely, fill a two-

dimensional region will be called simply *meander* patterns. Typical in this class are many of the patterns used in Islamic design [12].

Figure 6 gives an example of a multilinear fret [11]. It consists of two monolinear continuous curves superimposed on each other that intersect at the four crosses shown.

Figure 7 shows a two-dimensional meander pattern from a 15th century French artwork, inlaid in wood and ivory, that consists of two continuous curves that almost fill a two-dimensional region [2]. This figure illustrates another characteristic feature of some frets and meander patterns, and this is the three-dimensional *under-over* aspect of the curves, not present in the patterns in the previous figures. This type of meander art is often called *knot-work* because of its resemblance to two-dimensional projections of three-dimensional knots. Note that although the two curves are linked together and cannot be separated without cutting them, they are not really knots in the strict sense of the word. Both can be reconfigured to a topological circle by merely untwisting the small squares on the ends. Therefore they consist of two interlinked *unknots* [13].

Although the patterns in Figures 6 and 7 both consist of two continuous curves, and although they differ in several ways not relevant to the topic of this paper, they do differ in one significant way. While the two curves in Figure 7 may be identical in the knot-theory sense (since they are both unknots), they are clearly very different from each other geometrically. On the other hand, the two infinite curves illustrated in Figure 6 are geometrically identical to each other. Figure 8 shows a deconstruction of the fret pattern of Figure 6 into its fundamental generator curve shown at the top in blue. In the middle is the same curve translated to the right, and at the bottom we see the superposition of the two curves that yield the final fret.

The examples in Figures 6, 7 and 8 illustrate our new method of classifying fret and meander patterns, not in terms of the types of motifs used [15], or the symmetries present in the patterns [14], or whether they contain certain well known geometric patterns such as swastikas [4], but rather, in terms of the number of different continuous curves from which they are constructed, the geometric properties of these curves, and how they are related to each other. For example, are the curves congruent to each other by translation, reflection, rotation, or some other affine transformation? Do they possess chirality? Do they intersect at right angles to each other? If they are knots, what kind of knots are they? If they are linked, what kind of links are they? In the remainder of the paper we illustrate this new approach with a variety of examples from different cultures and historical periods.

2. Bilinear Fret Patterns

The Chinese fret of Figure 6 is a good example of a medium-complexity pattern composed of two continuous identical curves. However, a much simpler example of this class of fret shown in Figure 9 is given by Lewis Day [3]. The fret pattern at the top may be decomposed into two continuous curves (blue and red) that are translations of each other, and that when superimposed on each other, at the bottom, form the original fret pattern. We will call such frets *congruent*, and more specifically in this case, congruent by *translation*.

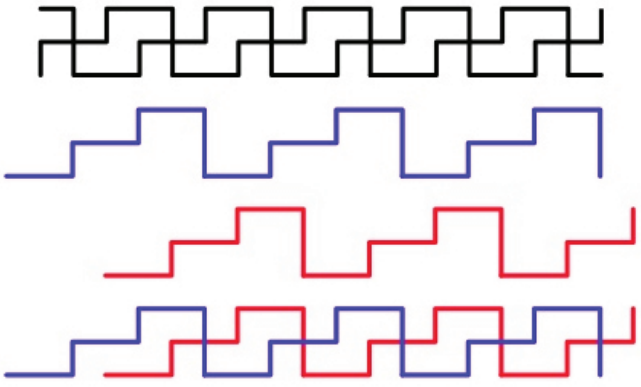

Figure 9: Simple bilinear fret composed of one generator curve.

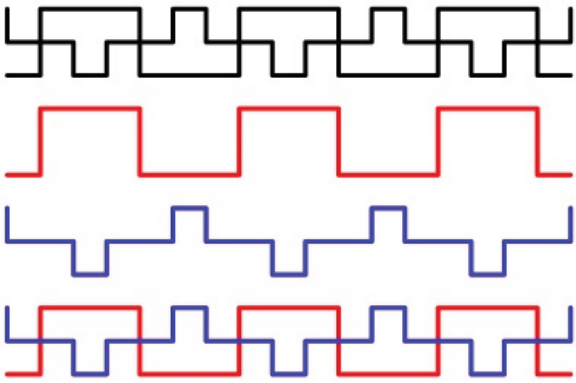

Figure 10: A simple fret composed of two non-congruent continuous curves.

Another very simple bilinear fret contained in Lewis Day's book is shown in Figure 10. As in the previous example, this fret pattern may be decomposed into the two continuous curves (blue and red) shown, such that when superimposed on each other (at the bottom) they form the original fret. However, The blue and red curves in this case are not congruent to each other.

A more complex bilinear Chinese fret pattern found on Ching dynasty carpets, and composed of two continuous curves is illustrated in Figure 11. Here also the two curves (blue and red) are congruent to each other by translation.

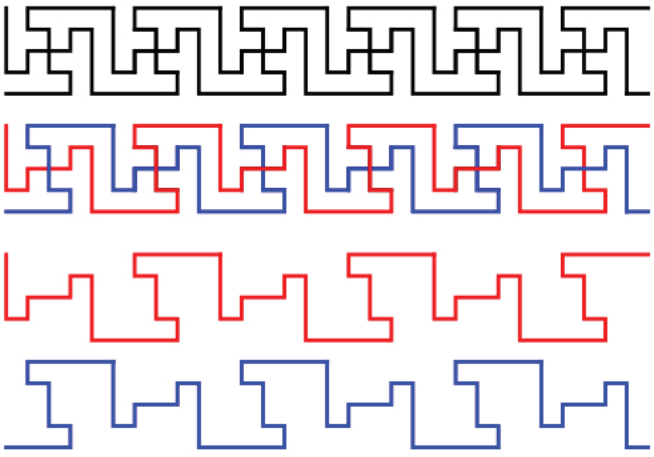

Fig. 11: A more complex congruent bilinear fret found on Ching dynasty carpets.

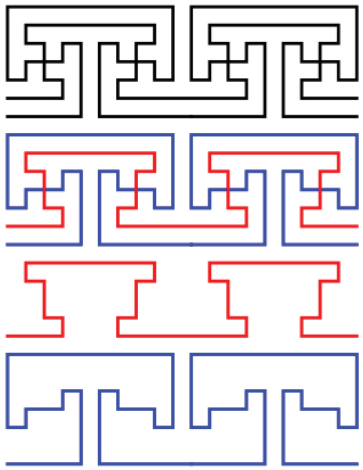

Figure 12: An even more complex fret pattern found on Turkmenistan carpets.

An even more complex bilinear pattern found on Turkmenistan carpets is given in Figure 12. Note that in this example the two curves are very different from each other, and suggest a method to measure the complexity of a fret. There are many ways to measure the complexity of a pattern. One way is by the amount of work (or the number of basic operations) necessary to obtain it by transforming it from the simplest possible pattern [8]. In the present context, a very simple way to measure the complexity of the fret pattern is by the height in units of the smallest segments used.

Thus the height of the frets in Figures 9 and 10 is two, the fret in Figure 11 has height four, and the height of the fret in Figure 12 is six. Since the curves are periodic, another possible way to measure the complexity of a fret is by counting the number of turns contained in one period of each curve.

3. Multilinear Meander Patterns in Roman Mosaics

Multilinear meander patterns (also called polylinear by Paulus Gerdes [6]) that fill either an entire area, or a large portion of the inner or outer boundary of a region were used extensively in Greek and Roman mosaics. In this section we give an example of our method of analysis applied to a Thmuis mosaic signed by the mosaicist Sophilos circa the year 200 B.C., and exhibited in the Graeco-Roman Museum in Alexandria [4]. The pattern may be viewed as a broad border pattern of a two-dimensional area. A reconstruction of the meander pattern surrounding a portrait (not shown here) is pictured in Figure 13. The original meander pattern is shown on the left. Analysis reveals that it consists of three closed continuous meandering curves here colored blue, red, and green for easy visualization, shown on the right. Upon inspection it becomes clear that the red and green curves are congruent to each other by a rotation of 90 degrees. Also, these two curves are not congruent to the blue curve. Therefore the pattern is made up of two non-congruent continuous closed meanders.

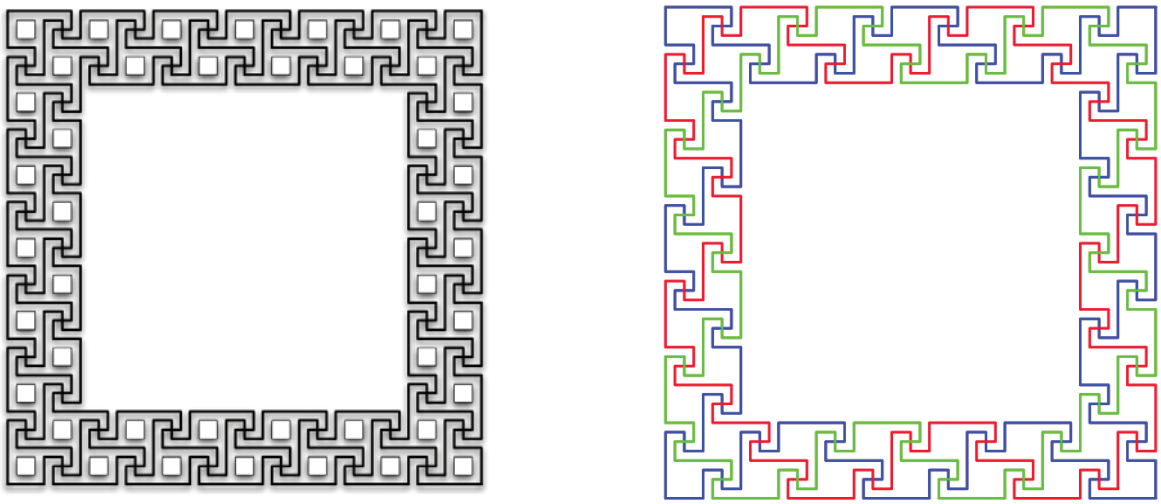

Fig. 13: Meander pattern on a Thmuis mosaic [4].

As already observed in the preceding sections, many meander patterns since antiquity exhibit the property that they form swastikas at their intersections. Indeed, Dunbabin [4] classifies these as *swastika meanders*. Since the swastika is considered to be the oldest symbol used by humans going back some 20,000 years, it has received much attention, particularly before World War II, when Hitler gave the symbol such a bad name [15]. The swastika is also a Chinese character that means ten thousand, pronounced *wan* in Mandarin. In many cultures it symbolizes wellbeing and good luck. In [4] swastika frets and meanders all fall in one category. Our method breaks this class down into many subclasses of swastika frets and meanders. There has been considerable debate in the literature as to whether the frets and meanders that contain swastikas were constructed to connect swastikas together, or whether the swastika pattern was discovered by extracting it from meander patterns such as those discussed here [7, 15].

4. Leonardo da Vinci and Albrecht Durer

Leonardo da Vinci was fascinated by meander patterns formed from knots of interlacing chords, and he produced several drawings of them [2]. It turns out that another famous contemporary painter, Albrecht Durer, was also fascinated with such knots, so much so that he copied Leonardo's drawings. One such drawing is that shown on the left in Figure 15. It consists of four small monolinear drawings in the four corners, and one large circular meander pattern that fills the entire space. The small curves are quite common in many cultural traditions around the world. For example, among the Angolan *sona* drawing tradition this pattern denotes an insect [6]. It is also almost identical to a pattern common in China that denotes eternity, and is pictured in Figure 14.

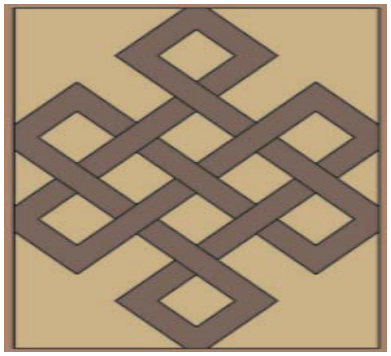

Fig. 14: Chinese symbol for eternity.

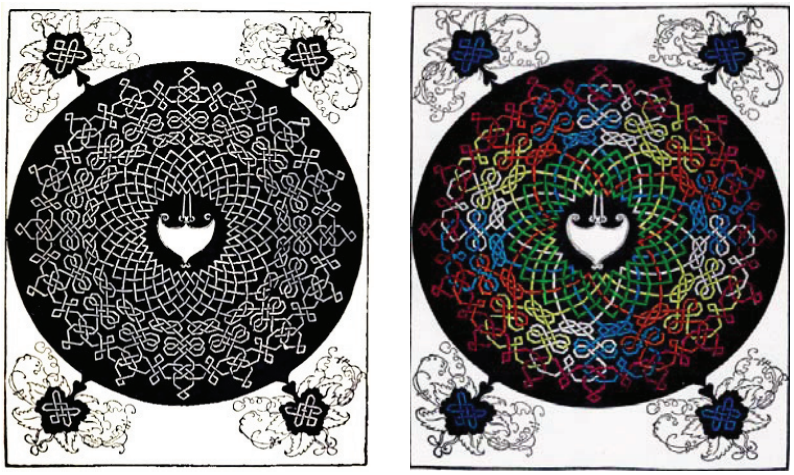

Fig. 15: Hexalinear meander pattern copied by Durer from Leonardo.

The large center pattern in Figure 15 consists of six continuous closed curves. To better see them we have colored them with different colors on the right in Figure 15. The simplest and most obvious curve is the green curve that stays near the center of the drawing. A slightly more complex curve colored red stays close to the outer boundary of the circle. The other four curves are quite complicated, travelling in a circular manner from the outside to the inside and back, four times. They are colored white, yellow, orange, and blue, consecutively in a clockwise manner. Each of these curves is knotted, links with the other knots, and reaches the center of the figure four times yielding 16 vertices. The green curve near the center provides another 16 vertices, for a total of 32 vertices at the center of the figure. Furthermore, these four curves are all congruent to each other by rotation. Therefore the centerpiece consists of *three* non-congruent curves.

5. Unbounded Number of Curves

In this section we give two examples to illustrate a category of frets that uses a combination of a fixed number of continuous main curves with an additional unbounded number of small curves. The term unbounded here refers to the fact that as the fret becomes longer, more of these small curves are required. The first example in Figure 16 is taken from the book by Lewis Day [3]. There is one curve

that traverses the entire fret forming circles, and each circle is interlaced with a closed cloverleaf shaped figure. As the fret grows, more and more of these cloverleaf patterns are needed.

Fig. 16: Fret consisting of one continuous curve and an unbounded number of small curves.

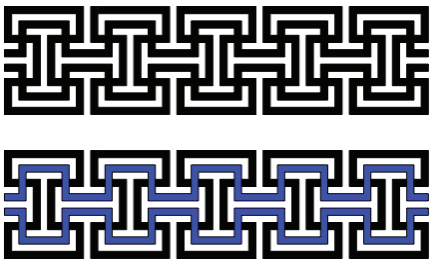

Fig. 17: Fret consisting of one (or two) continuous curves and an unbounded number of small curves.

The second example comes to us from Pompeii [5], and is illustrated in Figure 17. The original fret is shown at the top of the figure. The bottom of the figure shows the continuous curves in blue, which helps to see the five 12-sided `I`-shaped black polygons intersecting these curves. Note that as in Figure 16, depending on how the long curves are finished at the ends, they may consist of one or two curves.

Fig. 18: A set of points (left) and a monolinear symmetric tree-shaped sona drawing (right).

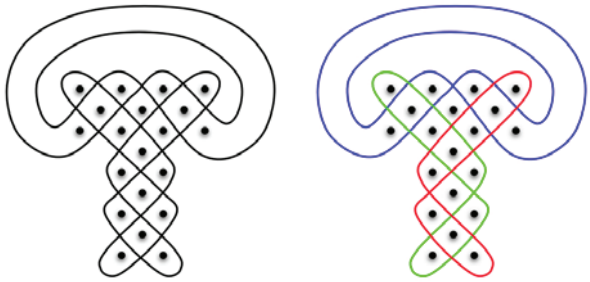

Fig. 19: Sona drawing denoting the Tshihongo mask composed of 2 non-congruent curves.

6. Sona Drawings

Many cultures all over the world have traditional visual art practices that unite them with a common thread: the use of meandering cyclic geometric curves that satisfy certain geometric properties. Aside from the ancient Roman and Byzantine mosaics discussed in the preceding, such practices include *sona* drawings from Angola in Africa, *kolam* drawings from South India, Celtic knots, sand drawings from Vanuatu in the South Pacific Islands, Islamic art, illumination of manuscripts, and Chinese decorative knots [4, 6, 8, 10, 12]. A typical sona drawing consists of a single curve that meanders around a group of points previously drawn, and ends at the point where it started. The pen or other tool used (finger in the case of sand) may not be lifted off the paper during the execution of the drawings, and it may not go over lines already drawn, except to cross over them. Sometimes more than one curve is drawn, but the most desirable drawings consist of one single curve, i.e., they are monolinear. Without any constraints it is easy enough to execute a sona drawing, since every set of

points admits a very large number of them [10]. However, once constraints such as connectivity and symmetry about certain axes are added, the task may become considerably more complicated. For example, take the points shown in Figure 18 (left). One solution of a drawing that has the topological shape of a tree, and is symmetric about a vertical line through the middle is shown on the right. A simple algorithm for constructing such sona trees is given in [8], where applications of the algorithm to art are also discussed.

In his book on sona drawings from Angola, Paulus Gerdes classifies them in terms of symmetries and the number of curves used in the drawing. Our classification method goes further by analyzing the properties of the curves used. We close our discussion by illustrating the method on a drawing of a *Tshihongo* mask [6]. The original sona drawing is shown in Figure 19 (left), and its decomposition into three curves of different color on the right. Gerdes classifies this drawing as 3-linear. On the right it may be observed that the red and green curves are mirror images of each other, and thus they are congruent. Therefore we classify this curve as being composed of two non-congruent curves.

References

[1] Belcastro, S.-M. and Hull, T. C., "Classifying Frieze Patterns without Using Groups," *The College Mathematics Journal*, Vol. 33, No. 2 (Mar., 2002), pp. 93-98.

[2] Christie, A. H., *Traditional methods of Pattern Designing: An Introduction to the Study of Decorative Art,* The Clarendon Press, Oxford, 1910.

[3] Day, L. F., *Pattern Design*, B. T. Batsford Ltd., London, 1903. Revised and enlarged by Amor Fenn in 1933. Dover,1999.

[4] Dunbabin, K. M. D., *Mosaics of the Greek and Roman World*, Cambridge University Press, Cambridge, U.K., 1999.

[5] Fenn, A., *Abstract Design and How to Create It*, T. Batsford Ltd., London, 1930. With new introduction by Richard M. Proctor in 1993. Dover 1993.

[6] Gerdes, P., *Sona Geometry from Angola*, Polimetrica, Monza, Italy, 2006.

[7] Goodyear, W. H., *The Grammar of the Lotus,* Sampson Low, Marston & Co., London, 1891.

[8] Liu, Y. and Toussaint, G. T., "A Simple Algorithm for Constructing Perfect Monolinear *Sona* Tree Drawings, and its Application to Visual Art Education," *Conf. on Artificial Intelligence, Knowledge Engineering and Data Bases*, Cambridge University, U.K., Feb. 21-23, 2009.

[9] Liu, Y. and Toussaint, G. T., "A Tessellation-Transformation Method for Categorizing and Generating Geometric Textile Design Patterns," *Design Principles and Practices: An International Journal*, Vol. 2, No. 4, 2008, pp. 101-111.

[10] Nagata, S., "Digitalization and Analysis of Traditional Cycle Patterns in the World, and Their Contemporary Applications," *Forma*. Vol. 22, 2007, pp. 119-126.

[11] Nakamura, S., *Pattern Sourcebook: Chinese Style*, Rockport Publishers, Beverly, Mass., 2008.

[12] Sutton, D., *Islamic Design: A Genius for Geometry*, Walker & Co., New York, 2007.

[13] Toussaint, G. T., "A new class of stuck unknots in Pol-6," *Contributions to Algebra and Geometry*, Vol. 42, No. 2, 2001, pp. 301-306.

[14] Washburn, D. K., Style, Classification and Ethnicity: Design Categories on Bakuba Raffia Cloth. *Transactions of the American Philosophical Society,* Vol. 80, No. 3, 1990, pp. 5-157.

[15] Wilson, T., *Swastika: The Earliest Known Symbol and its Migrations*, U.S. National Museum, 1894. Transcribed by Alfta Svani Lothursdottir, Northvegr and A. Odhinssen, 2003.

Order at the Edge of Chaos: Algorithmic Art Based on Completely Chaotic Rational Functions

Robert M. Spann
3001 Veazey Terrace, NW #802
Washington, DC 20008
Email: bobspann@gmail.com

Abstract

Rational functions are often used to generate algorithmic art. See for example Mandelbrot [7], Peitgen and Richter [10], Kalantari [6] or Sisson [11]. In many cases these computer images utilize the fact that most rational functions are well behaved in some regions and exhibit chaotic behavior in other regions of the complex plane. See for example Beardon [2]. In this paper I show how images can be obtained using rational functions that exhibit chaotic behavior everywhere in the complex plane. That is, rational functions for which the Julia set is the entire extended complex plane. Functions with this property have not been used to obtain algorithmic art in prior work. In doing so, I also use a measure of angular, rather than Euclidean distance. This use of angular distance, rather than some form of Euclidean distance to obtain images is also a new approach. The resulting images can be highly patterned and exhibit interesting symmetries. Finally, I show how the measure of angular distance described below can be used to create very different images from rational functions with very similar dynamic properties.

Introduction

This paper addresses the generation of images using the iteration of rational functions that are chaotic everywhere. Prior work has not used such functions to obtain images. Specifically, I consider a subset of rational functions of a complex variable, $R(z)=p(z)/q(z)$ where $p(z)$ and $q(z)$ are polynomials and z is a complex variable. A completely chaotic rational function is a rational function for which the Julia set is the entire extended complex plane or the Riemann sphere $C \cup \infty$ where C is the complex plane. The mathematical properties of iterated rational functions are well known. See, Keen [5], Beardon[2], or Milnor[9]. These properties are briefly discussed to provide the background for the images obtained below.

Rational Functions with a Julia Set Equal to the Extended Complex Plane

The forward iterates of any point z_0 are $R(z_0)$, $R^2(z_0)...R^n(z_0)$, where $R^n(z_0)$ is the n-fold composition of R. Let z_0 and z_1 represent two points that are close to each other. A rational function is chaotic everywhere if the forward iterates of these two points move further and further apart. Formally, a rational function is chaotic everywhere, if for all z_0 and arbitrarily small ε, $|z_0 - z_1| < \varepsilon$ and also
$|z_0 - z_1| < |R(z_0)-R(z_1)| <.....<|R^n(z_0)-R^n(z_1)|$.

I utilize rational functions of degree two. That is rational functions for which at least one of $p(z)$ or $q(z)$ is of degree two and the other is of degree two or less. There are numerous examples of rational functions of degree two whose Julia set is the entire extended complex plane. There are also methodologies for creating rational functions whose Julia set is the entire extended complex plane. See for example Barnes and Koss [1], Beardon[2], Hawkins [4] or Milnor[9].

The approach utilized in this paper is as follows. First, define a fixed or periodic point as a point z_0 such that $R^k(z_0)=z_0$. A fixed or periodic point is attracting if for any point z in the neighborhood of z_0, the forward iterates of z move closer to z_0 under iteration by $R^k(z)$. A fixed, or periodic point is repelling if for any point z in the neighborhood of z_0, the forward iterates of z move further away from z_0 under iteration by $R^k(z)$. If k=1, z_0 is a fixed point; otherwise z_0 is a periodic point. See Beardon [2].

If a rational function is chaotic everywhere, there can be no points z_0 such that for arbitrarily small ε, $|z_0 - z_1|< \varepsilon$ and also $|z_0 - z_1| > |R(z_0)-R(z_1)| >.....>|R^n(z_0)-R^n(z_1)|$. That is, there can be no attracting fixed or periodic points.

The dynamics of a rational function in the complex plane are determined by the forward iterates of its critical points. The critical points of a rational function are points where the function R(z) fails to be a local homeomorphism. In general these are the points where the first derivative of R(z) is equal to zero. A rational function of degree m has at most 2m-2 distinct critical points. When the degree of R(z) is 2, there are at most two critical points. A rational map of degree 2 has at most 3 distinct fixed points and may have numerous other periodic points of varying orders. See Beardon [2] or Milnor [8].

It is well know that each attracting fixed point or attracting cycle of a rational function must have a critical point in its basin of attraction. If one can show that the forward iterates of each critical point include a repelling fixed point or a repelling periodic point, then there are no attracting fixed (or periodic) points and the Julia set is the entire extended complex plane. See Beardon [2] or Hawkins [4].

Let z_{p1} and z_{p2} denote two distinct repelling periodic points, and let z_{c1} and z_{c2} denote the two critical points of a rational function of degree 2. There are three generic ways the critical points and periodic points of a completely chaotic rational function of degree 2 might be structured. They are:

a) $R^k(z_{c1})=z_{c2}$ and $R^j(z_{c2})=z_{p1}$ for integers k and j.
b) $R^k(z_{c1})= z_{p1}$ and $R^j(z_{c2})=z_{p1}$ but $R^i(z_{c1}) \neq z_{c2}$ for any i.
c) $R^k(z_{c1})= z_{p1}$ and $R^j(z_{c2})=z_{p2}$

This classification can be used to construct rational functions whose Julia sets are the entire complex plane.

Obtaining Images from Completely Chaotic Functions

I obtain images from completely chaotic functions by iterating the function n times, for n not too large. The colors in the images I create are based on a measure of angular distance, not the Euclidean distance between each initial point and the n^{th} iterate of that point.

For each point $z_0=r_0\exp(i\theta_0)$ let $R^n(z_0)=r_n\exp(i\theta_n)$ and let $\theta=\theta_n-\theta_0$. Next let $d=\frac{1-\cos\theta}{2}$ This is a measure of the angular distance between z_0 and $R^n(z_0)$ Note that $0 \leq d \leq 1$. The value of d is zero when $\theta_n = \theta_0$. The value of d is equal to one when $\theta_n-\theta_0$ is 180 degrees.

I then define a map from the interval [0, 1] to the indices {1,2,...,k} of a list of k colors as follows: Let $z = x + iy$. For fixed $x_1 < x2$ and fixed $y_1 < y_2$ construct a grid of n_x x n_y points. I have used a grid of 2000 x 1500. Iterate the rational function R(z) n times over this grid. Compute d, the angular distance between z

and $R^n(z)$, for each discrete point in the grid. Next compute the mean and standard deviation of the angular distance d for all points in the grid. Then if we want the image to consist of k colors of approximately equal area, the map is:

f(d) =j if $\frac{j-1}{k} < N(d) \leq \frac{j}{k}$ for d in the interval [0,1] and j one of the indices {1,2,...,k}

where N(d) is the cumulative normal distribution with mean and standard deviation equal to the calculated mean and standard deviation of d over the preselected grid.

To create an image with n < k colors of unequal areas create a many to one (i.e. non injective) map h: j → m for integers $1 \leq j \leq k$, $1 \leq m \leq n$ Then, the map h∘f will result in an image with n colors and (possibly) unequal areas for the different colors.

Images

The first image, Figure 1 *Star Wheel* is created using the equation $f(z) = \frac{(z^2 - 2)}{z^2}$. This is an example of case a) above. The critical points are z= ∞ and z= 0. The forward obit of 0 is $f(0) = \infty$, $f(\infty) = 1$, $f(1) = -1$, and $f(-1) = -1$. The fixed point z = -1 is a repelling fixed point. This equation is from an example in Beardon [2].

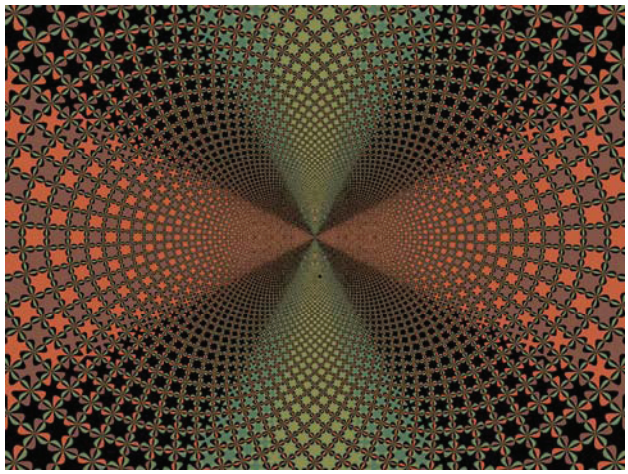

Figure 1: *Star Wheel*

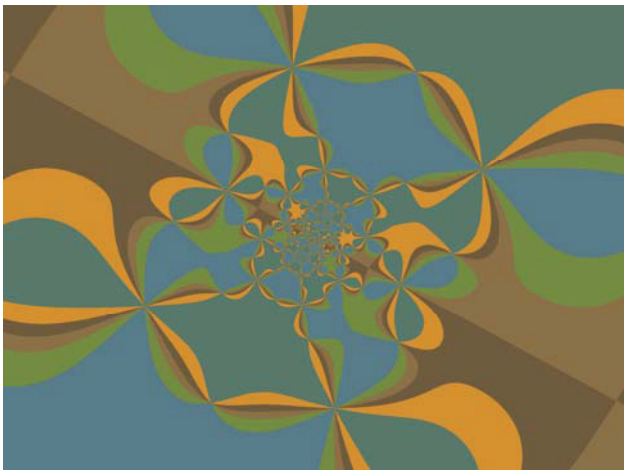

Figure 2: *Folk Dances I*

This function is iterated 15 times for x in the interval [-10,10] and y in the interval [-8,8]. Even though the function used to create Figure 1 is completely chaotic, the resulting image is highly patterned and symmetric. This conclusion builds upon earlier work of Field and Golubitsky [3]. My approach differs from that work in that I start with functions that are chaotic everywhere whereas Field and Golubitsky start with functions that already exhibit symmetry properties, but are not necessarily chaotic everywhere.

Figure 2, *Folk Dances I,* is created using the function $f(z) = -.5^{\frac{1}{3}} \exp 4i\frac{\pi}{3} + \frac{1}{z^2}$. This equation is from an example in Milnor[8]. It is easy to check that this equation satisfies case a) above. This function is iterated seven times for x in the interval [-10,10] and y in the interval [-8,8].

The dynamics of the rational function used to create Figures 1 and 2 are very similar. In both cases, the critical points are zero and infinity. In both cases $f(0)=\infty$ and $f^2(\infty)=z_f$ where z_f is a repelling fixed point. The difference is primarily the result of the number of iterations used to generate the image.

There is an axis of mirror symmetry along the 45 degree line in Figure 2. The symmetry is with regard to shape, but not color. Colors are reversed above and below the 45 degree line.

Figure 3 *Lava I* is created using the same function as Figure 2. The difference is that Figure 3 focuses on an region that is contained within the iteration region of Figure 2, but is only about two percent of the area of the region of iteration for Figure 2. Figure 3 is created by iterating the equation seven times for x in the interval [-1, 1.51] and y in the interval [-8.7935, -.000001]. Figures 2 and 3 illustrate the fact that these equations with Julia sets equal to the entire complex plane do not necessarily lead to images with self similarities. This result suggests that iterating R(z) in a different region of the complex plane might also result in very different images. This is an area for further exploration.

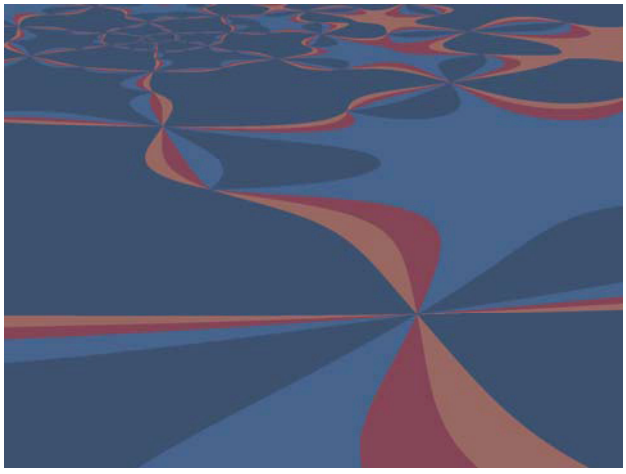

Figure 3: *Lava I*

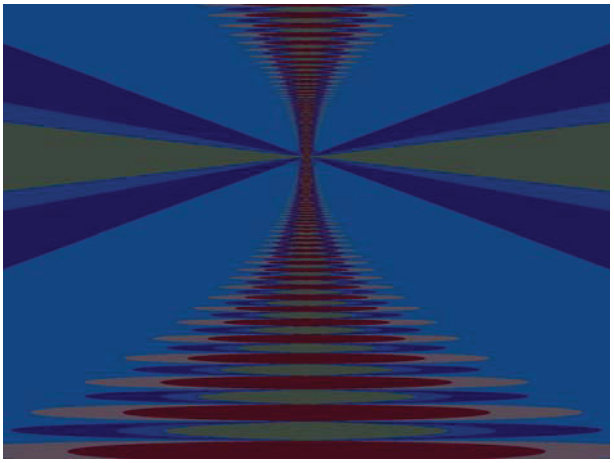

Figure 4: *Stairway1A*

Figure 4 *Stairway1A* is created using the function $f(z)=-.5\dfrac{z^2+1+z\sqrt{8}}{z}$. This is an example of case b) above. The critical points are -1 and 1. Straightforward calculations show that $f^2(1) = f^2(-1) = 0$, and $f(0)=\infty$. The point $z=\infty$ is a repelling fixed point. This function was determined by finding values for a and λ in the equation $R(z)=\lambda\dfrac{z^2+az+1}{z}$ such that $f^2(1) = f^2(-1) = 0$ and $|\lambda|<1$. This parameterization of a rational polynomial of degree 2 and the use of a numerical approach to determining the parameters of a rational function such that the Julia set is the entire extended complex plane is based on Hawkins [4]. My approach differs from Hawkins [4] in that Hawkins restricts the search to the slice of parameter space for which a=2.

This equation is iterated seven times for x in the interval [-0.75, 0.75], and y in the interval [-12, 6].

The resulting image has mirror symmetry, just like Figure 2, but without the color reversal in Figure 2.

Figure 5 *Cederick* is created using the function $f(z)=(-.0868+.68923i)\frac{(z+1)^2}{z}$. This is an example of case c) above. As in the function used to create figure 4, the critical points are -1 and 1. However, the dynamics are different. The dynamics are $f^2(-1)=\infty$ (a repelling fixed point), and $f^3(1)=z_{f2}$ where z_{f2} is a repelling periodic point of order 2. This function was determined by starting with the equation $R(z)=\lambda\frac{z^2+az+1}{z}$, setting a=2 and then finding λ such that $f^3(1)=z_{f2}$ where z_{f2} is a repelling periodic point of order 2 and |λ|<1. The latter condition insures that infinity is a repelling fixed point. See Hawkins [4] or Beardon [2].

The function is iterated eight times for x in the interval [-1, -0.2] and y in the interval [1, 1.6]. Figure 5 does not exhibit the symmetry properties exhibited by the images in Figures 1, 2, and 4.

Figure 5: *Cederick*

Conclusion

I have shown how images can be obtained using rational functions for which the Julia set is the entire extended complex plane. Prior work has not used such functions to generate algorithmic art. I also use a measure of angular, rather than Euclidean distance. This use of angular distance, rather than some form of Euclidean distance to obtain images is a new approach. Extensions of this work might include examining rational functions of odd degree greater than two and the use of alternative maps for coloring the images obtained from completely chaotic rational functions.

Acknowledgement: I would like to thank Gary R. Greenfield for helpful comments and criticisms of an earlier draft of this paper.

References

[1] Barnes,J. and Koss. L., A Julia Set That is Everything *Mathematics Magazine* Vol 76 pp. 255-263. 2003.

[2] Beardon, A.F., *Iteration of Rational Functions* Springer-Verlag 1991

[3] Field, M. and Golubitsky, M., *Symmetry in Chaos; a search for Pattern in Mathematics, Art, and Nature* Oxford University Press 1992.

[4] Hawkins, J., Lebesque Ergodic Rational Maps in Parameter Space *International Journal of Bifurcation and Chaos* Vol. 13, pp. 1423-1447. 2003.

[5] Keen, L., Julia Sets in Devaney, R. and Keen, L. (eds) *Chaos and Fractals Proceedings of Symposia in Applied Mathematics* American Mathematical Society 1989

[6] Kalantari, B, Polynomial Root Finding and Polynomiography World Scientific 2008.

[7] Mandelbrot, B, *The Fractal Geometry of Nature*, New York, W.H. Freeman 1983

[8] Milnor, J., Geometry and Dynamics of Quadratic Rational Maps *Experimental Math* 2 pp. 37-83. 1993.

[9] Milnor, J, *Dynamics in One Complex Variable* Princeton University Press 2006

[10] Peitgen, H, and Richter, P. H., *The Beauty of Fractals* New York Spring-Verlag, 1992

[11] Sisson, P. Fractal Art Using Variations on Escape Time Algorithms in the Complex Plane *Journal of Mathematics and the Arts* Vol 1, pp. 41-45. 2007.

Collapsed Orbs: Astroidal Sculptures from the Breakdown of the Sphere

Stephen Luecking

School of Computer Science and Digital Media
DePaul University
sluecking@cs.depaul.edu

The sculptor discusses his sculptures derived from his investigation of super-spherical surfaces. Recounting methods he developed for modeling super-spheres in NURBS geometry, he introduces the computer-aided design of the sculptures based on astroid-like surfaces. He also presents techniques for a computer-assisted translation of the digital models into physical patterns for casting the sculptures.

Introduction

Super-spheres are surfaces that result when the formula for a sphere no longer remains quadratic, but has had its exponents substituted by a value other than 2. This simple change in parameters yields a vast array of surfaces arranged in various symmetries along the x, y and z axes of Cartesian space. The possibilities for sculptural exploration are therefore extensive and have occupied much of this sculptor's activity during the past three years.

One set of explorations, entitled "Shot", are a set of 21 permutations involving the inversion of different quadrants of the sphere into various combinations of astroidal surfaces within a sphere. The sphere is broken down, or collapsed, into inward curving surfaces. This paper presents the methodology for designing these sculptures within a spline modeling environment and for reproducing these into patterns suitable for casting.

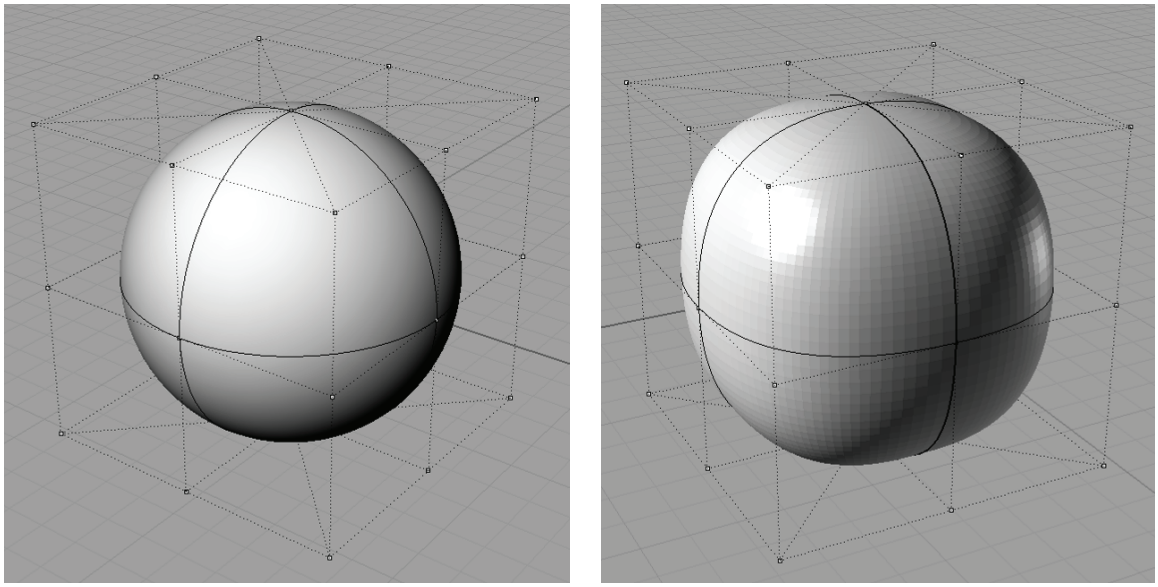

Figure 1 and 2. *Spline representation of a sphere (left) and supersphere (right). Both are shown within the same bounding box formed by the control points.*

Superspheres and Splines

The general formula for the sphere with the Cartesian co-ordinates 0,0,0 as its center is $x^2 + y^2 + z^2 = R^2$, or $x^2 + y^2 + z^2 = 1$ for a unit sphere, while the generalized formula for a super-sphere centered at the same point becomes $x^n + y^n + z^n = 1$. Values of n greater than 2 will extend the quadrants of the sphere toward the eight points determined by the corners of a circumscribed cube. At $n = \infty$ the sphere transforms into the cube marked by these points. Powers less than 2 cause the sphere to collapse inward. At 1 the quadrants of the sphere flatten into the triangular faces of an octahedron. At values less than 1 the sphere collapses into a concave surface. At a power of 0.5 the surface dips into an astroid. When the value of the exponent reaches 0 then all that remains of the supersphere are the three lines of the x,y,z axes.

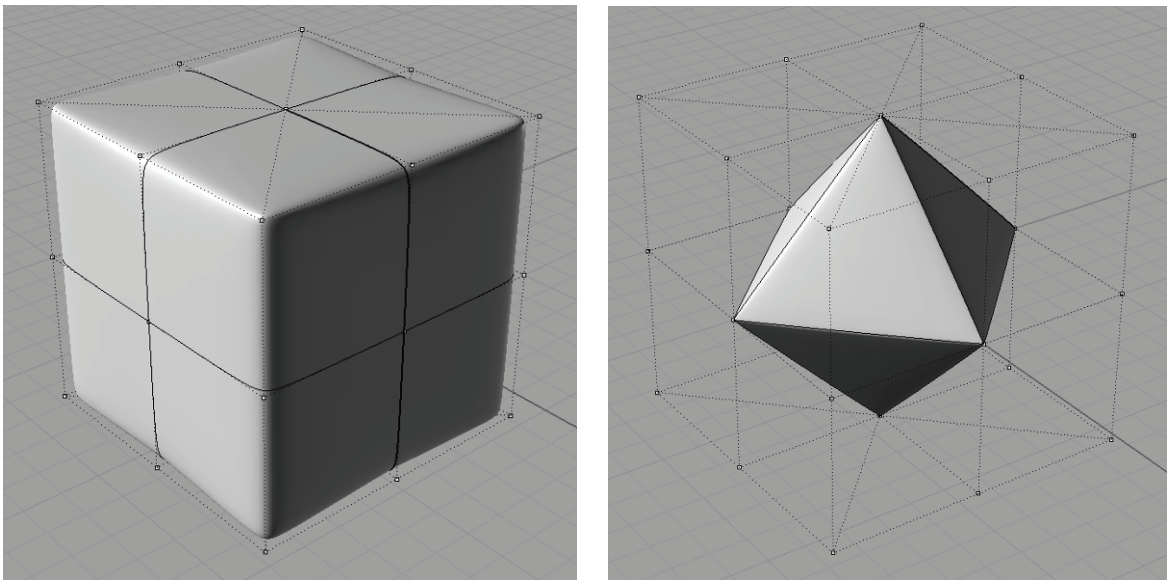

Figures 3 and 4. *Superspheres nearing the shape of a cube (left) and an octahedron (right).*

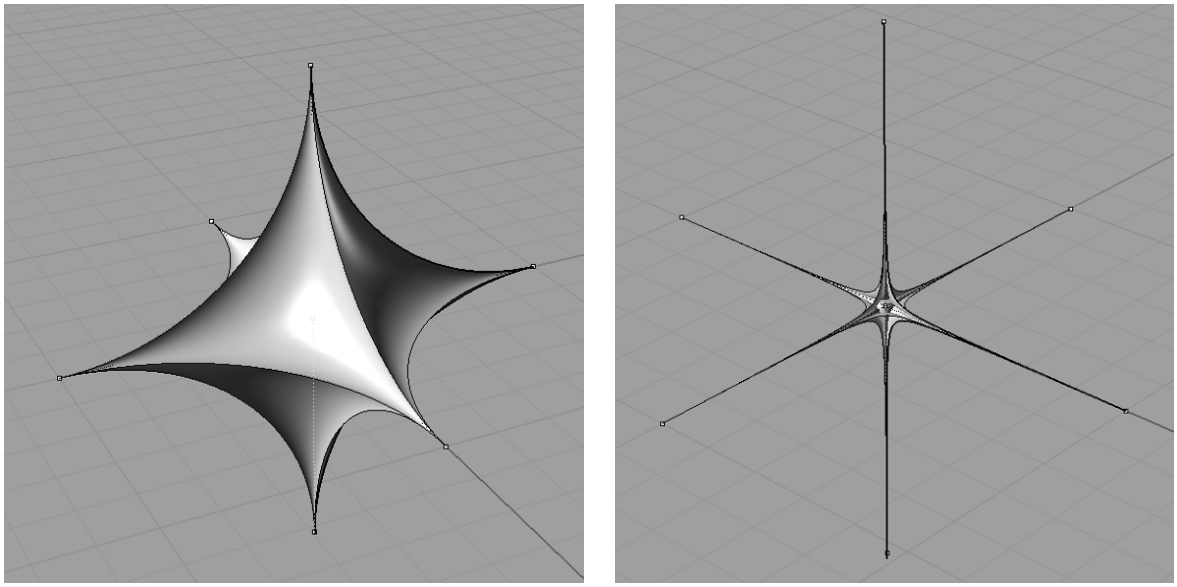

Figures 5 and 6. *Astroidal supersphere (left) and a supersphere approaching n=0.*

The sculptor models superspheres by modifying the position and weight of the control points on a spline replication of a sphere. The position of the control point determines the direction of the surface's distension and its weight determines the mathematical strength of the pull on a surface. Figure 1 illustrates a spline model of a sphere with its control points visible. Note that the control points form a cube. At this stage the vertex control points have a weight of 0.5. In Figure 2 that weight has doubled to 1. The control points on the supersphere model in Figure 3 have a weight of 100, accounting for its nearly cubic form. Figure four depicts the supersphere with its point weight reduced to 0.01 – its form approaching an octahedron.

A similar process of convergence also occurs when all twenty off-surface control points – the eight vertex points and the twelve edge points on the cube – are dragged to a point at the center of the sphere as in Figure 5. Only the six face points remain to hold the ends of the three orthogonal axes in place. Subsequent increasing of the weight of this central singularity to 10 produces a surface clearly converging into three axial lines, as in Figure 6. Selectively dragging some points to the center while keeping other points outside allows for a number of other familiar surfaces, like the astroid of revolution demonstrated in Figure 7.

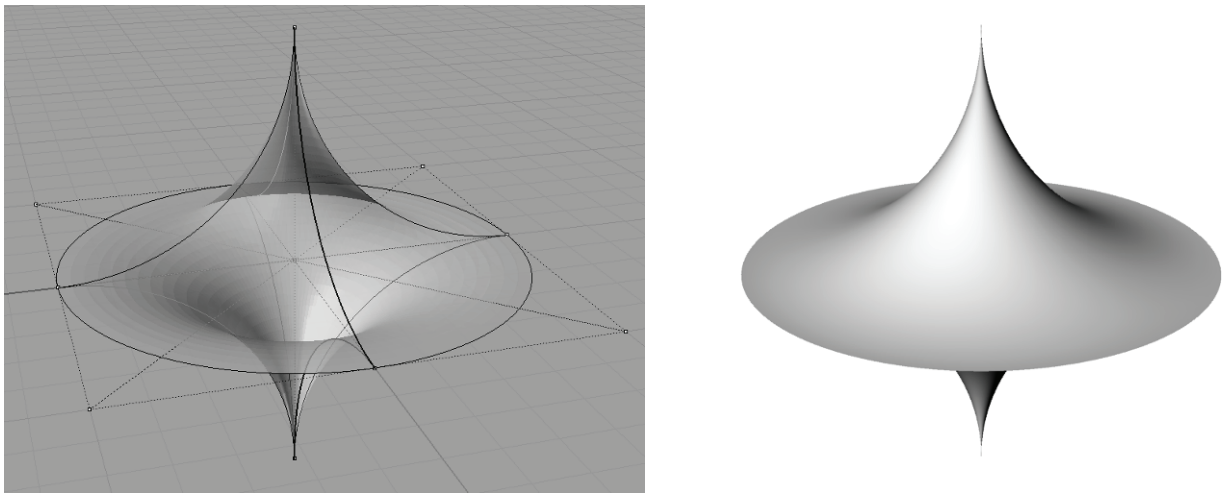

Figure 7. *Astroid of revolution. The external control points on the x,y plane define the equator.*

Sculpture Design

This series, entitled "Shot", sought to explore the partial inversion of the sphere: it would retain some of its convexity. The most intriguing solution was to deflate the surface quadrants of the sphere into strong negative forms. Convexity resulted by retaining the orthogonal great circles of the sphere and then to selectively invert quadrant arcs of those circles. Changes in the location of the collapsed arcs accounts for a number of potential permutations allowed by this format. For the purposes of this series half of the great circle arcs have been collapsed and half remain standing.

In the spline modeler these possibilities were quickly realized by dragging the appropriate control points to the center. Figure 8 presents the development on one such permutation. The finished design removed the inside edges by modifying the surface into a continuously sweeping surface (Figure 9).

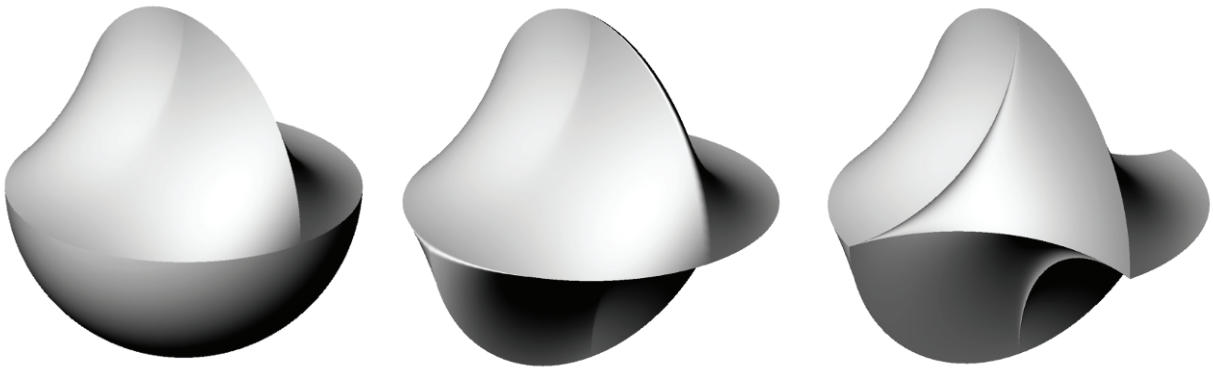

Figure 8. *Study for "Shot". Spline surface model from Rhino 3D.*

Pattern Construction

Each physical pattern begins as an armature created by three intersecting planes (Figure 9), sawn from $^{1}/_{8}$ inch Baltic birch plywood and then slotted to permit their intersection. Once glued these three mutually supporting planes became a strong armature. The pattern strengthened much more after applying a fast-setting putty of filled polyester – better known as Bondo. The edges of the plywood function as guides in determining the smooth sweep of the surfaces. The finish surface of the patterns is a durable alkyd-based spackle manufactured for exterior uses. While the Bondo catalyzes quickly, the spackle must dry overnight. However it is much easier to finish than Bondo and once sprayed with lacquer it is quite hard and smooth. (Note that water-based spackle formulations do not work over the polyester.)

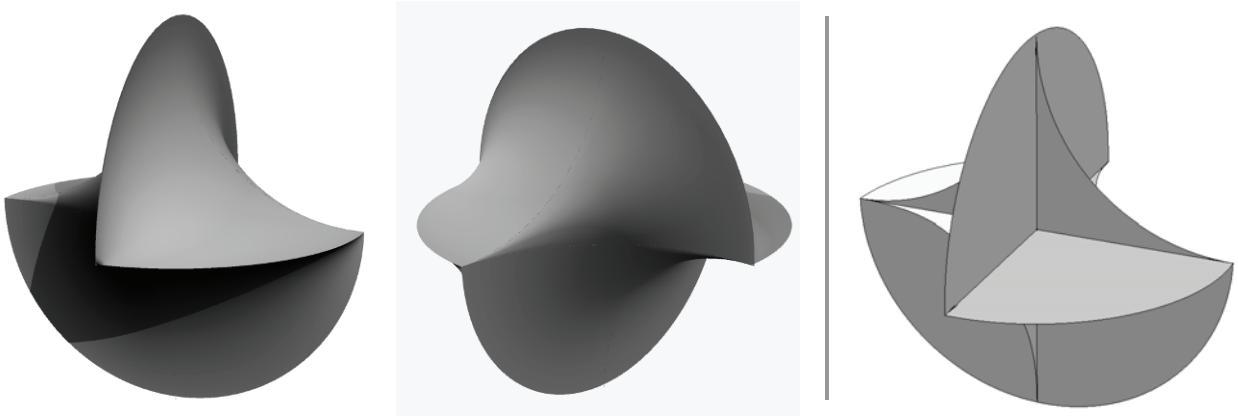

Figure 9. *Studies for "Shot").* **Figure 10.** *Armature planes for "Shot"..*

The sharp-edged fins of the digital models are impossible to achieve and so in the pattern they widen into ridged arcs. For purposes of casting their thickness must be at least ¼ inch to permit flow of the metal to the perimeters of the sculpture. Bronze casting is even more problematic, since the cooling differential between the more massive center and the thin ridges can easily lead to cracking in the final sculpture. Consequently the pattern's ridges were widened to $^{3}/_{8}$ inch.

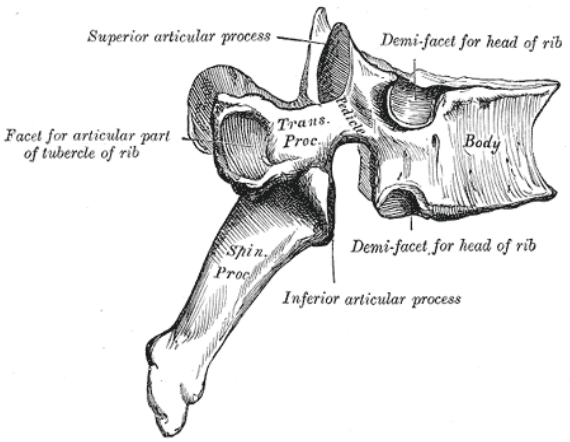

Figure 11. *A diagram of a human thoracic vertebra from the 20th U.S. edition of Gray's Anatomy of the Human Body, 1918.* **Figure 12.** *Patterns after initial application of polyester putty to plywood armature.*

Figure 13. *Patterns after top-coating of alkyd spackle.*

Conclusion

At this writing the "Shot" sculptures are at the pattern stage with all 21 underway. Though the exigencies of pattern construction and casting has led to forms that sacrifice some of the sharpness and mathematical crispness of the digital designs, another set of qualities appeared as the forms took on more organic qualities. While they still hold most of their geometric character, they also evince some of the character of bone segments. The ridges recall the rounded outcrops, or processes (Figure 11), by which tendons attach

to bones, while the concave surfaces reflect the inward arcing structure that help to define and support these processes.

This to a sculptor is a positive change: when the sculpture, on its way to physical realization, takes on a multi-valence that the abstract design alone could not provide. The physical should exert its own meanings and associations. These are as much felt as observed.

Exploring Foldable Great Circle Geometries

CJ Fearnley
Executive Director, Synergetics Collaborative
240 Copley Road, Upper Darby, PA 19082-4016
cjf@SynergeticsCollaborative.org

In his magnum opus, Synergetics, R. Buckminster Fuller develops a folklore of great circle ``railroad tracks" which transit ``energy" inwardly and outwardly through the center of a sphere or omni-directionally around the great circles or to other inter-connected systems. In this context, Fuller documents a number of interesting geometries by folding discs into modules which dovetail together to build a great circle tessellation of the sphere. These easily built, tangible models show whole planar great circles (not just the surface graph) and how they subdivide omni-directional space with angle and frequency. Fuller's models have the remarkable property that the number of modules (each identical or in mirror image pairs) exactly equals (or is a multiple of) the number of great circles in the spherical tessellation.

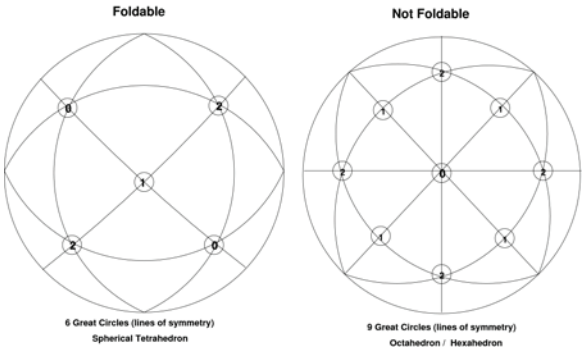

In the critical case and more precisely, foldability is the property of being able to put together N origami folded unit discs (the modules) to form a unit sphere that is tessellated by exactly N great circles. So foldability is, mathematically, the property of a great circle spherical tessellation that can be partitioned into Eulerian circuits (the modules) each of which has exactly 360 degrees in its arcs (edges). That is, foldability implies an equivalence relation on the set of origami modules composing a great circle tessellation.

In my exploration of this property, I found that not all great circle spherical tessellations can be subdivided in this way (e.g., the nine great circle net formed by the ``lines of symmetry" of the octahedron). Moreover, I have discovered that many more great circle tessellations than the ones described by Fuller have this foldability property. So the phenomenon of foldability in only some great circle nets is an interesting property of omni-directional space.

My investigation is a work in progress. In my presentation, I will explore the artistic and mathematical elegance of those spherical tessellations of great circles with this new property that I call ``foldability" or ``great circle foldability". I will describe the models, demonstrate them, and outline my on-going search to characterize those spherical tessellations exhibiting foldability.

Study of Foldability in Simple Spherical Great Circle Nets

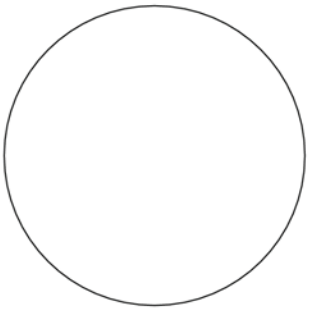

One Great Circle

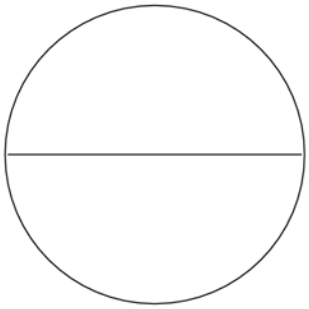

Two Great Circles

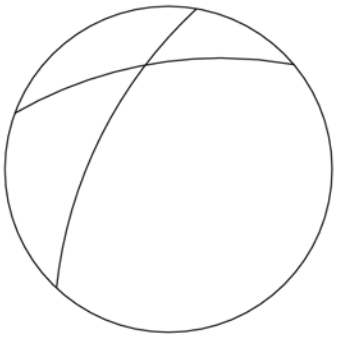

Three Great Circles

Parts of interior arcs sum to 180 degrees
"Slide" the arcs around to explore each possible 3 great circle net.

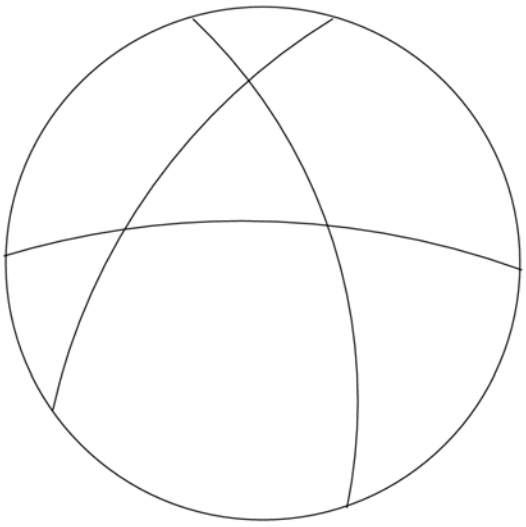

Four Great Circles

Are all variations foldable?

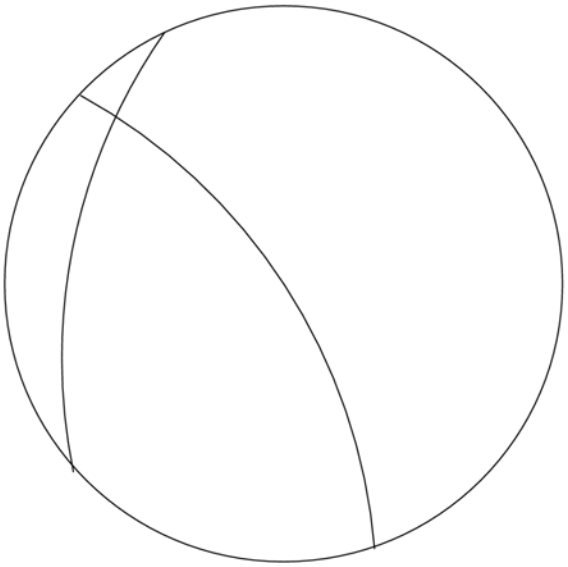

Four Great Circles

With fewer intersections
The geometry changes
Never foldable???

Intaglio Monoprints

Benigna Chilla
bchilla@berkshirecc.edu

Abstract

These are a selection of my intaglio monoprints that were introduced in [1].

Ten Intaglio Monoprints

A selection of ten intaglio monoprints are shown below. The first four pieces were some of the first experiments to serve as ideas and possibilities for larger pieces, which materialized in pieces that followed.

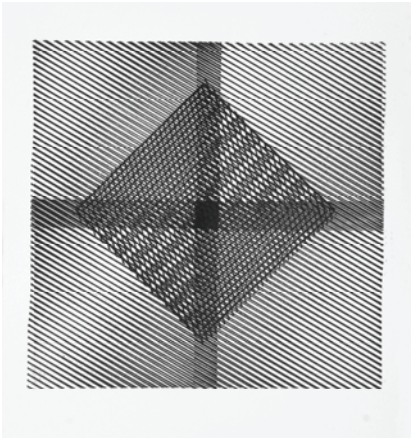

Number 1. Floating Diagonal Squares Within A Square I, 9” x 9”.

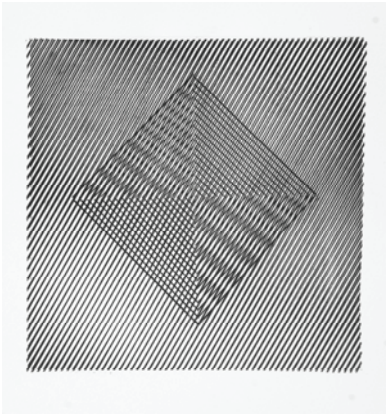

Number 2. Floating Diagonal Squares Within A Square II, 9” x 9”.

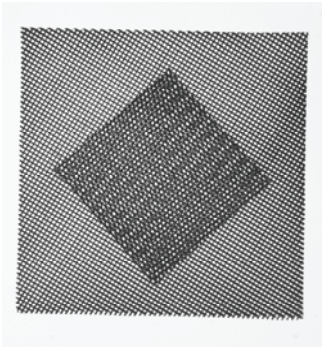

Number 3. Floating Diagonal Squares Within A Square III, 9” x 9”.

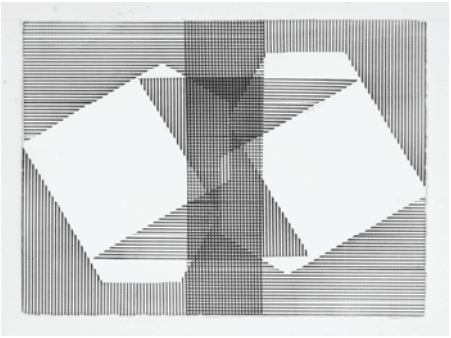

Number 4. Space Rotation, 11” x 15”. One plate was used: printed four times while rotated to the right 90^{o}, always lining up with a corner of the page.

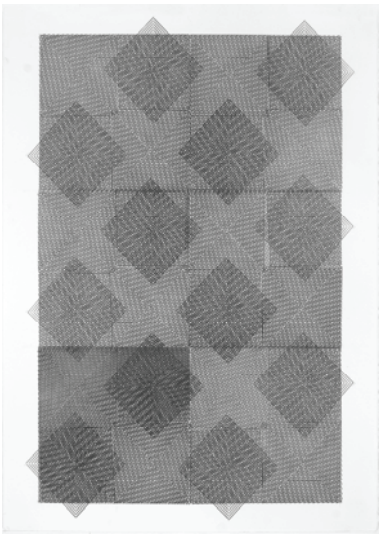

Number 5. Floating Squares, 30” x 32”. On six squares, twenty-four squares were printed, and the twelve squares were added moving on a diagonal across the existing surface.

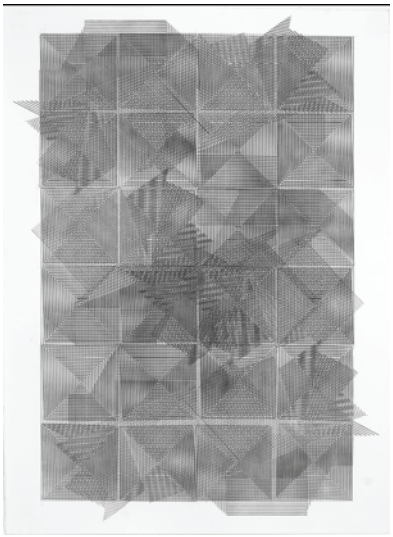

Number 6. Kaleidoscope Surface, 30” x 22”. Over twenty-four squares, different linear plates were printed focusing on the center of the page and then moving in all directions of the piece.

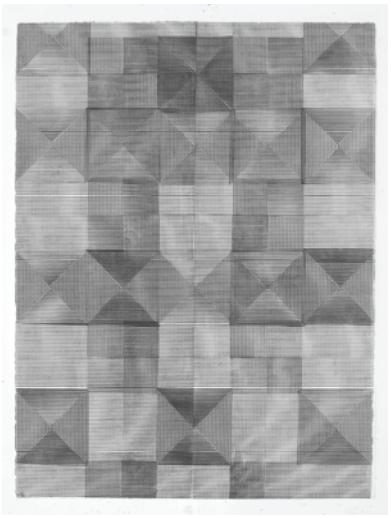

Number 7. Woven Structure, 30” x 22”. The idea for this piece was based on an old hooked rug. The design followed a grid-system, which consisted of only squares. I departed from this design while overlapping different layers of squares with horizontal lines and squares divided through triangles within a square, appearing like a three-dimensional pyramid.

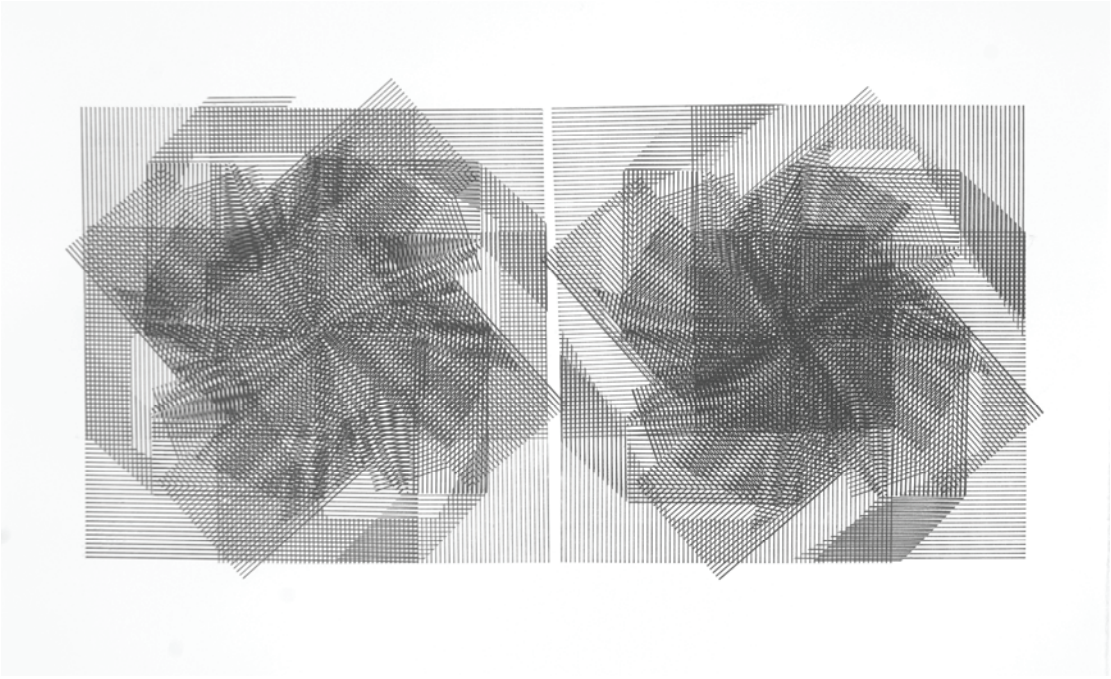

Number 8. Double Rotation, 22” x 30”. A group of linear plates were rotated from the center either to the right or left, always keeping the same point of the plate at the center of each square.

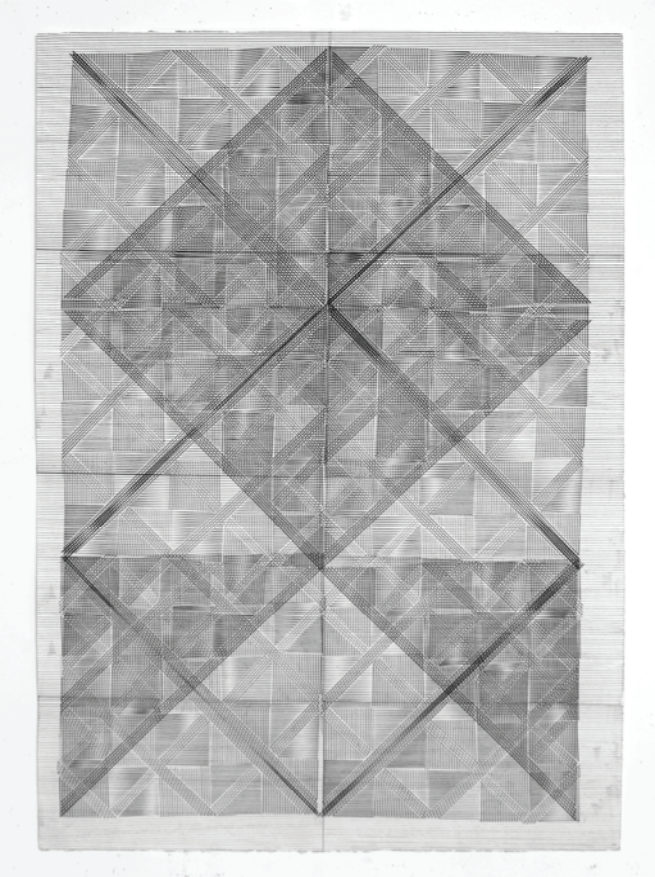

Number 9. Woven Structure II, 42” x 30”. The idea for this piece also came from a hooked rug, looking at the overlapping of designs of squares. I started with printing horizontal lines over the entire page and then using smaller plates moving back and forth over the surface. The imperfection of the hand printed page added a more lively quality to the piece.

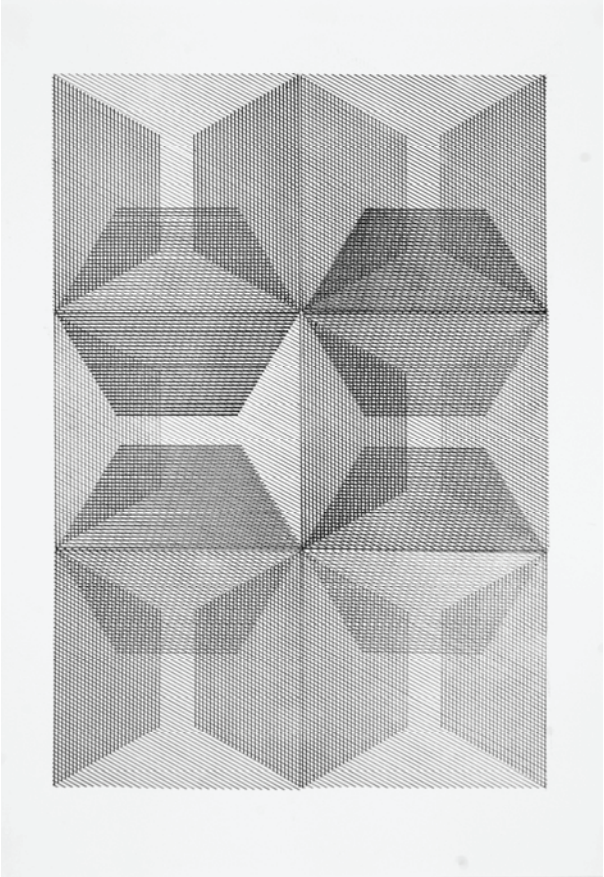

Number 10. Spaces, 22” x 30”. First six squares of diagonal lines were printed. In each square the same trapezoid is printed 3 or 4 times, rotated from each corner of the square.

Reference

[1] Benigna Chilla and Nat Friedman, *Benigna Chilla: Intaglio Monoprints, Line Patterns, Line Surfaces,* Hyperseeing, November/December 2008, www.isama.org/hyperseeing/.

Transforming "Circle Limit III" Patterns - First Steps

Douglas Dunham
Department of Computer Science
University of Minnesota, Duluth
Duluth, MN 55812-3036, USA
E-mail: ddunham@d.umn.edu
Web Site: http://www.d.umn.edu/~ddunham/

Abstract

M.C. Escher's *Circle Limit III*, a repeating pattern of fish, is often considered to be the most appealing of his four "Circle Limit" prints. The fish meet four at each right fin tip, three at each left fin tip, and three nose-to-nose. The concept of this pattern has been generalized to allow any number of fish at those meeting points. But currently there is no computer program to draw such general patterns. In this paper we make progress toward that goal and show some new patterns in this *Circle Limit III* family.

Introduction

Figure 1 below shows a computer rendition of the Dutch artist M.C. Escher's pattern *Circle Limit III* which he realized in the Poincaré disk model of hyperbolic geometry. Figure 2 shows another pattern from the *Circle Limit III* family. In the next section, we review a bit of hyperbolic geometry. Then we describe the

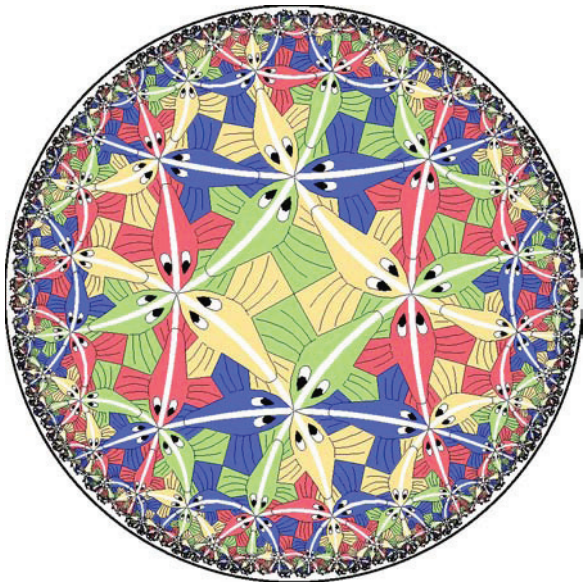

Figure 1: A rendition of Escher's *Circle Limit III*.

Figure 2: A $(4, 4, 3)$ pattern in the *Circle Limit III* family.

3-parameter family of *Circle Limit III* patterns. Next, we show how to create patterns from two special subfamilies. Finally, we discuss a possible attack on the problem of drawing general patterns.

The Family of *Circle Limit III* Patterns

In a 2006 paper [Dun06], I introduced the concept of a 3-parameter family of *Circle Limit III* patterns indexed the numbers p, q, and r of fish meeting at right fin tips, left fin tips, and noses respectively. Such a pattern was denoted by the triple (p, q, r), where p, q, and r should all be greater than or equal to 3. So the patterns of Figures 1 and 2 would be denoted $(4, 3, 3)$ and $(4, 4, 3)$ respectively. Following Escher, we place some restrictions on the patterns in this family. First, r should be odd so that the fish swim head-to-tail. Second, right fin tips should be at the center of the bounding circle. Another condition is that colors of the fish should obey the map-coloring principle: fish that share an edge should be different colors. The fish should also be colored symmetrically and fish along the same "backbone line" should be the same color. Figures 3 and 4 show $(3, 4, 3)$ and $(5, 3, 3)$ patterns. Note the differences between Figure 3 and *Circle Limit III*. In particular, requiring that a right fin tip be at the center allows us to distinguish between (p, q, r) and (q, p, r) when $p \neq q$.

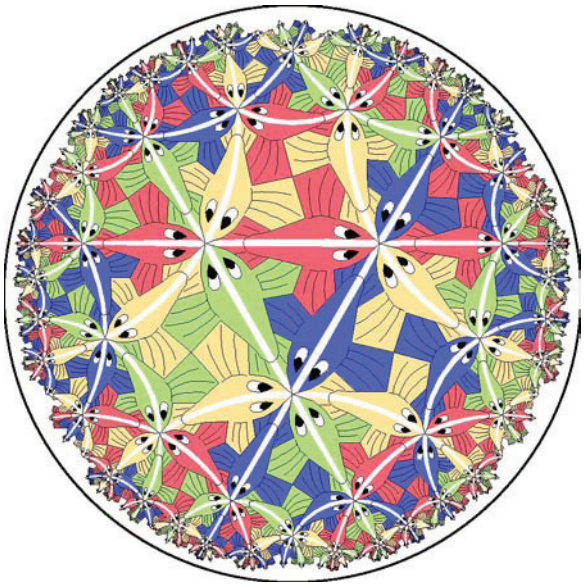

Figure 3: A $(3, 4, 3)$ fish pattern.

Figure 4: A $(5, 3, 3)$ fish pattern.

Hyperbolic Geometry

Escher's "Circle Limit" patterns realized his goal of representing an infinite repeating pattern in a finite area. He used Euclidean constructions to make his patterns, but they could also be interpreted as repeating patterns in the Poincaré disk model of hyperbolic geometry. We must rely on models of hyperbolic geometry in which Euclidean constructs have interpretations as hyperbolic points and lines, since there is no smooth embedding of the hyperbolic plane into Euclidean 3-space [Hil01]. The hyperbolic points in this model are just the (Euclidean) points within a Euclidean bounding circle. Hyperbolic lines are represented by circular arcs orthogonal to the bounding circle (including diameters). For example, the backbone lines of the fish lie along hyperbolic lines in Figure 2. Also, equal hyperbolic distances correspond to ever smaller Euclidean distances toward the edge of the disk. For example, all the fish in Figure 1 are hyperbolically the same size, as are all the fish in Figure 2.

One might guess that the backbone arcs of the fish in Figure 1 (*Circle Limit III*) are also hyperbolic lines, but this is not the case. They are *equidistant curves* in hyperbolic geometry: curves at a constant hyperbolic

distance from the hyperbolic line with the same endpoints on the bounding circle. For each hyperbolic line and a given distance, there are two equidistant curves, called *branches*, one each side of the line at that distance from it. In the Poincaré disk model, those two branches are represented by circular arcs making the same (non-right) angle with the bounding circle and having the same endpoints as the corresponding hyperbolic line. Equidistant curves are the hyperbolic analog of small circles in spherical geometry: a small circle of latitude in the northern hemisphere is equidistant from the equator (a great circle or "line" in spherical geometry), and has a corresponding small circle of latitude in the southern hemisphere the same distance from the equator. For more on hyperbolic geometry see [Gre08].

Creating Patterns from the $p = q$ Subfamily

When $p = q$, the backbones lie along hyperbolic lines, not equidistant curves, so that the fish are symmetric by reflection across their backbones. Thus, in this case we only need to usd half a fish as a motif since we can get the other half by reflection. Figure 2 shows the $(4, 4, 3)$ pattern, an example from this subfamily.

To transform one half-fish motif to another in this subfamily, we can proceed as follows. A half-fish motif (or more accurately, pieces of it) with right fin at the center of the bounding circle and backbone line perpendicular to the positive x-axis fits into a hyperbolic isosceles triangle symmetric across the x-axis, with apex at the origin. When such an isosceles triangle is transformed into the Klein disk model of hyperbolic geometry, it become a Euclidean isosceles triangle, since the hyperbolic lines in the Klein model are represented by Euclidean chords of the bounding circle (a chord in the Klein model corresponds to the orthogonal circular arc in the Poincaré model with the same endpoints as the chord) [Gre08]. Any one of these Euclidean isosceles triangles can be mapped onto another by a differential scaling — having different x- and y-scale factors. So the transformation process is: map the original half-fish from the Poincaré to the Klein model, apply the differential scaling to get the half-fish into the new Euclidean isosceles triangle, and finally map the new isosceles triangle and its half-fish back to the Poincaré model. Figures 5 and 6 show $(5, 5, 3)$ and $(3, 3, 5)$ patterns that were created this way.

Figure 5: A $(5, 5, 3)$ pattern.

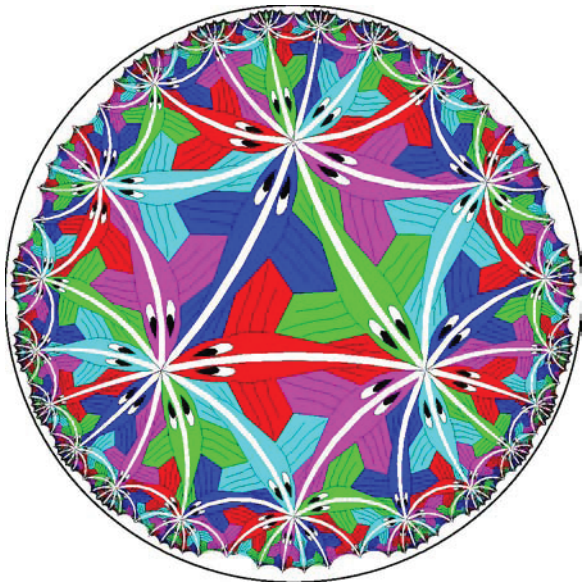

Figure 6: A $(3, 3, 5)$ pattern.

Creating Patterns from the $p = r = 3$ Subfamily

When $p = r = 3$, the backbone lines nearest the origin in the Poincaré model form a Euclidean equilateral triangle, as can be seen in Figure 3 above in the case of $(3, 4, 3)$ and Figure 7 below which shows $(3, 5, 3)$. This fact can be exploited to generate new patterns using the Euclidean scaling mentioned above — but only for right halves of the fish. Figure 8 shows the right halves of the fish of Figure 7.

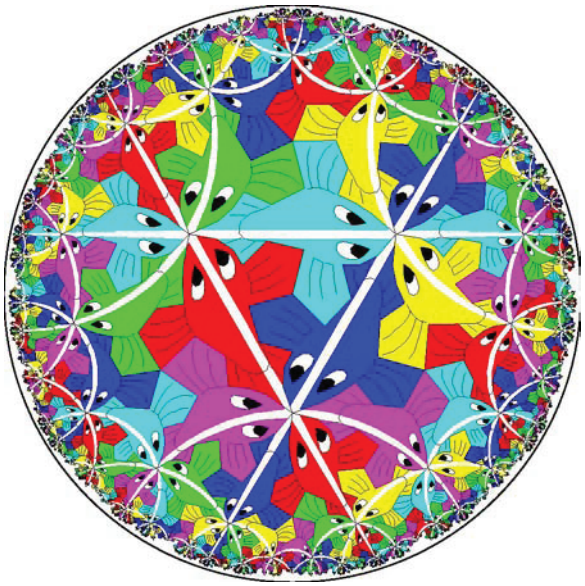

Figure 7: A $(3, 5, 3)$ pattern.

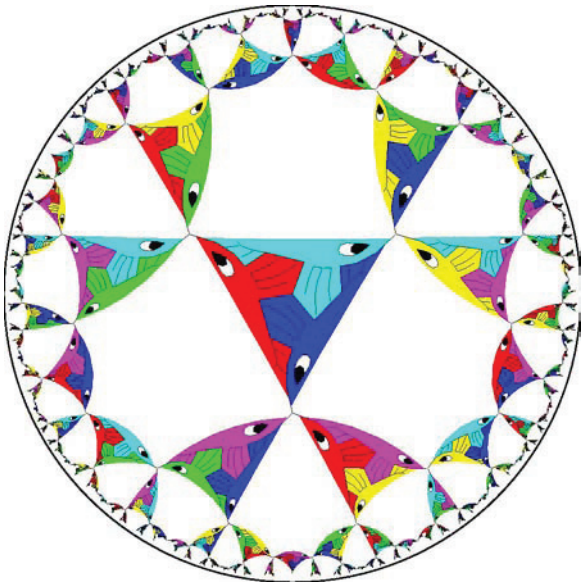

Figure 8: The right sides of the fish in the $(3, 5, 3)$ pattern.

Figure 9 below shows the right sides of the fish in the $(3, 4, 3)$ pattern of Figure 3. Figure 10 shows the right sides of fish in the $(3, 6, 3)$ pattern. Actually, the "seed" right fish-half was taken from the $(3, 4, 3)$ pattern of Figure 3 and it was scaled to form the right fish-halves of Figures 8 and 10. Close examination reveals that the fish halves in Figure 8 are slightly different than the corresponding ones in Figure 7.

A Possible Solution for the General Case

We have seen in cases of the two subfamilies of the previous sections that transforming a hyperbolic motif so that it fits inside a Euclidean isosceles triangle allows us to transform that motif so that it can form any pattern in that subfamily. But in both cases, only half a fish was transformed. Thus it would seem that to transform a fish from a (p, q, r) pattern to a (p', q', r') would require separate processes to transform the left half and the right half. One possible idea would be to find a model of hyperbolic geometry the right "distance" in between the Poincaré model and the Klein model so that the backbone line (equidistant curve) would "flatten out" to a Euclidean line. This would handle the right half-fish. To take care of the left half-fish, we could hyperbolically translate its fin tip to the origin, find the correct "in between" hyperbolic model (probably different than for the right half), apply the transformation, then hyperbolically translate back.

Conclusions and Future Work

For two subfamilies of (p, q, r) *Circle Limit III* patterns, we have shown how one "seed" half-fish motif can be transformed to create any pattern in that subfamily. In the case $p = q$, the backbone lines are hyperbolic

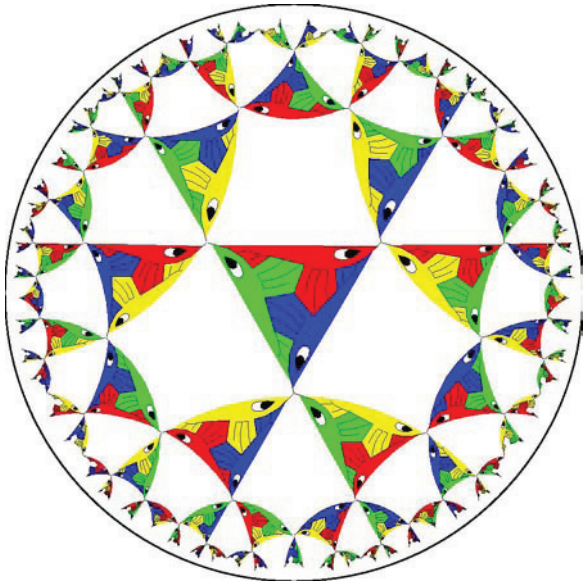

Figure 9: A $(3, 4, 3)$ pattern of right fish-halves.

Figure 10: A $(3, 6, 3)$ pattern of right fish-halves.

lines, so that we can get the other half-fish by reflecting across those lines, and thus obtain the entire pattern. We have also indicated a possible direction of attack for the general case of transforming from and (p, q, r) pattern to any other such pattern.

Another seemingly difficult problem is to automate the process of coloring a (p, q, r) pattern so that it has the same color along any line of fish and adheres to the map-coloring principle that adjacent fish have different colors. I determined the colorings of all the patterns above "by hand", except for Escher's *Circle Limit III* pattern (and the related patterns of Figures 3 and 9). Although it may be possible to program symmetric colorings of any repeating pattern, the requirement that fish along a backbone line be the same color adds an extra degree of difficulty to coloring (p, q, r) patterns.

Acknowledgments

I would like to thank Lisa Fitzpatrick and the staff of the Visualization and Digital Imaging Lab (VDIL) at the University of Minnesota Duluth.

References

[Dun06] D. Dunham, *More "Circle Limit III" Patterns,* in Bridges London: Mathematical Connections in Art, Music, and Science, (eds. Reza Sarhangi and John Sharp), London, UK, 2006, pp. 451–458, 2006.

[Gre08] M. Greenberg, *Euclidean & Non-Euclidean Geometry, Development and History,* 4th Ed., W. H. Freeman, Inc., New York, 2008. ISBN 0-7167-9948-0

[Hil01] David Hilbert, Über Flächen von konstanter gausscher Krümmung, *Transactions of the American Mathematical Society,* pp. 87–99, 1901.

The Boy Surface as Architecture and Sculpture

C.P. Bruter
ARPAM, Gometz-le-Chatel, France

Abstract

The Arpam project proposes to construct several small buildings, referred to as follies, in a large verdant park. Each folly will illustrate mathematical concepts of a particular chapter of the mathematical universe. We will discuss using the Boy surface to generate the structure of a folly. We will also discuss four sculptures related to the Boy surface and illustrating various aspects of knot theory that will be placed in the vicinity of the folly.

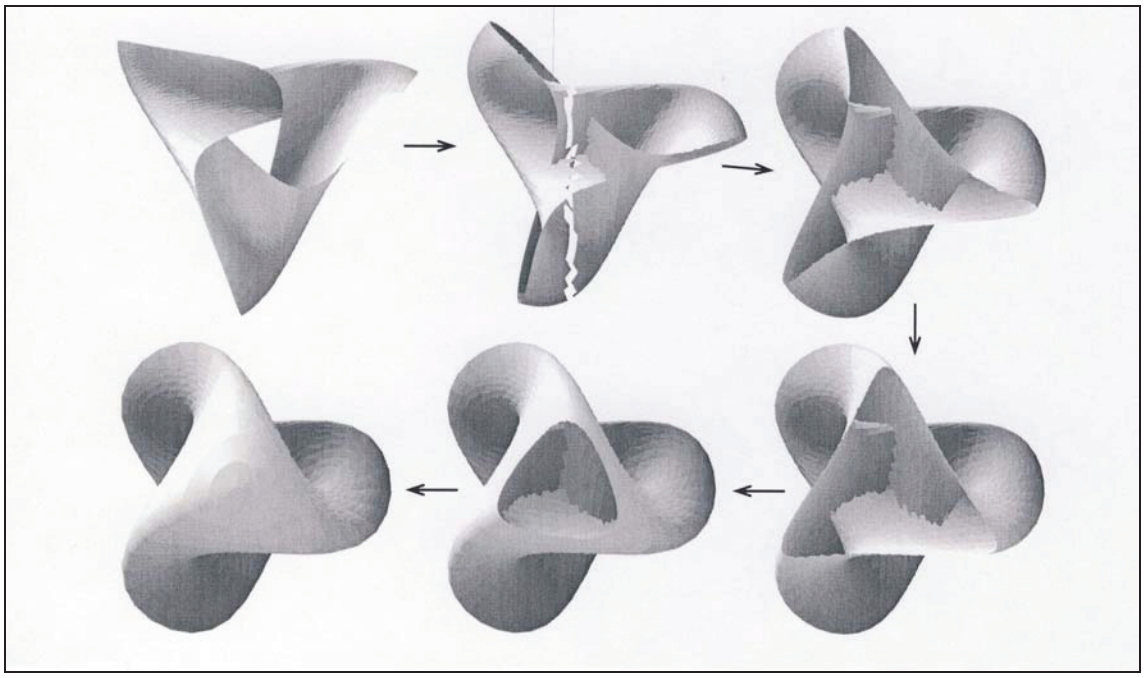

Figure 1. Morphing a triple-twist Mobius band into a Boy surface.

1. Introduction

According to [14], Jean-Pierre Petit had suggested to the French artist Max Sauze a sculpture of the Boy surface. Petit' observations have been developed and expressed in fine mathematical terms by François Apéry [1] [2]. From the equations he established, François has produced several wire models of the Boy surface (a photo of the first one can be viewed in [3] ; also see Figure below of the most recent one). Apéry'student in Cagliari, Gregorio Franzoni, has made a similar model in Teflon. Several beautiful classical views of the Boy surface can be seen on Internet. Wikipedia gives a recent (2008) good animation showing its construction, it seems to be inspired by the static visual construction given in [18] (via the cross cap and the Roman Steiner surface) ; this web site also shows a wire sculpture inOberwolfach. Classical visual and mathematical presentations of the Boy surface can also befound in the books by Anatoli Fomenko [8] and George Francis [9]. Polyhedral constructions of the surface have also recently been made by Ulrich Brem [5], Richard Denner [7], Rob Kirby [12], and Konrad Polthier through an animation [16].

2. The Boy Surface

The projective plane RP^2 is obtained from a disk by identifying diagonally opposite points of the circular boundary of the disk. A cross cap is a representation of RP^2. The boundary of a disk and the boundary of a half-twist Mobius band are each a circle. The projective plane RP^2 is also obtained by identifying the two circular boundaries. Thus the projective plane can also be considered as sewing the boundary of a disk onto the boundary of a half-twist Mobius band. The boundary of a triple twist Mobius band is also a circle in the shape of a trefoil knot. The Boy surface can be considered as sewing the boundary of a disk onto the boundary of a triple twist Mobius band. A very nice morphing of a triple twist Mobius band into the Boy surface is shown in Figure 1. This sequence of images is from the website of Brian Sanderson

In Figure 1, images 1-6, we start with a triple twist Mobius band in image 1. In image 2, the three arcs of the edge, in orthogonal directions, pass through the center forming a triple point as the surface self-intersects. The outer ends also start to curve to form the beginnings of "tubular" spaces that can be seen at the top left and lower center. In image 3 the complete boundary is visible as the three outer ends are now starting to curve inward. Three "tubular" spaces are also now visible. In image 4 the surface continues to curve inward and the rounded triangular boundary starts to shrink. In image 5 the triangular boundary shrinks further and finally shrinks to a point as the surface closes in image 6. Here are a few graphic works made the French team :

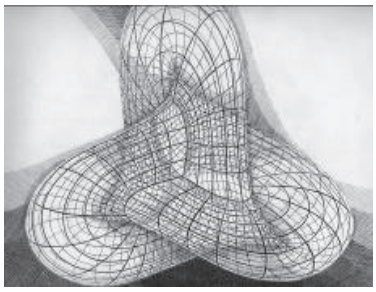

Figure 2. Surface de Boy. Patrice Jeener, 33x25, 2003

Figure 3. The Boy surface. J.-F.Colonna, 2002, screen scale

Figure 4. Ecorché de la surface de Boy. Patrice Jeener, 33x25, 2003

Figure 5. Surface de Boy, François Apéry, 30x30x30, 2002

Let us first consider parallel sections of the Boy surface (Figure 6). One can track their evolution in the following horizontal sections.

Note that Apéry's wire model lies at the singular "north pole". It allows us to interpret the Boy surface as a fiber space. Its basis is a convenient horizontal section of the surface : one can understand it as a plane knot. There are at least two ways to look at the fibers : according to the first one, they are ellipses. Now, consider two infinitesimally close ellipses, they define an infinitesimal band : this band, which now plays the role of a fiber, is in fact a Möbius band having the north pole as a singularity where the twist happens ; it induces the non-orientation of the surface. The usual general theory of fiber spaces does not take into account the intersections of the basis and the fiber. But this intersection plays a role in the topology of the total space. Here each fiber, say each ellipse, intersects the basis in two points. This property and the fact that the basis is a closed plane curve induces the presence of the self-intersection curve in the surface.

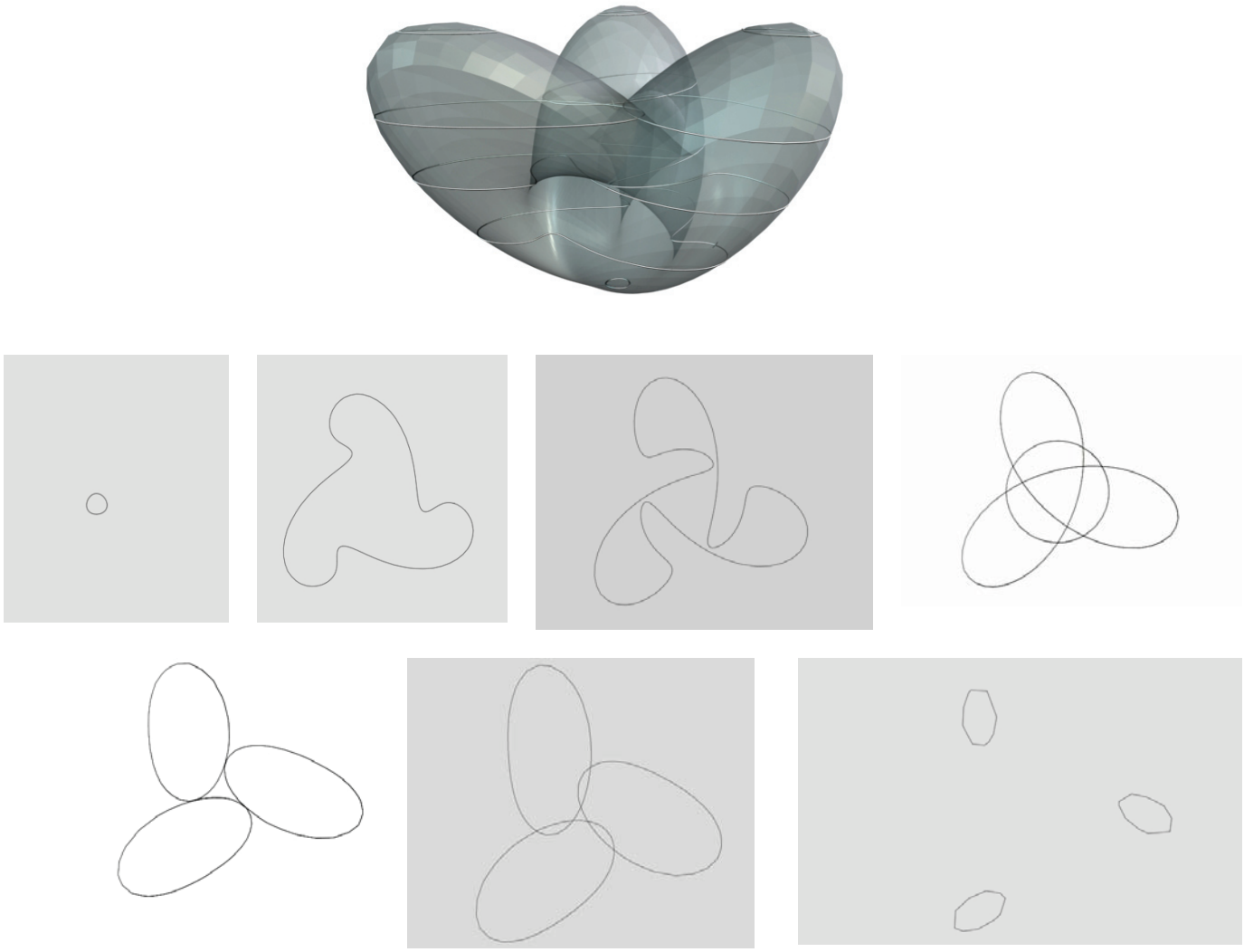

Figure 6 : Horizontal sections of the Boy surface, Christophe Delsart, 2008

3. The Stained Glass Folly

Some well-chosen ellipses of the Boy surface, materialized in chrome steel, constitute the main part of the frame of the folly. This one has two parts : one which is visible from the outside, and the other one which can only be visible from the inside of the folly. Its floor lies on a perpendicular plane to the axis, located at approximately one third of the height of the construction, starting from the singular north pole. This floor is transparent so that one can see the lower part of the construction from inside the folly. This lower part lies inside a cylinder plastered with broken mirrors which reflect the internal lights illuminating the frame.

A few Möbius bands are materialized with stained glass. By looking up and down, one can see them completely from inside the folly. The outside part of the folly has three pieces, but only two of them will serve as rooms for visitors. A series of vertical arches in the same material as the frame will cover the entrance of the two symmetric

rooms. Here are a few preliminary shots of the folly (Figure 7), without any decoration, giving an idea of its structure.

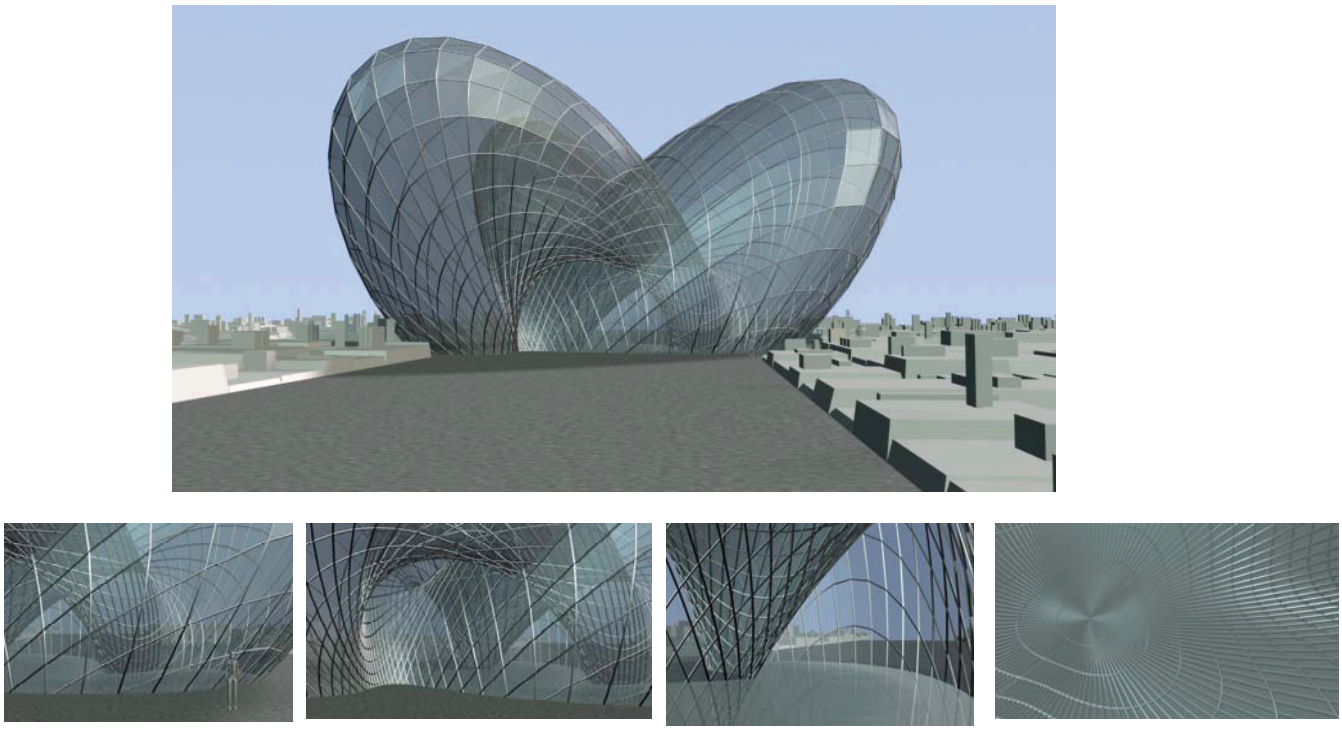

Figure 7. Preliminary images of the stained glass folly, Christophe Delsart and Yvan Ngnodjom, 2008

Convenient transversal rods to the elliptic frame will define panels and allow us to cover the outside part with glass and mirrors. The elliptic curve will be replaced by a piecewise linear approximation. Then some of these panels will be partly stained glass windows showing either tilings or knots and braids with symmetries. LEDs inserted in some panels will follow curves from knots : their representation in space will be improved using the fact that the angle between two consecutive panels of glass is not flat.

Beams of search-lights with convenient colours will illuminate the folly, and four sculptures placed around the folly as well.

4. The Four Sculptures

These sculptures will relate to the Boy surface. This surface has three visible lobes, it has one interior singular point, four exterior singular points : down, the “north pole”, and outside the submits of the three lobes. These singular points can be viewed as the centre and the vertices of a tetrahedron.

Its projection on the ground is an equilateral triangle. A tetrahedron will be placed in its centre. Each of its visible faces will be divided into three horizontal parts lying one upon the other. In each one, one or several knots linked together will be inserted. They can be made with different materials. Some of them will be screwed on so that they can be taken off and replaced by others.

A sculpture conceived by Philippe Charbonneau will be placed in a rear vertex of the triangle. It is a transparent ball made of resin or of glass, containing a part of a coppery ruled surface of degree 3. The intersection of this surface with the sphere is a double figure eight knot, that is three loops, the loop in the middle having one point in

common with the left one, and another point in common with the right one - this knot is the symbol of a Lens space **L**(5,1). Here is a model of this sculpture (Figure 8) :

Figure 8. Ruled surface inside a sphere, Philippe Charbonneau, 1987

A third beautiful shining sculpture (Figure 9), made by Philippe Rips, shows a knot-network made with triangular rods. Such a shape was created maybe first by Alan Holden([10], p. 125 and p.182 of the English edition, figures 171 and 243 of the French edition). I am indebted to Gary R. Greenfield of the knowledge of this fact. Indeed the two realizations are quite independent, and based on different ideas. In the present case, the idea was to look for simple knots from some of the internal edges of a dodecahedron (an internal edge, joining two vertices, is located inside the convex hull of a polyhedron). The sculpture will be placed in the other rear vertex of the triangle.

Figure 9 : Holden-Rips 4- Link, Philippe Rips, 15x15x 15, 2007

The last sculpture, again made by Philippe Rips, will be placed in the front vertex of the triangle. It needs some preliminary comments.

The general starting idea was to try to relate an object to some knots that may characterize it. At the last ISAMA Conference in Valencia, I learned about the works of Dmitri Kozlov [13] who has been independently working

with this idea. My own approach was to begin with polyhedrons. A preliminary study should be to know which knots can be made from a given polyhedron considering not only its exterior edges, but also its interior edges. The first step is to look for the simplest non trivial knots, the trefoils then more generally the n-foils. Cellular decompositions of polyhedrons should be used in a second step.

Frames in our space, which do not need to be orthogonal, are attached with trefoils : they are represented by three rods in general position. So that when one looks for trefoils created from the edges of a polyhedron, one has to look at trios of edges defining a frame.

Philippe Rips, who first worked on tensegrity and tepees and then on some classical objects, got interested in the problem. Given its complexity, he chose to work on the truncated tetrahedron : note immediately that it looks a little bit like the Boy surface. Here is this truncated polyhedron (Figure 10), with a circular hole in each face in order to show some convenient internal edges.

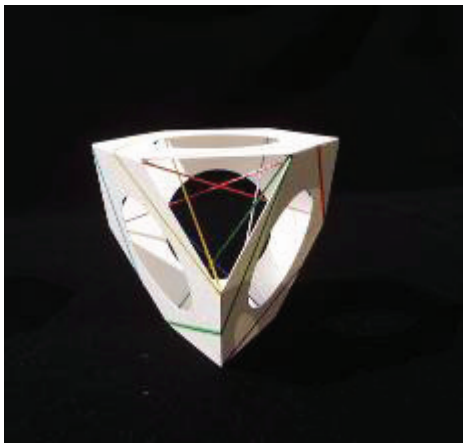

Figure 10 : Philippe Rips, Two internal views of a truncated tetrahedron, up and down, 2008

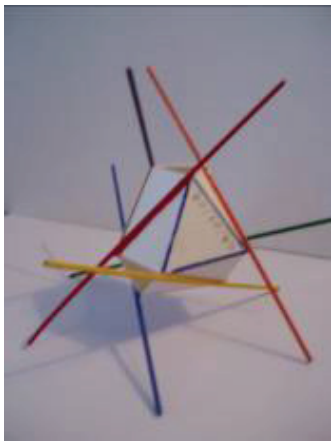

Figure 11 : Philippe Ripps, The heart of the tetrahedron, 2008

As one can see better from figure 11, by a circular permutation, we get five internal edges from one first, joining a vertex of the polyhedron to an opposite one. We get three couples of edges A = (a, a'), B = (b,b'), C = (c,c'), two edges of any couple being more or less parallel, so that the edges of any triple (x,y,z) such that x is in A, y is in B and z is in C and x,y,z are in general position.

Starting with the triple (a, b, c) and, in order to illustrate a self-intersection, imposing that any letter appears twice, we get the four triples of frames : (a, b, c), (a, b', c'), (b, c', a'), (c, a', b') The code of colours is here : a = blue, b = yellow, c = red, given rise to a trefoil coded in white; a' = green, b' = orange, c' = violet , so that (a, b', c') (respectively (b, c', a'), (c, a', b')) gives rise to a trefoil coded in blue (respectively in yellow and red).

We now have a few pictures of the set of the four trefoils associated with the truncated polyhedron (Figures 12 and 13):

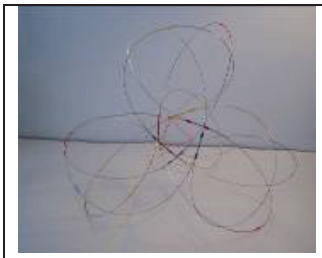

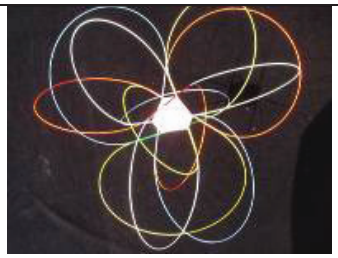

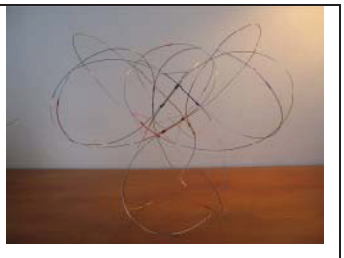

Figure 12. Philippe Rips, The Treasure of the Tetrahedron, 30 x30x 30, 2008 (middle :

Figure 13. Philippe Rips,

view from the top, left and right : front view)	**The Treasure of the Tetrahedron, 2008** (up or down)

As we know, Philippe Rips likes to produce flexible objects ; his home will resist any kind of seism.

Figure 14. Philippe Rips, Rips home, 2008

The man sitting is a mathematician thinking about the open problem of finding the equations of the trefoils, (right, left, linked) related to a Boy surface.

Acknowledgements : Cyril Vachez put me in contact with Christophe Delsart and Yvan Ngnodjom, two students, first ignoring mathematics, from the Institut Multimedia of the Pôle Universitaire Léonard de Vinci. François Apéry gave them the equations of the 3-Boy surface so that Christophe and Yvan succeeded in visualizing the folly. I am happy to thank Cyril, Christophe, Yvan, François and Philippe Rips who has built such an interesting home. It is a pleasure to thank Nat Friedman for his linguistics improvements and for introducing B. Sanderson presentation of the Boy surface.

References

[1] Apéry F. La surface de Boy, Advances in Math., 61, 3, (1986) 185-266.

[2] Apéry F. Models of the Real projective Plane, Vieweg Verlag, Wiesbaden, 1987.

[3] Apéry F.Constructing wire models, in Mathematics and Art (C.P. Bruter Ed.), Springer,

Berlin, 2002, 179-200.

[4] The ARPAM project. Available on line at httt://arpam.free.fr and http://hermay.org/ARPAM/

[5] Brem U.: How to Build Minimal Polyhedral Models of the Boy Surface, The Mathematical

Intelligencer,12, (1990) 51-55.

[6] Colonna J.F., http://www.lactamme.polytechnique.fr/Mosaic/images/SBOY.41.D/display.html

[7] Denner R. , Versions polyédriques minimales de la surface de Boy, Quadrature, 70 (2008), 31-35.

[8] Fomenko A. Visual Geometry and Topology, Springer-Verlag, Berlin, 1994.

[9] Francis G. A Topological Picturebook, Springer-Verlag, Berlin, 1987.

[10] Holden A. Shapes, Space, and Symmetry, Columbia University Press, 1971 (published in French by CEDIC-Nathan, Paris, 1977)

[11] Jeener P. http://www.poleditions.com/jeener/biblio.htm

[12] Kirby R. What is Boy surface, Notices of the AMS, 54, 10 (2007) 1306-1307.

[13] Kozlov D. Topological Knots and Links as Point Surface Structures of 2D manifolds, Proceedings of ISAMA '08, 79-87, www.isama.org/hyperseeing/, May/June 2008.

[14] Petit J.-P. et Souriau J. Une représentation analytique de la surface de Boy, http://www.jp-petit.com/science/maths_f/boy/f5101.htm

[15] Petit J.-P. Représentation …d'une surface de Boy,

[16] Polthier K. http://plus.maths.org/issue27/features/mathart/index.html

[17] Sanderson B. Boy's will be Boy's, http://www.warwick.ac.uk/~maaac/proj.pdf

[18] http://en.wikipedia.org/wiki/Boy's_surface and http://fr.wikipedia.org/wiki/Surface_de_Boy.

Period in Progress: Painting Music

Douglas Peden
3327 RT 22, Essex, NY 12936-0003
Email: *dpeden@westelcom.com*

Abstract

This paper discusses a recent development in my painting style, which is translating real sound and music into painted images. This is an extension and new direction of my "Wave Space," gridfield paintings last discussed in the electronic journal *Hyperseeing*, July-August 2008 issue. The procedure and results are discussed with a concluding example of a finished painting. In that my paintings are based on a concept called Gridfield Geometry, a pictorial review of its construction is given in the Appendix for those unfamiliar with my work.

Thesis Development & Discussion

We are familiar with the fact that the purpose of a music score is to communicate to a musician, from *symbol to sound,* a piece of music. Indeed, we can sometimes appreciate the score itself as visually beautiful — a work of art. However, my thought was to turn the process around and transform a piece of music from *sound to symbol* in a painting. While others may have pursued this goal, for me it was "another road never traveled by [1] [2] [3]." So, let's travel it and see where it leads.

To illustrate how I transform music to gridfield imagery, I have composed a short melody of seven measures, as scored in Figure 1. I will demonstrate the procedure using a *crossfield* [4] grid system (see Appendix). An *interfield* [4] example will be shown later for comparison. First, I translate the melody to a Cartesian grid (graph paper geometry), as illustrated in Figure 2. This grid defines my initial sound and time coordinates and most accurately translates the sound of music to images. In the following examples, I will treat the y-axis as tone, or pitch, and the x-axis as time. For my y-axis, I assume a chromatic, i.e., semitone, scale; that is, a 12 step scale of distinct sounds that is repeated every 12 units at a higher or lower pitch. The time scale can be in units of time or in the form of music symbols, i.e., notes, such as whole, one-half, one-quarter, one-eighth, etc., that have their own time durations. I chose a time scale measured in 16th note units, based on the shortest sound interval in the piece.

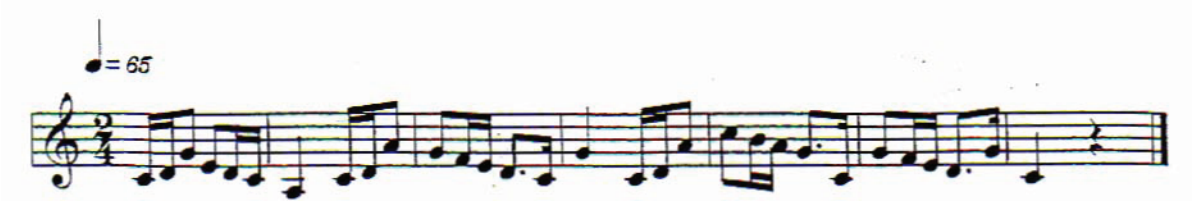

Figure 1: *Score for a* **s***even measure melody.*

This simple translation gives my first example of music represented as a gridfield — an image familiar to musicians as piano roll notation. By erasing the visual distraction of the grid, the isolated sound events and melody are represented simply as a relationship of rectangular shapes — Figure 3.

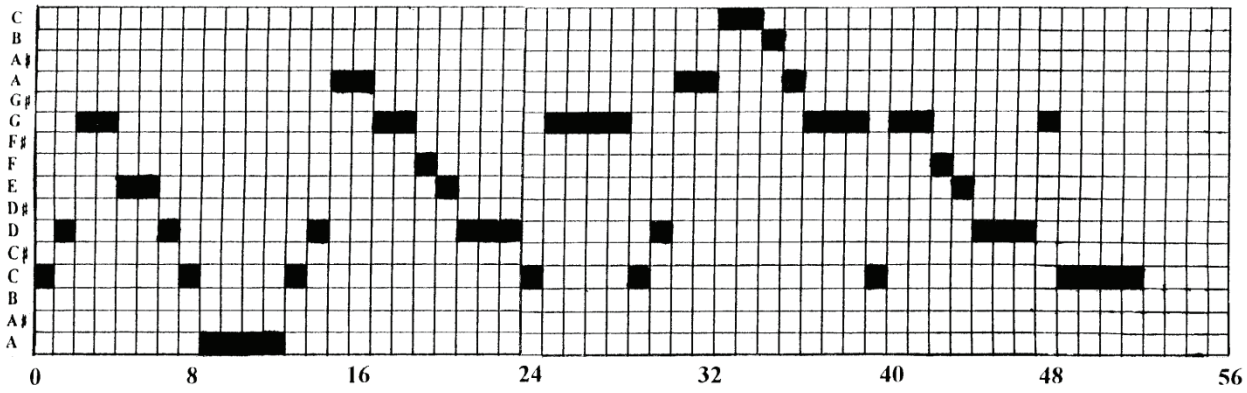

Figure 2: *Melody translated to Cartesian grid — piano roll configuration.*

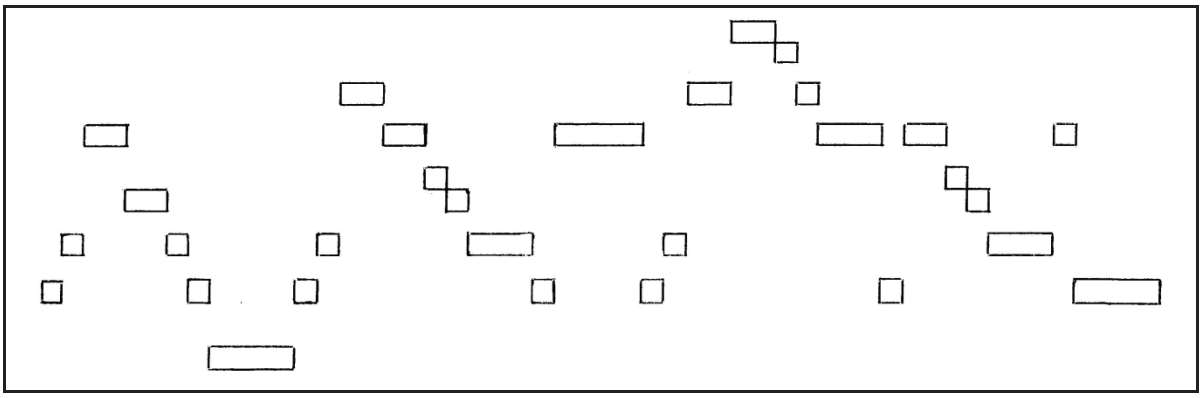

Figure 3: *Gridfield piano roll configuration of melody.*

For my next transformation, to a 1st generation crossfield grid (Figure 4), I chose a wave/wave field oriented in the y-axis direction with parameters wavelength λ=12 units, amplitude a=2. I then

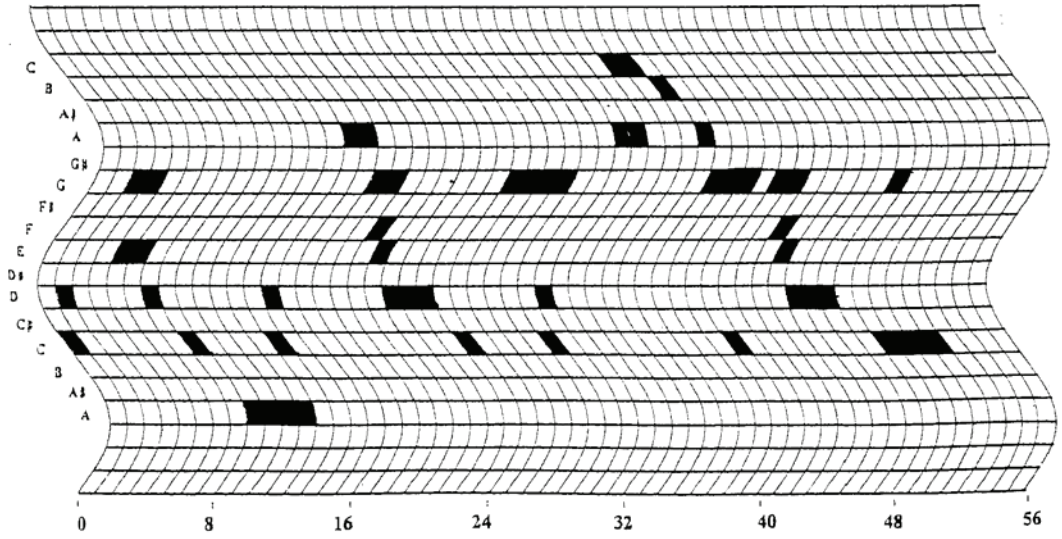

Figure 4: *1st generation gridfield with melody translation.*

translated the melody to the new coordinates as illustrated in Figure 4. Note that I have started the chromatic scale with "middle C" placed at the beginning of the wave cycle which, coincidentally, is the

starting note of the melody. One could start with any of the possible cell positions on the wave cycle; however, a different relationship of notes would result which may or may not satisfy the artist's expressive intent. After erasing the grid, the 1st generation gridfield melody is isolated as shown in Figure 5. For the melody to be transformed to a 2nd generation gridfield (Figure 6), I chose an x-axis wave field whose parameters are λ=8 and a=2 and plotted it into my 1st generation gridfield (Figure 4). I then erased the underlying *x*-axis field to create a 2nd generation gridfield, as in Figure 6, and translated my melody to it. Erasing the grid structure gives the final free-flowing imagery illustrated in Figure 7.

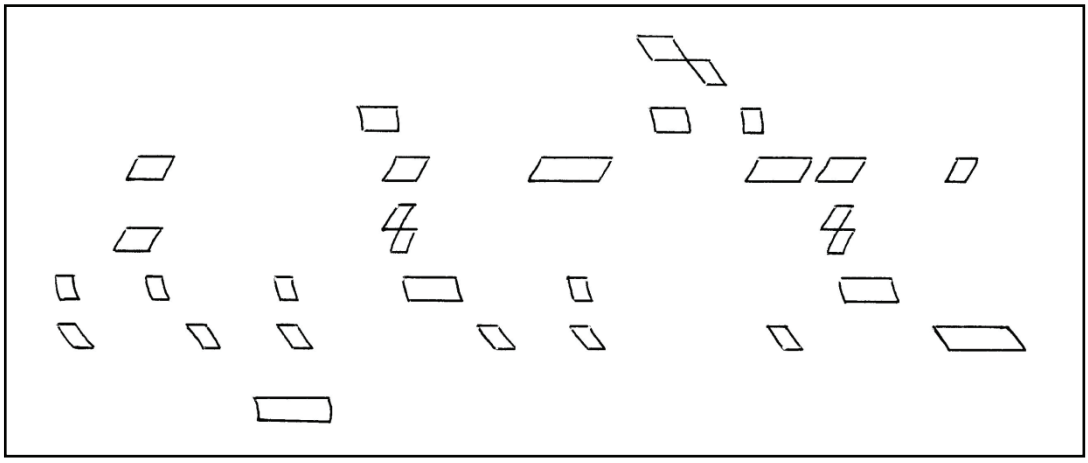

Figure 5: *1st generation gridfield melody.*

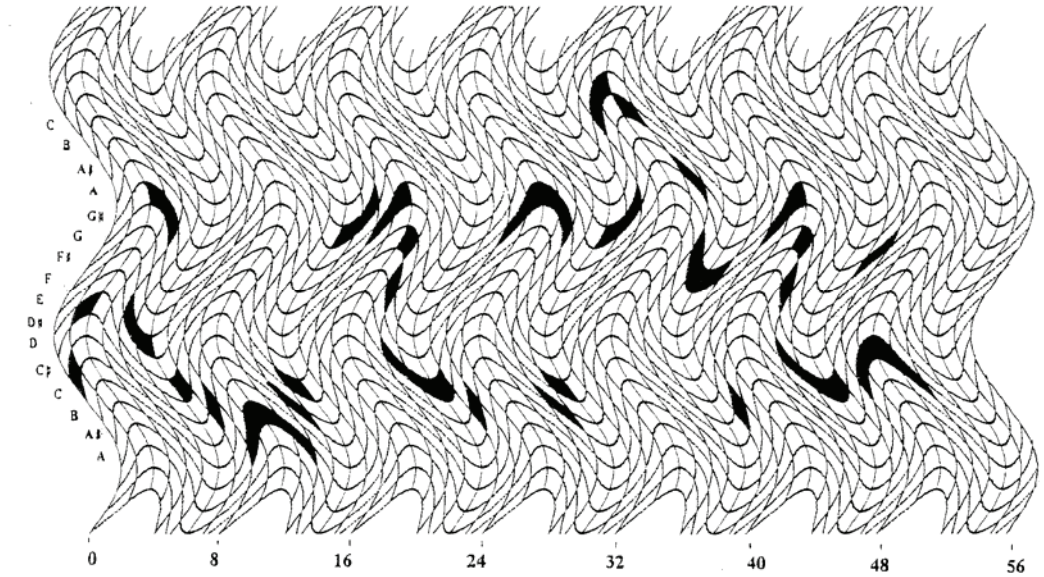

Figure 6: *2nd generation gridfield with melody translation.*

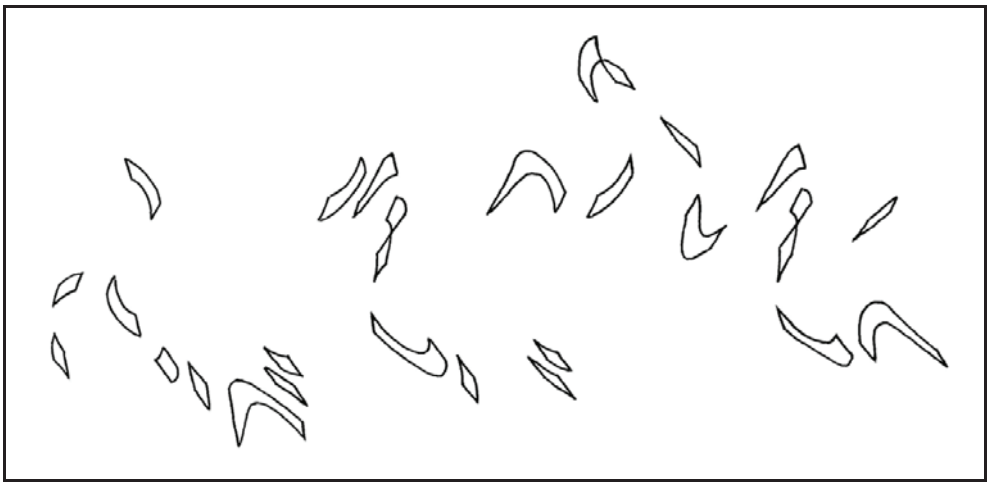

Figure 7: *2nd generation gridfield melody.*

This example could easily be seen as an arabesque, reminiscent of Arabic writing, but the message being presented in the imagery of the symbols of *visual music* rather than words.

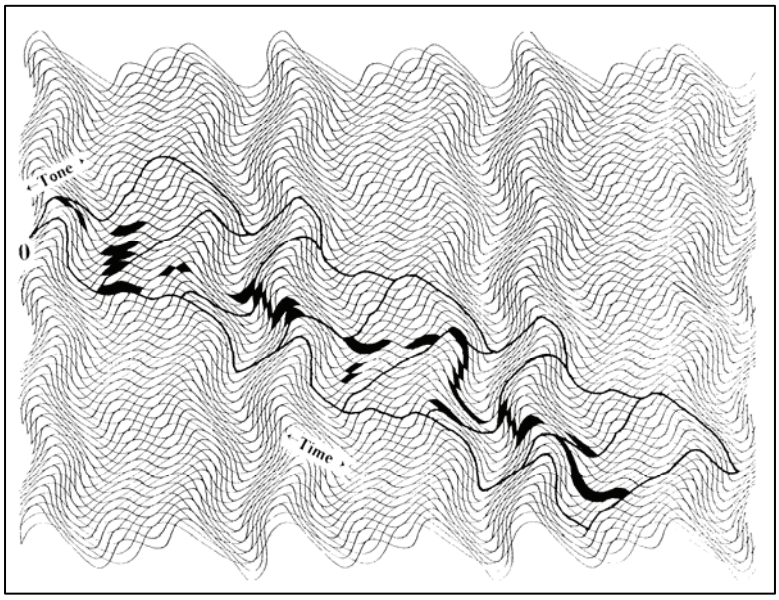

Figure 9: *Interfield Grid with Seven Measure Melody.*

A possibility that I haven't explored in a major work is using the above approach with an Interfield Geometry. In my Appendix review, I have included the development of an interfield grid at Step 10i. Figure 9 is an extended version of Step 10i, using the melody encapsulated in 7 measure sections (heavy outline) and 14 stave lines. The difference between this grid and a crossfield grid can be seen in the cell/note structure and the orientation of the coordinate axes, where we have in the interfield grid an x and y coordinate axes that has a variable, angular relationship dependent on the parameters chosen [4]. Though interfield grids are more complex and challenging, they are certainly open to added creative possibilities. Indeed, where there are computer solutions to the graphing a crossfield grid, as far as I know, there are no such interfield solutions beyond its 1st generation, and past this, I have to draw the grids.

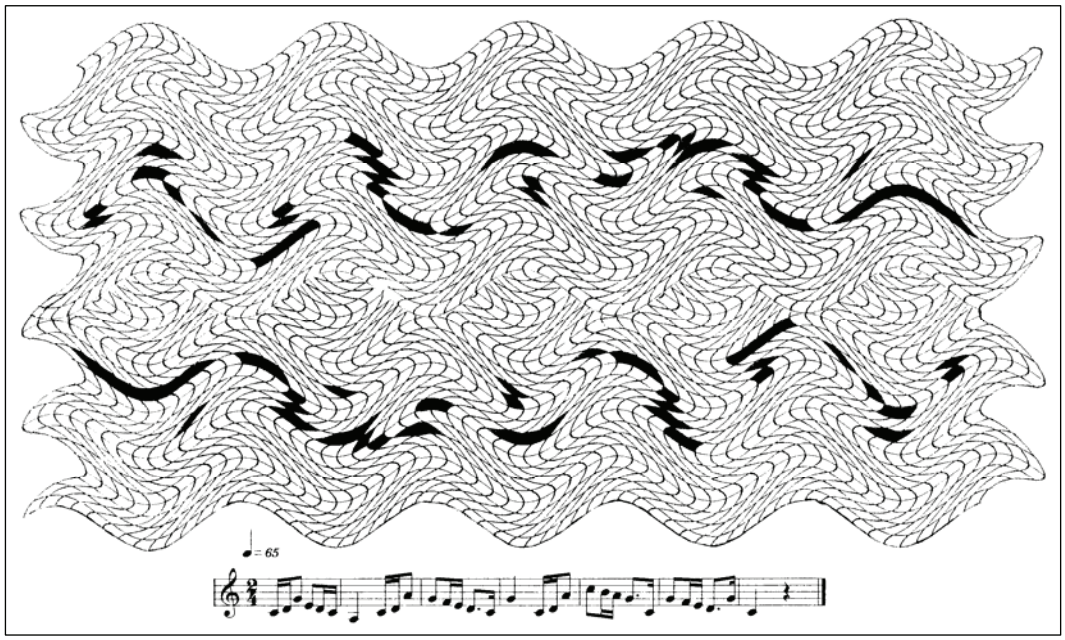

Figure 10: *Study #1.*

To further examine the process of translation and transformation of music to painting, I have included two study sketches, Figures 10 and 11. In both examples, I have used my 7 measure melody as the main theme. Indeed, the use and placement of the imagery of the actual score suggest to me the possibility of itself being the title of the painting. Arguably this is the same as a painting being identified by a foreign language which we may not understand. In fact, a musician, if asked where and/or what is the title could just whistle it. Or, we could have a computer button of sorts attached to the painting, as in some birthday cards, to periodically or on command play the tune or an orchestration of it — an electronic accompaniment to the piece. Reacting to the two sketches, I see the composition of Figure 10 expressing elegance — a comfortable symmetry brought about by the melody simply being repeated, rotationally translated 180 degrees. Figure 11 appears much more complex intellectually and emotionally — not as "comfortable" as Figure 10 — especially in the dynamically contorted center section. The addition of color could even make it more expressive.

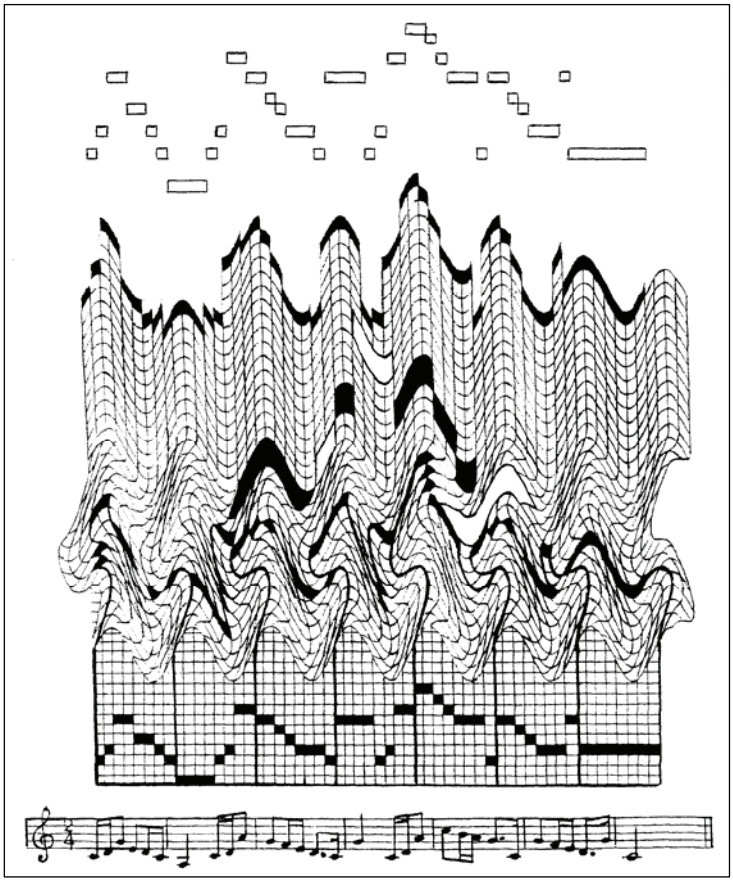

Figure 11: *Study #2.*

Using the ideas and melody presented above, the following two panel painting (Figure 12) is introduced.

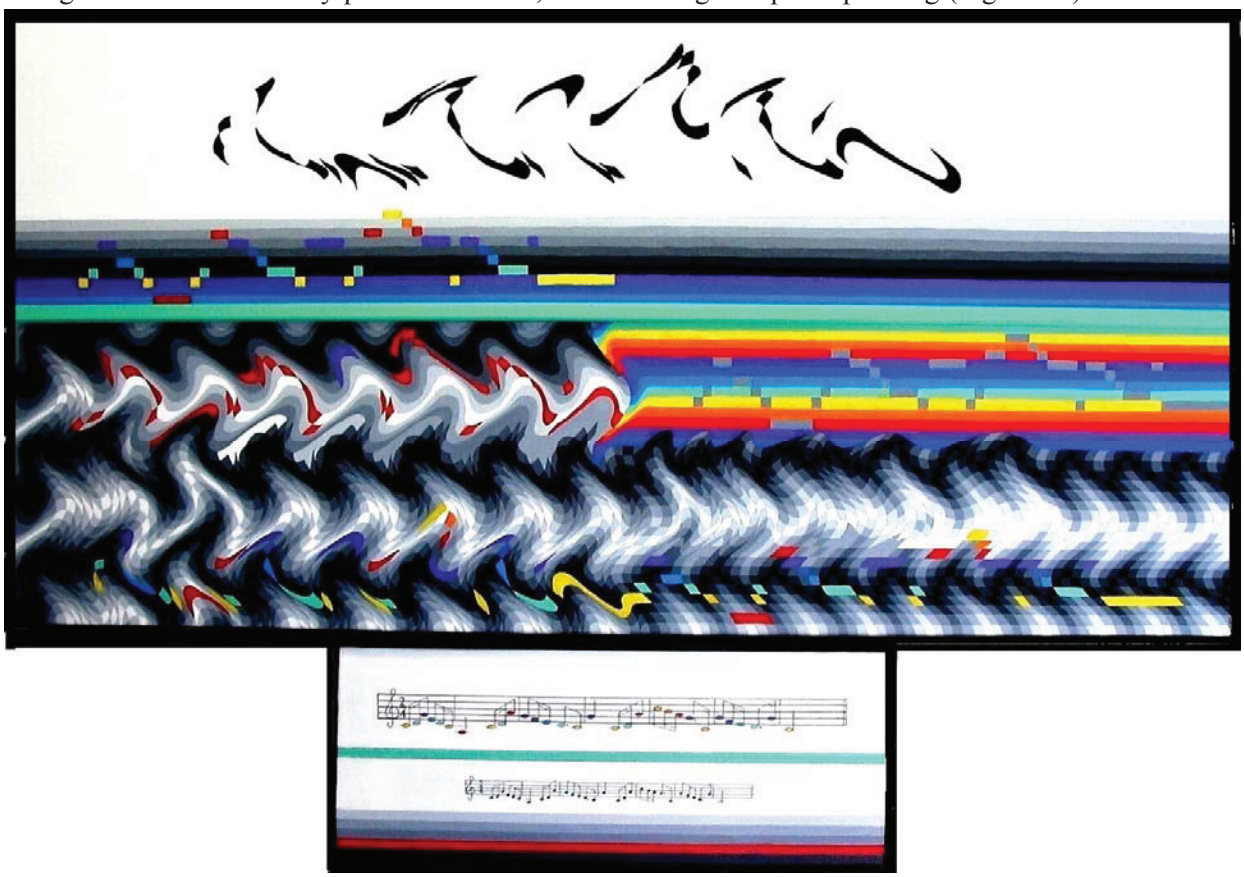

Figure 12: *Painting # 209: Variations on a Seven Measure Melody (2007).*

The design of this piece is taken from the *classical sonata form* in music literature, where the music begins with an introductory theme and progresses in time through a developmental stage, where the theme is subjected to various melodic alterations, inversions, fragmentations, and such, and is finally recapped, most often, to a clear and comfortable conclusion. In our case, the painting is designed to be read from the bottom to the top. For a detailed examination of my intention, start at the bottom panel where the melody is presented in its original score (the smaller image). Above this, the score/theme is enlarged and repeated, but with the black notes changed by a color coding based on the seven color sequence of the rainbow — red, orange, yellow, green, blue, indigo, and violet (ROYGBIV), to complement the seven notes of the whole-tone scale, i.e., the octave. I then intuitively chose the color yellow to represent the musical pitch of C and matched the remaining rainbow sequence to the pitch sequence. In the same manner, where the music staff is divided by line and space to indicate seven levels of pitch, the rainbow sequence is similarly applied as seen in the middle right side of the main canvas. Also, to complement the seven pitch octave, I used the option of coding the stave spaces according to seven levels of tone from white, through shades of grey, to black. This is seen in the tonal layering leading to the white space at the top of the painting. The technique was also used in defining the gridfield waves in the middle left section of the painting and in the cell variations so dramatically displayed in the supporting rhythmic structure in the lower section of the main canvas. The melody itself is seen painted in different gridfield

transformations, sometimes maintaining the color coding of the musical notes originally assigned to the score: One example is in the upper left section in the piano roll configuration. Two other examples can be seen in the lower section of the main canvas — one on the left in a 2nd generation gridfield; the other on the right in a 1st generation gridfield. Sometimes the melody is painted in a single color, as in the center left section of the main canvas in red, in grey on the right, and black at the top of the painting.

The reader may have noted a preference for the number 7 in this painting, including 7 color and tonal variations, 7 variations of the melody, and the melody being divided into 7 measures — even the date of completion '07. Believe it or not, this was not intentional.

Indeed, one might ask if this painting has any meaning beyond an exercise in pure design. Is there a more personal feel to it? In truth, as in my previous work [1], I have tried to present a narrative, or metaphor, through the organization of the abstract elements of art, i.e., line, space, color, rhythm, tone, texture; and certainly in this case, equivocate it to *program music*. Program music is where a composer attempts to interpret a scene or situation in the language of music — such as a landscape, as expressed in Beethoven's Symphony #6; or, a narrative, such as a hero's life reflected in Richard Strauss's *Ein Heldenleben*. Though this may seem a bit fanciful, I see the melody in my painting as a living thing, divided in a genetic structure of notes, episodically influenced and changed by its environment which is represented by color, line, texture, and gridfield space; and, in conclusion, emerging "triumphant" as a clear, "confident" and unencumbered entity at the top. Of course, any interpretation of such abstract work would ultimately come from the viewer's own experience and discretion, whether in some intellectual and/or emotional sense; or, it could simply be enjoyed as pure decoration — akin to a musical background.

All in all, this essay simply represents how my style has again changed from my various artistic periods, particularly through the inspiration of music. I have also tried to express an artist's constant search for personal meaning; and hopefully, suggest to others new ways to express themselves through art.

References

[1] Electronic Journal *Hyperseeing*: Issues: 04/07; 06/07; 09-10/07; 11-12/07; 01-02/08; 03-04/08; 07-08/08.

[2] Douglas Peden. (2001) The Influence and Use of Music and Mathematics in My Art, *Bridges: Mathematical Connections in Art, Music, and Science,* (ed. Reza Sarhangi). Central Plain Book Manufacturing, Winfield, Kansas, pp 223-233.

[3] Douglas Peden. The Sounds of Silence, *Symmetry: Art and Science - 2004-Sixth Interdisciplinary Symmetry Congress and Exhibition of ISIS-Symmetry*, pp 198-206.

[4] Douglas Peden. (2002) GridField Geometry, *Bridges: Mathematical Connections in Art, Music, and Science,* (ed. Reza Sarhangi) Central Plain Book Manufacturing, Winfield, Kansas, pp 117-123.

Appendix: GridField Construction Pictorial Review

Steps 2, 5, and 8 indicate a set of wave/wave fields chosen in the construction of the three crossfield grids at Steps 4, 7, and 10c respectively. These grids were achieved by erasing the y-axis field at Step 3, the x-axis field at Step 6, and the x-axis field at Step 9. The interfield grid at Step 10i was realized by erasing the y-axis field at Step 9. I have also shaped it to its coordinate axes, as done in Figure 9. The black cells represent the 12 notes of the chromatic scale and their transformations in space and time in the 1st, 2nd, and 3rd gridfield generations, Steps 4, 7, 10c and 10i respectively (10i is a 1st generation interfield grid). The second set of black cells in Steps 10c and 10i show how the shape and time of the same 12 notes change if I had extended the starting sequence for another wave cycles in either direction in order the raise or lower the pitch.

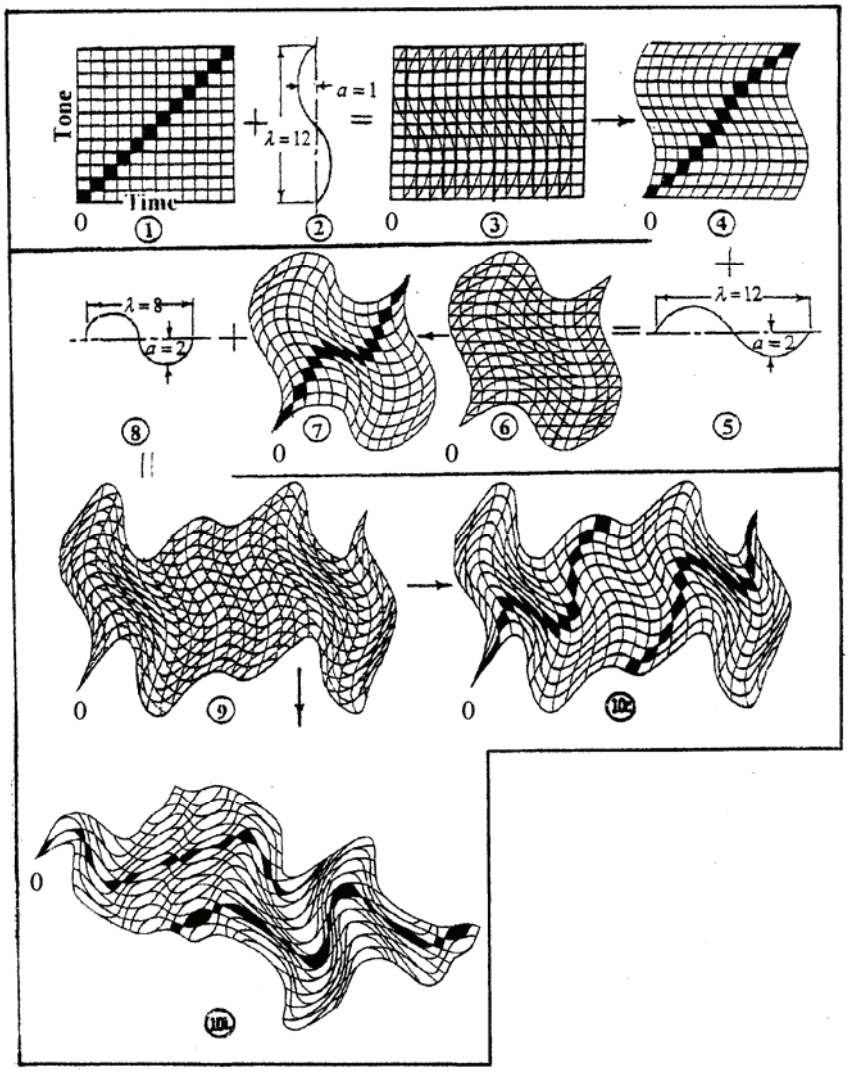

Three Crossfield transformations at Steps 4, 7, 10c. One Interfield transformation at Step 10iStep 10i.

Beading in the Stream of Consciousness

Donna L. Lish
129 Center St.
Clinton, NJ 08809
Web: www.libeado-designs.com
Email: *dlish5@embarqmail.com*

Abstract

Beading, using the anti-clockwise spiral of the peyote stitch is implemented in the progression of thought processes as a meditative art form. A sequence of mandala-like studies exemplifies diverse departures of time-marking experiments in design and color.

The supreme meditative element in my sculptural textiles is the repetitive rhythm of stitching: crocheting, knitting, and beading. Coalescence of each process, integrated with psychological foundations that impact the work is the main concentration which conducts each construction.

For the beaded forms featured here, the spiral, emulated from nature and considered in certain points the most perfect of shapes, is the chosen application. The peyote stitch and network of one threaded bead at a time in ascending rows form the strategic sequence of the circular or elliptical array, as in Figure 1.

Figure 1. Coptic Key- the center of the spiral progression, regarding light, photon, in the quantum realm

Figure 2. Embrace depicts 3 cylindrical spirals

Spirals exist plentifully in the natural world (the nautilus, ram's horn, sea horse tail, pine cone). Spirals have been key to mathematical applications (golden mean spiral, female- curved; male-angled spiral). They have

reference to infinity, having no beginning and no end. They have been integrated in circuitry, where the life of electronic elements is extended due to the spring-like form, making the technology conducive to physiological implementation. Forty five rpm, seventy eight, and LP records mimic the smoothness of playing one side of the vinyl/celluloid disk or the other, in a spiral groove.

Figure 3. Channels was a challenge in design contrast.

Figure 4. Continuity, 16 in.hx8x5, liner fits in the spiral beaded tower storage- a funerary urn.

Artists have cited the spiral as symbol of continuity and have applied it to three dimensions. The linear helical rotation conforms to iteration of motif, as in the figure eight looping of rows in basketry, coiling in ceramics, and crocheting. Samples of cylindrical beading are seen in Figures 2, 3, and 4.

Figure 5. Fixation has additional rows in areas which yield an oval configuration.

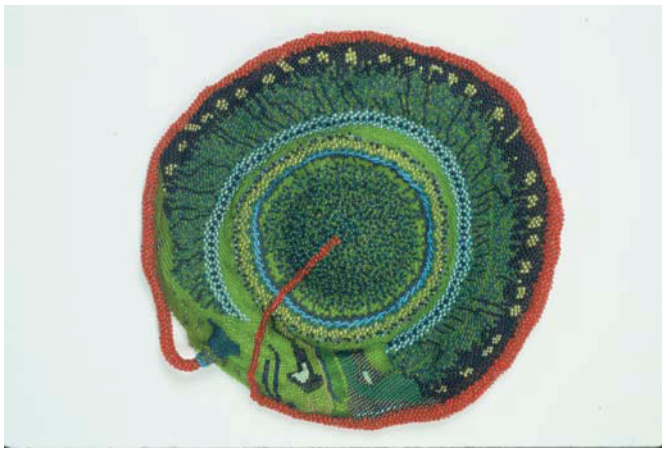

Figure 6. Red Sanity infers the frequency of crypts and furrows in the human eye. The red line is a way out.

Patterns may be accurately graphed prior to beading, recognizing how the beads acquiesce into the half-step format of the peyote stitch, linking beads alternately between those of the previous row. Though this method of planning in advance yields more probable outcomes, intuitive prediction in the stream of consciousness is my preferred means of formulating a pattern. As each addition relies on what preceded, a spiral progression provides the departure point for motif and scale to emerge. I commence with an extensive palette of compatible colors and a theoretical concept that are reconsidered in various degrees of detail, from one row to the next and one design segment to the next.

Figure 7. Yellow Quake has a crater as centrality.

Figure 8. Blue Quake is a monochromatic study.

In the anti-clockwise spiral (for this right handed beader) there is a starting point of 3 beads and there is a conceptualized design in mind generated and altered as successive complexities evolve. In the progression of the mandala shape, there is a definitive beginning and ending, the completion of which is often intuitively realized. Figures 5 through 10 illustrate six variations.

The stream of consciousness, comprehensively, is the resultant correlation of diverse elements: thoughts, dreams, images, sensory stimulation, mnemonic content; altered by possible physiological fluctuations. While progress ebbs and flows in art-making, the stream of consciousness moves forward and additions interplay. In this process, given any occurrence of variables, the direction could verge on chaos, which has its own set of laws. The objective is to maintain balance in orderly increases, which aligns anticipated results.

As mindset directs the chosen moment of consciousness, beading is the visual construct of communication on that predictable plane, like the scroll of script in a hand-written journal; internalized in an abstract realm. Additionally, beading is the collation of continuously refined influences in components of the stream of consciousness during art-making. In consciousness and divergent thought, my focus is on spontaneity- one bead increments, cumulative design elements in the marking of time where color and pattern syncretize and intertwine.

References

[1] John Briggs, *Turbulent Mirror,* Perennial Library, 1989

[2] Melchizedek Drunvalo, *The Ancient Secret of the Flower of Life,* Clear Light Trust, 1990

[3] Robert Feldman, *Understanding Psychology,* McGraw Hill, 1996

[4] Adam T. Hadhazy, *Twisted Transistor,* Discover Magazine, March, 2009, p. 12

[5] David Meyers, *Psychology,* Worth Publishers, 1998

[6] John White, *Frontiers of Consciousness,* Julian Press, 1974

Figure 9. Spectral Quake, with edging details for balance.

Figure 10. Galactic Quake is edged in a crocheted t of reflective fiber.

Comet!

George W. Hart
Dept. Computer Science
Stony Brook University
Stony Brook, NY 11794 USA
george@georgehart.com

Abstract

Swooshing across the science center atrium at Albion College, my sculpture *Comet!* is over 100 feet long from one end to the other. It consists of nine different orbs of powder coated aluminum suspended by chain from the ceiling, each between 42 and 48 inches in diameter. They can be seen as 3D slices of a four-dimensional sculpture which is visibly polyhedral at the start and gradually morphs into an intricate flower-like final form. Each stage has a darker core structure intertwined with a lighter tangle. The initial orb is colored with two shades of light yellow, successively deeper shades of orange are used in the middle of the room, and rich reds appear at the far end. Viewing each component in turn, the final orb can be understood in logical steps, like a mathematical derivation. On the construction day, after three years of planning, over one hundred members of the Albion college community—students, faculty, and others—worked with me to assemble it at a large public "sculpture barn-raising."

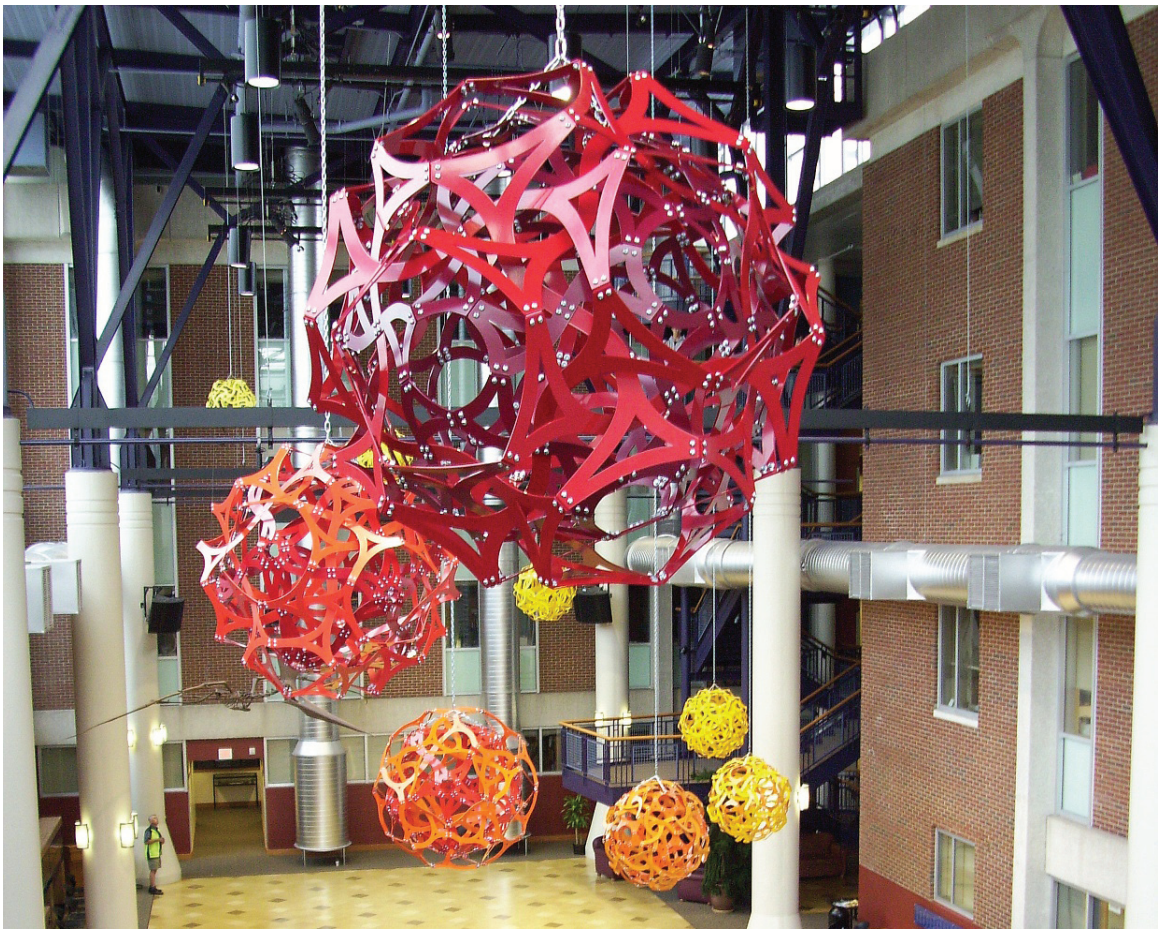

Figure 1: *Comet! aluminum, with steel connectors, 100'*

Design and Preparation

Mathematical sculpture celebrates the aspect of what it means to be human that centers on our innate attraction to form, pattern, and structure. I enjoy creating such artwork and involving others in the assembly process. Spread out over a period of more than three years, I led a project to create a large mathematical sculpture for the newly constructed Science Center atrium at Albion College, in Albion, Michigan. The project culminated in a public assembly event on Saturday, September 13, 2008, where thousands of precut metal parts were assembled into a series of colorful orbs and lifted into the air. The sculpture, called *Comet!,* is permanently suspended along a curved path in the atrium for all to enjoy. Figure 1 is a view from the end of the room closest to the ninth orb.

Comet! consists of nine orbs, each made of 90 laser-cut aluminum parts joined with 120 laser-cut steel brackets and held together by 600 nuts, 600 washers, and 600 bolts. That makes a grand total of 18090 parts not including the suspension chain and connection hardware. The laser-cut steel and aluminum parts were first powder coated in ten different shades, being careful to keep track of different shades for connector brackets with two different dihedral angles. Although I designed the sculpture and supervised its construction, this was certainly not a one-man job!

I was first contacted early in 2005 by Albion faculty with the idea that their new Science Center would be enhanced by the inclusion of a mathematical sculpture. After some discussions and planning, I visited the campus in October 2006 to present a talk on mathematical sculpture and view the site. On seeing the atrium space, I was attracted to the architectural design, which includes a floating bridge with a floating staircase down to the ground level, plus a well thought-out four-story staircase with varied projections into the space. Large glass walls to the outside and windows from surrounding offices allow viewing objects in the space from additional points of view. My main concern was the large size. I didn't think I could make something sizable enough to fit properly in such a vast volume. In discussion with the core group of Albion faculty on the project—David Reimann, Darren Mason, and Gary Wahl—we came up with the idea to have a multipart sculpture which would span across the space. They wrote a proposal for funding the project, emphasizing interdisciplinary connections between mathematics, computer science, and the arts, and pointing out the value of a public sculpture barn raising to the academic and broader community.

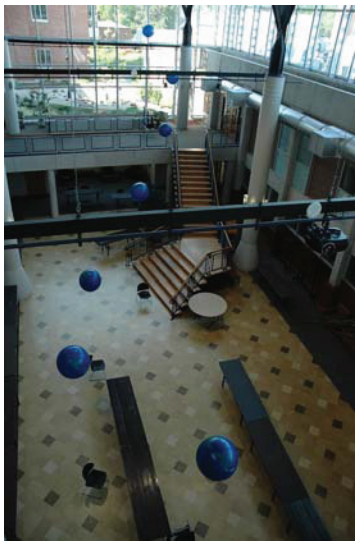

Figure 2: *Helium balloons, for positioning*

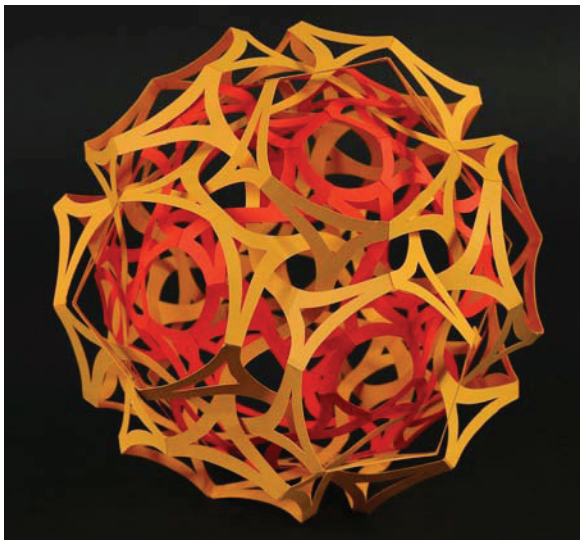

Figure 3: *Six-inch paper model of orb nine*

The proposal was approved, additional funding was also found, and I began detailed work on the design. The atrium roof is divided into nine bays by support beams and there were lights, dinosaurs, and projection equipment already suspended from those beams that had to be worked around. From the architectural plans, I selected approximate locations for the nine orbs to hang at the midlines of the nine bays. They would each hang from a "V" of chains tied to two dividing beams, so as to be clear of the existing obstacles. On my second trip to the campus, we placed nine helium balloons in the space to get a sense of the nine positions. We tied these to chairs so we could move them around and adjust the height of the strings. We viewed them from all vantage points and measured their positions. Figure 2 shows the balloons in place. From the balloon measurements, we made plans for chain to be suspended down from the beams to the appropriate height for each.

The path of orbs starts high at one end of the room, where it can be seen through windows from the outside street, swoops dramatically down towards the floor to engage the viewer, bends back and up to follow the curve of the internal stairway, then makes a reverse hook over the floating bridge for a close-up finish. Along the way, the path stays clear of the suspended fossil dinosaurs and tries not to block the light beam between a digital projector and its screen. By walking around and through the space, the viewer has opportunity observe the sculpture from above, below, and all sides.

I had considered many ideas and made many sketches for the design of the nine individual orbs. In the end I narrowed them down to two design proposals which I brought to the faculty at Albion for feedback. In Plan A, the nine orbs were identical in structure except that small curving appendages varied from one to the next to give a sense of a swimming motion. This underlying uniformity of design would have simplified the logistics significantly. Plan B involved nine different structures, entailing a much more complex design, fabrication, and assembly process, but would result in a much richer final result. I made a paper model of the ninth orb from the Plan B design, shown in Figure 3, to help communicate the richness of its ideas. In the end, the Albion faculty opted for the more complex Plan B, in part because math faculty liked the analogy between a formal mathematical proof and a series of sculptural forms which start at a familiar place and evolve stepwise to an ultimate result.

To deal with the assembly-day logistics of making nine distinct orbs simultaneously, we expanded the faculty committee by a dozen members. Each orb involves a highly

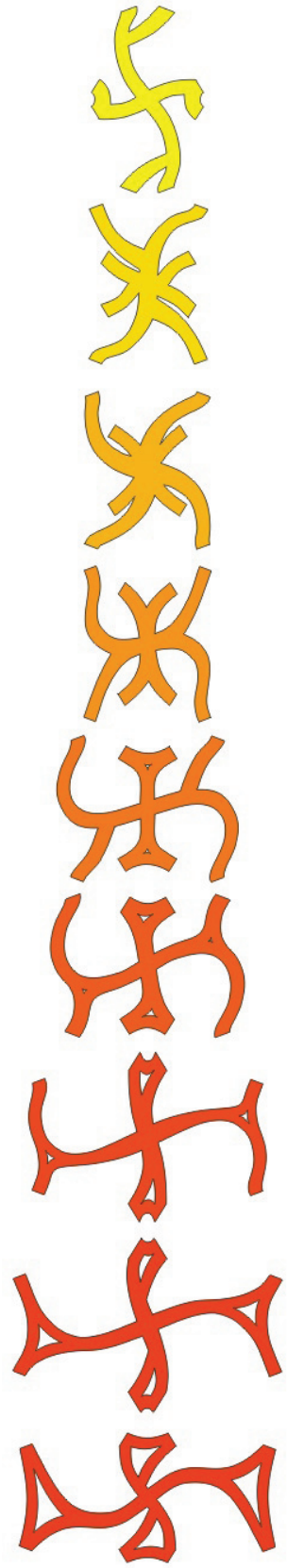

Figure 4: *Nine orbs' component parts*

intricate and slightly different interweaving of component parts, so there would be too much going on for me to supervise alone. We planned instead to build one orb the evening before the main event, with a committee of sixteen faculty members helping me. I would train them in the procedure and coach them about foreseeable problems to be alert for. Then on the assembly day, the remaining eight orbs could be assembled by the public in eight groups, with two trained faculty serving as leaders at each table. Additional faculty enlisted and this plan turned out to work well.

Figure 4 gives a summary of the nine shapes in glyph form. Each pattern shown is repeated 30 times, rotated once into each of the 30 face planes of a rhombic triacontahedron. [1] Thus the overall form can be understood as a subset of a stellation of the rhombic triacontahedron. This is not a familiar structure for people unfamiliar with polyhedral geometry, but if we draw the two diagonals in each rhombic face of a rhombic triacontahedron, one sees that the short diagonals form the edges of a dodecahedron and long diagonals form the edges of its dual icosahedron. As these Platonic solids are well known, I chose a design very close to this structure for orb one. To enrich it and provide landmarks, the vertices of the dodecahedron are shown as open circles and the vertices of the icosahedron are made in a pentagrammatic star form. From that starting point, a series of gradual morphings, crossings, and piercings lead ultimately to the final orb nine.

The next step was to make detailed engineering designs and prepare files to send to the laser cutter. This involves keeping track of thousands of little details involving spline curves, bolt sizes, hole diameters and clearances, material thickness, bending radii, dihedral angles, weight, tensile strength, etc., while not losing sight of the overall artistic vision. For visualization of the nine overall forms and verifying that the components can be physically positioned without intersecting each other, I used my own sculpture design software, described in [1]. Final drawings were prepared with general purpose drawing tools and sent to the laser cutter. As a check, to make sure that all the parts actually mate together as planned, we asked the laser cutter to prepare an initial ten parts of each shape to use in a fit-test.

I flew out to Albion for a third visit in August 2008. We put together the test parts and verified that no corrections were needed in the parts design. Figure 5 shows one of the test assemblies of the uncolored aluminum components. At that visit, we also finalized the color choices to tell the powder coating company. I wanted the orbs to gradually change in color from one end of the room to the other. I also wanted each to be two colors: one color for the 60 outer components and a slightly darker color for the 30 inner components. In addition there are 60 brackets connecting inner parts and another 60 connecting outer parts, and each bracket must match its part in color. To minimize the number of colors required and introduce another level of continuity, we chose to have the darker color of each orb be the same as the lighter color of the next orb. With this design, a total of only ten colors were needed: yellows, oranges, and reds. The remaining parts were cut, all were powder coated, chains were suspended from the ceiling beams, the sculpture barn raising was advertised, food was ordered, etc.

Figure 5: *Test fit, with David Reimann*

Figure 6: *Sculpture barn raising activities.*

Construction

After careful planning and organized worry on my part about every possible thing which might go wrong, the assembly itself went off with no problems. Nothing got lost; not too many parts got scratched; nothing fell and was bent; no maniacs ran off with key components. One connection was a bit tight and it helped to have small hands to get its bolts in place. Some scratches occurred, but we had planned for this and had enough spares. Overall, everything went smoothly.

On the afternoon before the construction, I flew out to Albion for my fourth time. On the way from the airport, we picked up the parts from the powder coater, finished just-in-time. That evening, the sixteen group leaders and I assembled orb number nine and got it suspended it above the atrium bridge. The parts went together exactly as planned and we worked out a good way to lift orbs into position and shackle them to the chains, which had already been installed. In preparation for the next day's construction, I explained to the group leaders how each of the remaining orbs was in some ways the same and in other ways different from the one we had built.

At the barn raising, over one hundred members of the Albion college community—students, faculty, and others—participated in the construction over a period of several hours. We worked around eight tables, each with two faculty build leaders and changing groups of volunteers who came and went according to the free time in their schedules during the day. I ran back and forth between all the tables checking on everything and debugging occasional problems. Figure 6 shows various views of the day.

Each orb has 30 inner parts, which each mate via angle connectors to four others. The participants must be careful not to reverse parts or mis-connect them. The bolts must be tightened securely, so we checked there is no vibrational buzz when tapping on everything. Then the 60 outer parts were connected. Each mates to the center of one inner part and to two other outer parts. At this stage there plenty of room for confusion and mis-connected parts. Occasionally, components had to be unbolted and replaced in the correct orientation. Getting every single bolt tight was something of a challenge because if we tapped and heard a rattle it was not always easy to locate the source of the sound. Eventually everything was ready to hang. Three of the bolts in each orb were replaced with eyebolts for the chain to connect to. These points were chosen symmetrically so each orb hangs with a three-fold axis vertical. We took a documentary photo of each (see Figure 7) and then the buildings staff were able to raise them up into position with no difficulties.

At the end of the day, it was deeply satisfying for this artist to see the fruits of so much labor hanging ripe for all to savor.

Conclusion

A collaborative artwork such as *Comet!* is an iconic way to illustrate the ties that connect art, math, computer science, and engineering. Academics sometimes need to be very narrow and compartmentalized when working deeply in their own specialties, so it is useful to also create a social event and a permanent sculptural reminder of the broader inter-relatedness of our fields. A sculpture barn raising event creates a community while creating a tangible focal point that manifests the common bonds between disciplines. In the process, many students are exposed to a new perspective on mathematics and computer science, which may have a subtle long-range impact on their career decisions. Informal feedback from students, faculty, and community members indicates that the *Comet!* project was a great experience for all participants. For more information, many additional images documenting details of the design, preparations, and the construction event are available online at [2]. In addition, there is an entertaining time-lapse video of the entire construction and hanging process.

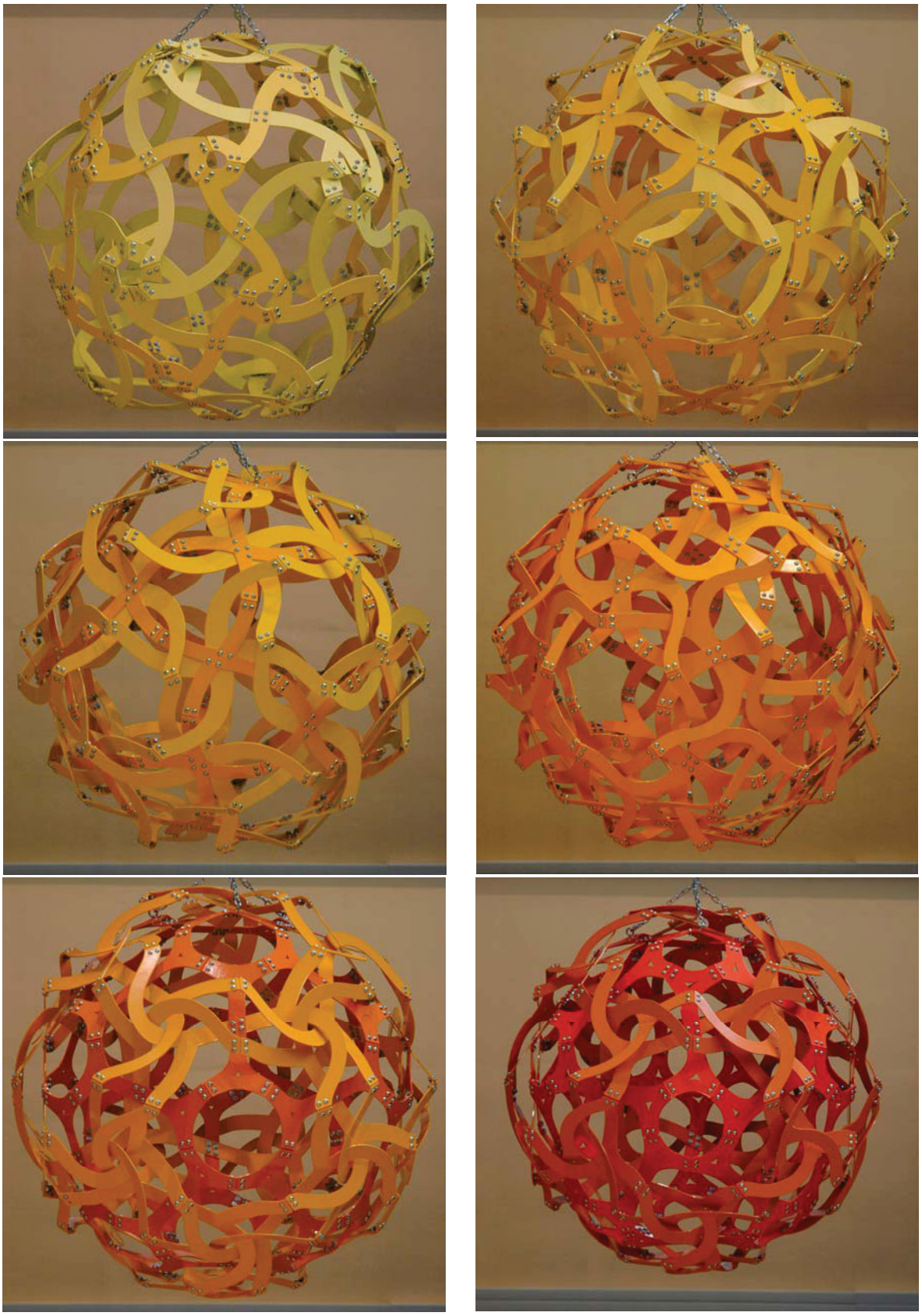

Figure 7 (begins): *Comet! nine individual orbs*

Figure 7 (continued): *Comet! nine individual orbs*

Acknowledgments

This was a community art project and I am happy to thank many people who contributed in many ways, especially all the students and others who attended and participated in the assembly event. Prof David Reimann, chair of the Albion Mathematics and Computer Science department championed this project, found funding, and took care of many aspects of the organization. Professors Darren Mason (Math/CS) and Gary Wahl (Art & Art History) provided a great deal of additional support throughout all its stages. The additional group leaders who participated by attending the previous night's practice preparation and then leading the construction all day at one table are: David Anderson (Math/CS), Amy Bethune (Chemistry), Mark Bollman (Math/CS), Lynne Chytilo (Art & Art History), Michael Dixon (Art & Art History), Andrew French (Chemistry), Vanessa McCaffrey (Chemistry), Karla McCavit (Math/CS), Carrie Menold (Geology), Robert Messer (Math/CS), Aaron Miller (Physics), Daniel Mittag (Philosophy), and Martha O'Kennon (Math/CS). The local company Caster Concepts provided the laser cutting and Finishing Touch did the powder coating. Figure 7 photos courtesy of Gary Wahl; others by the author.

References

[1] G.W. Hart, "Symmetric Sculpture", *Journal of Mathematics and the Arts*, 1:1, pp. 21-28, March, 2007.
[2] G.W. Hart, http://www.georgehart.com

Stephanie Strickland's Poems

Stephanie Strickland and Nat Friedman

Abstract

Stephanie Strickland will present her collaborative digital Flash poem slippingglimpse. *Here, she includes ten of her print poems influenced by mathematics, on which Nat Friedman offers his reflections. The first four poems are from* True North*, University of Notre Dame Press, 1997.*

STRIVING ALL MY LIFE

Maxwell said: There is no more powerful way
to introduce knowledge to the mind than...as many different
ways as we can, wrenching the mind

away
from the symbols to the objects and from the objects
back to the symbols.

Maxwell said: I have been striving all my life to be free
of the yoke of Cartesian co-ordinates. I found
such an instrument in

quaternions. Do I need *quaternions*
to talk about light?
Alas,

the square of quaternions
is negative. But Gibbs's vectors, uncouth
seemingly, work

well, in *any* dimension, with a very
great capability for
interpreting space relations.

Rukeyser said: Critical minds
that approach the world with love
have but one possible

defense—to build a system.
Rayleigh said, I protest
the compression.

Gibbs: I myself concluded
that the paper was
too long.

What struck me in the first stanza was that "different ways" referred to hyperseeing, seeing from multiple viewpoints, which I feel is super basic. This is also particularly true in personal relations. Concerning symbols, I recall Paul Halmos saying that you have to explain it in words, not symbols. That is, words were more intuitive, and closer to the essence. NF

WHO COUNTS, COUNTS

Baby and you
—and me,
we will make three,

but baby-and-me
are different: we're two-
who-are-one.

So, together, five—or we *were,* when
I-was-two-in-one,
but

wishing, it was so hot
that summer, I was wishing
we were two.

You and me, we've been two
who were one as well, but nobody thinks
that's the same, or

a problem. How
many of us were there *really,*
when

I-was-two-who-were-one? Was it
five: us-two + we-three?
Or three?

Or two.
You said, “If it came
—God forbid—to that, well then,

just
two.” You meant, should it come,
Godsent, to some crux,

should push
come to knife,
just

Baby and you.

Having created sculptural forms, I've imagined what an amazing miracle to have a person forming inside yourself. NF

THE WHOLE

—it means force is deformation,
it means
what is assumed
fundamental

is derived: it means a point is a collection—reform-
ulating physics—a collection of twistors (there) at that point: all possible
lightpaths. Maybe all

calculation

should use complex numbers.
Maybe

the real world we see
is a real projection of something
—complex: the solid

part of a table, *one part,* each quadrillion. And between these
bullets?

Nothing

is less certain. The party of the hard part, the a-for-apple
real part, halts and stops us: where and when;
but the b-for-broom sweeps

through in flashing angular directions,
set spinning as it swings—and
going somewhere:

homing to the pole
of its Polar-i-
za-tion.

It was an epiphany when I realized the world was described by complex numbers, and i *was really as real as 1, in the sense of mathematical reality, which is our description of physical reality. Richard Feynman describes properties of light beautifully via complex numbers. But the question remains, how can light be both a wave and a particle? NF*

PRESTO! HOW THE UNIVERSE IS MADE

On your Mark, one first O/riginal Form; *Get set,* a second
angular Segment; *Go*—the next step, a Rule replacing
each straight side in the first by the second; if I take

a box and for each side of that box substitute a cone
or peak, to make a kind of star—then do *again*
what I did before: take the star-box

and where I find a straight-line replace it
with a peak, to make a *starrier* star, nesting the shape
even deeper in the figure, re-placing

peaks to make a Star-in-the-Box! Or, a Diamond-heart-
Star at *every* level (a shape self-similar); a shape
of extreme complication, in only a few—in five—

iterations, it already reads as texture and is rapidly
sinking as it plummets, repeating, into bonded
lock, where photons mediate, shunting between

heavy center, vibrant orbit. Or *deeper,* look. No,
look, a quantum leap: the burst box—the born star—is re-
emerging on the line, on the line *or/and*.... Repeat:

Maybe life did begin fractally. Benoit would like that. NF

The next six poems are from the manuscript, "Huracan's Harp": 150 was published in MiPOesias *2007; 6 and 69 were published in* Critiphoria *1, 2009; 35 and 64 will appear in* P-Queue *6, forthcoming 2009; 120 makes its first appearance here.*

150

how cuppa joe and doughnut are the same
what's one without the other everything
the other is or ever could be not twins

not reduplications the very tinny taste
of these militate against them what
matters Mo are holes and those no joke

The first line is already wonderful. I just had a vision of a doughnut morphing into a cuppa joe.

120

God having no need of names pre-Adamic Alone Prior
all ferriage raging crooning urge orchestrated if at
all in musing chaosmosis in some brico-logic order

all roiling vacuum mass/equivalent eager to emerge
or hardrock pulse liable to erupt but no well no faultless
glance no direct inspection or candid reflection

prompts muttering of good Whoa dude that's good
or hold on not good enough no God's template trigger
tripped by missing signatures like any other highspeed

collider detector system for matter supermatter metamatter
maybe metametamatter mother's name for mathematics
writing straight through space with curly angled fluid lines

Concerning seeing, Robert Irwin wrote an excellent book, Seeing Something Is Forgetting Its Name. *NF*

6

Grothendieck
sees everything globally from the beginning Hironaka
said *no coordinates no*
*equation*s

roller coasters have no sudden on
a dime
change of direction however steep
no cusp
no crossing through themselves—
their shadows do : sharp projections of the smooth

pulling back
to the smooth
from tangle local
problem disappears : only *global* lift
left

inside the crush cross point so multifarious—a many nenny
whorled
blow it up (gentle difficult
balloon work) make it
smooth

Roller coasters are great "curve in space" sculptures. Usually not knotted. NF

35

minimum somethings consist altogether of

4	corners
4	faces
6	edges
12	angles
1	insideness
1	outsideness
1	concavity
1	convexity
2	poles of spinnability
32	features

behavioral potential

axial rotation
orbital travel

expansion-contraction
torque (axial twist)

inside-outing (involuting-evoluting)
precession (axial tilt)

interprecessionings among plural systems
self-steering of a system (precessionally done)

some **powers** are only otherness-viewable
some only multi-otherness-realizable

"…not until a six
otherness appears remotely, approaches, and associates
with the fivefold system can the latter learn
from the newcomer of its remote
witnessing that the fivefold
system has indeed
been *rotating*
axially…"

I just learned that a tetrahedron has 32 features. NF

69

yes Jane it is regrettable that the mathematical
with so much to offer
by way of reframing should be in thrall
to such a degree to the defense & security retrenchment
agenda complete with strong support
for money-changers
the field's heavy lifting toward promotion of some singular
global threat (say terrorism) or space
settlement (after
the bombing stops) an Archimedean
precedent
http://www.google.com/search?hl=en&rls=GGLD,GGLD:2005-05,GGLD:en&sa=X&oi=spell&resnum=0&ct=result&cd=1&q=Grothendieck+mathematics&spell=1 Grothendieck
like Bartleby
refused

Makes one think mathematics can be a WMD! NF

∞ infinite ways to change continuously lapping licking staying
at (near) equilibrium

7 but seven stable ways to change abruptly *jump*
Hell's kitchen smoke plume fire cat
something's got to give it *duh*
does spectacular
collapse
or the baby's nap unfolding

stably disappearing stability a
ha downdraft snowflake oh also snow
ball rolling into mind soot chippiness ice

utter irrelevance
scale | laws | causes | radiation
to the form to
the gliding shape the wind the word the (class 4)
computation

The only stability is instability. NF

WORKSHOP: Unit-Weave the Cubic Polyhedra

James Mallos
3101 Parker Avenue
Silver Spring, MD, 20902, USA
E-mail: jbmallos@gmail.com

Abstract

The class of cubic polyhedra, i.e., the polyhedra having exactly three edges incident on every vertex, includes the tetrahedron, cube, dodecahedron, the fullerenes, and many others less well-known. They make a nice model-building playground for the beginner, yet there is a universality beneath. All polyhedra can be triangulated; the cubic polyhedra are exactly the duals of those triangulations. Cubic polyhedra can be *unit-woven* from identical die-cut shapes I call *twogs*. A deck of twogs small enough to store in the palm of the hand while weaving can make over 300 different cubic polyhedra. We will learn how to weave and unweave, spider-like from the hand, without the aid of a work surface; how to join three twogs at a vertex (that bit, always the same, is endlessly repeated;) how to close *rings* (borrowing terms from fullerene chemistry comes naturally;) and how to follow a *ring spiral code.* We will follow a ring spiral code to weave a shape someone else has "teleported" to us by text-message. We'll go on to discover and name some polyhedra ourselves. We'll finish with the brainier aspects as time allows.

Introduction

Building polyhedron models is always an exciting classroom activity, one usually associated with lots of building components spread out on a table, and a single model taken home. The power to build is the sort of power children yearn for, so no wonder model building gets their attention. It would feel even better to gain a power that is word-like in its ability to be reused and explored in new combinations. Weaving polyhedron models from *unit weavers* allows students to take home an inexpensive building set that can be worked entirely from the hand (in a car or on a plane) to make hundreds of different models from memory or written codes.

Unit Weaving

As has recently been proven [1], it is possible to weave any compact surface, so weaving all of the convex polyhedra is now small potatoes. We will tame ambition even further, limiting ourselves to weaving just the polyhedra where three edges meet at every vertex, the so-called cubic polyhedra. Given such a strong constraint on vertex-valency, it is possible to weave a polyhedron using short, identical, die-cut shapes. I term these flat identical shapes *unit-weavers*. The first unit-weavers, *IQ's*, were invented by Holger Strom [2]. My new unit-weavers, *twogs*, are easier to weave, and easier to understand visually, partly because they do not attempt to weave a closed-up

Twogs made their West Coast debut at the Bay Area Maker Faire in 2008 .

surface. (Twogs and IQ's are related to each other by a graph transform, so they essentially can weave all the same shapes.)

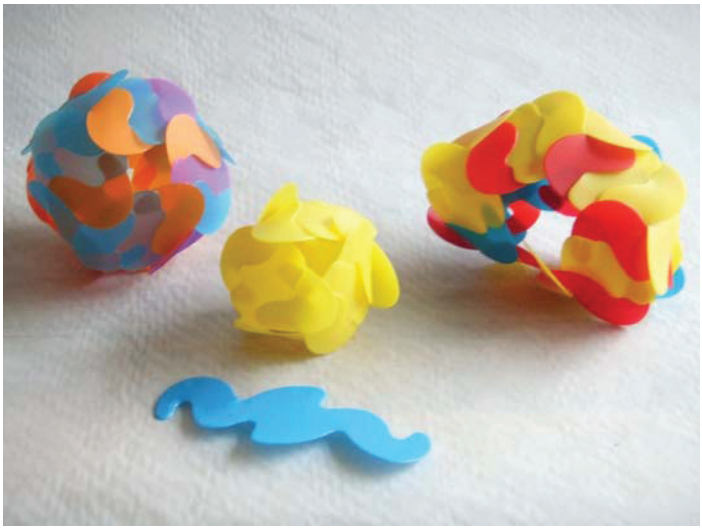

A twog with basic unit-woven polyhedra. L to R: cube, tetrahedron, and "tuic" (**t**he **u**nique **i**somer of the **c**ube.)

The Great Barrier Reef one must pass over to sail to the kingdom of unit-woven polyhedra is getting one's fingers to learn the moves needed to weave three twogs together. After that, it's all smooth sailing. Some children, as young as seven, quickly become adept at the basic moves, some adults struggle. In the workshop we will focus on holding the deck properly in the hand and making the basic weaving moves in a repeatable way. This is the hard part. The building of polyhedra can then almost be self-discovered. As time permits, we will cover the mathematical aspects outlined below.

Ring Spiral Codes

Chemists studying the cage-like, all-carbon molecules called fullerenes (corresponding to the cubic polyhedra having exclusively 5- and 6-sided faces) have found that there is a simple way to construct these cages in a face-by-face sequence—one that just happens to be ideal for unit-weaving. This special construction sequence is expressed in a sequence of numbers called a ring spiral code. The simplest version of the ring spiral code suffices for most cubic polyhedra, the more complicated generalized code [3] yields a practical weaving order for any cubic polyhedron. We will weave some text-messaged ring spiral codes in order to "teleport" an unknown polyhedron into the room.

Just as for life's genetic codes, an arbitrarily generated ring-spiral code can be unbuildable nonsense. Likewise different polyhedral genotypes (ring spiral codes) can encode the same polyhedral phenotype (isomorphically equivalent polyhedra.)

Boundary Words

When a ring-spiral sequence is followed, each partially completed stage, upon the closing of the latest ring, can be described by a binary word [3] that is cyclic in the sense that all cyclic permutations are considered equivalent. By convention, perimetral vertices that are already three-connected are coded as zeros, and vertices that are as yet only two-connected are coded as ones. As far as the ensuing weaving is concerned, a completed patch is fully described by its boundary word. Since all sequences of ones and zeroes are possible, there is a sense in which the information content (entropy) of a completed patch is proportional to its perimeter. Valid weaving moves can be identified with grammatical operations on the boundary word.

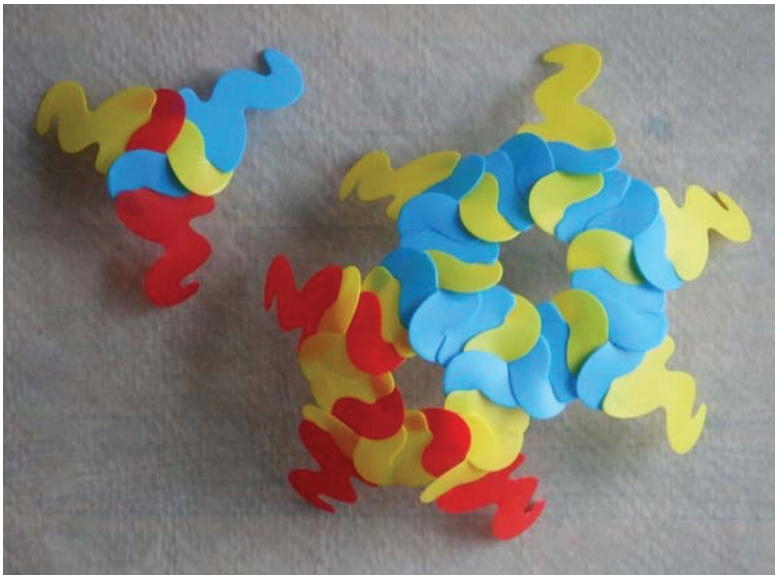

Three interwoven twogs, and a patch of partially completed unit-weaving having the boundary word (arbitrarily starting at the lowest red twog and proceeding counter-clockwise) 101111011.

Combinatorics

The software program Plantri [4] can efficiently explore the whole combinatorial space of cubic polyhedra. We borrow from fullerene chemistry to give cubic polyhedron a *carbon number* denoted C_n where n is the number of vertices, and likewise usurp the use of the chemical term 'isomer' to mean a cubic polyhedron having the same number of vertices but a different shape (polygonal faces of any size are permitted.) Plantri's explorations can be summarized in this table:

Carbon Number	Number of Twogs Needed	Number of Isomers
4	6	1
6	9	1
8	12	2
10	15	5
12	18	14
14	21	50
16	24	233
18	27	1249
20	30	7595

Table. Counts of the number of *isomers* of C_n . Adapted from [4].

Euler's Formula

An assiduous weaver of any age will eventually discover a version of Euler's Formula. Each n-gonal face cubic polyhedron can be assigned (what is usually termed a topological charge) what I will term a topological *gravity* g, where g = 6 - n. The basket can close when the net gravity of the weaving is +12.

In a completed basket, a patch of weaving that has positive topological gravity will bend straight weavers (geodesics) convergently, just as normal, positive gravity bends starlight convergently. This provides reasonable support for the sign convention of curvature (i.e, "why not n - 6?") that is lacking for basket makers not familiar with the definition of Gaussian curvature.

Coloring Problems

An n-coloring of the edges of a cubic polyhedron can be identified with a weaving using twogs of n colors. A perfect edge coloring can be identified with a weaving where no two twogs of the same color touch. So, following Tait's Theorem, the now-proven Four-Color Conjecture could be stated: "Any cubic polyhedron can be woven from twogs of three colors, twogs of the same color not being allowed to touch."

Motivation

Unit-woven polyhedra not only look organic, they inspire an approach to the polyhedra that is quintessentially biological: a lessened interest in symmetry, and a deepened interest in complete taxonomy and close visual observation. A too-easy academic course is sometimes labelled "basket weaving." How ironic it is, that in the twentieth century considerable intellects were surprised that carbon would preferentially form molecules of 60 atoms, found it difficult to grasp that a certain mass density is required for the cosmos to close, and were surprised to discovery that the entropy of a black hole is proportional to its surface area. If only they had done more basket weaving as kids!

Experience in weaving gives students the basis for a physical intuition different from ours, and prepares them to go beyond us. I once sat in on a meeting of biologists at NIH who struggled to understand why a rat's brain maps its surroundings in a demonstrably hexagonal grid—rather than a Cartesian one! We've gone through life with strange, Cartesian-wired brains, let's help our kids escape our fate.

References

[1] Akleman, E., Xing, Q., and Chen, J. "Plain Woven Objects." Hyperseeing, November-December 2008.

[2] Strom, H., U. S. Patent 3,895,229, 1975.

[3] Fowler, F. et. al., "A Generalized Ring Spiral Algorithm for Coding Fullerenes and Other Cubic Polyhedra." in Discrete Mathematical Chemistry, DIMACS Series in Discrete Mathematical and Theoretical Computer Science, 2000.

[4] Brinkmann, G., McKay, B., "Fast Generation of Planar Graphs." Communications in Mathematical and in Computer Chemistry, 2007.

Fractal Tessellation

Mehrdad Garousi
Freelance fractal artist, painter and photographer
No. 153, Second floor, Block #14, Maskan Apt., Kashani Ave, Hamadan, Iran
E-mail: mehrdad_fractal@yahoo.com
Mehrdadart.deviantart.com

Introduction

As a fractal artist, two areas I am most interested in are fractal tessellations and combining fractal geometry with other areas of traditional and modern mathematics. Therefore, I have attempted to create sets of fractal tessellations with simultaneous application of the rules of Euclidean and hyperbolic geometries, some of which are shown here.

I avoid interwoven and ambiguous dusty fractal shapes and I use very simple Euclidean forms as the basic materials of the tiling. This is because in a tiling I want clear shapes with clear forms that follow from a step by step geometrical process.

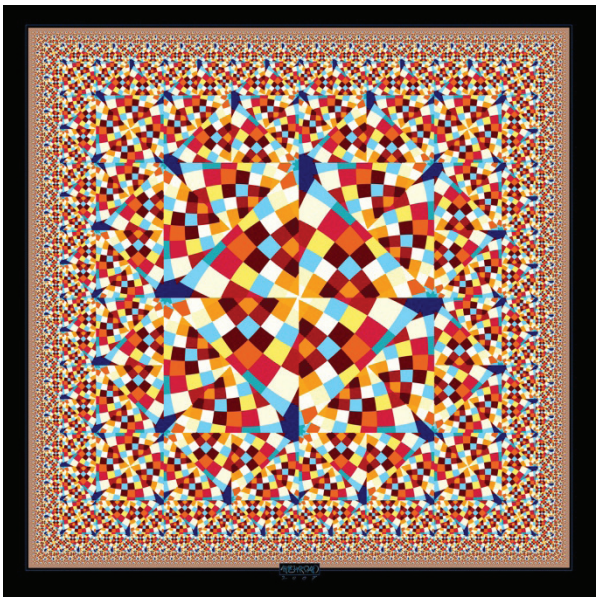

Figure 1: The Carpet (2007; © Mehrdad Garousi).

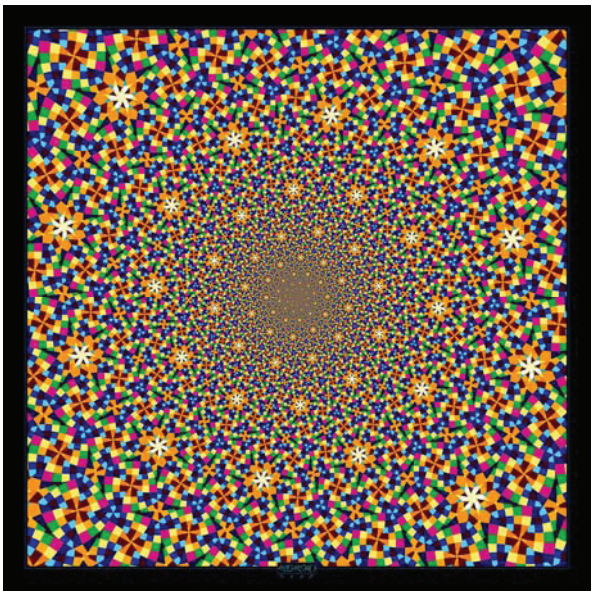

Figure 2: *The Dome (2007; © Mehrdad Garousi).*

A complex example of this kind of fractal tiling is *The Carpet* (Figure 1). This image is completely made of very small colorful square tiles arranged side by side. The main pattern of this tessellation at the center consists of four right triangles that form a square. Each of them, with two other smaller right triangles, each one exactly half of the larger right triangles, form another smaller square. This process goes on toward infinity and provides a square carpet with 4-fold rotational symmetry.
The Dome (Figure 2) fractal image has more complexities. Although, its basic formative shapes, like those of *The Carpet*, are very small Euclidean tiles, the pattern consists of two fractal spiral

lines interwoven at the center of the image to infinity. Connecting orange stars will display these two spirals more clearly. This fractal image is similar to the interior tiling of the domes of Islamic mosques, presenting a modern fractal tiling for the domes with the difference that the center of the domes continue to infinity inside the sky.

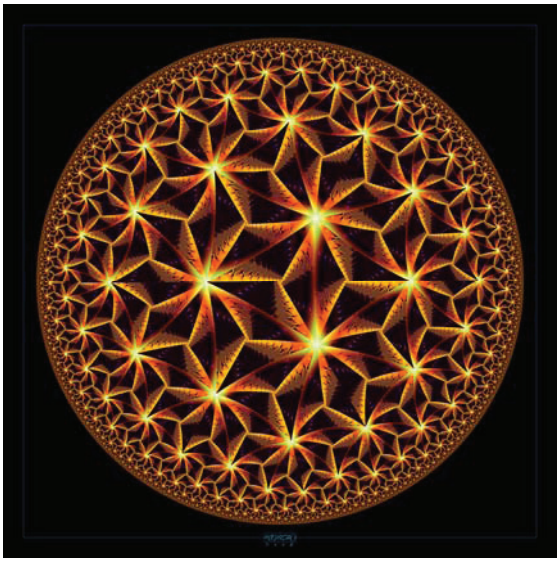

Figure 3: *Gestalt (2008; © Mehrdad Garousi).*

Figure 4: Iron Tortoise (2008; © Mehrdad Garousi).

Another group of fractal tessellations are those which have been generated by applying hyperbolic geometry principles. Images *Gestalt* (Figure 3), *Iron Tortoise* (Figure 4) and *Indian Globes* (Figure 5) are good examples of this property. All these images are created by fractal formulas and by applying hyperbolic geometry and some basic rules of tiling of the hyperbolic plane. Even their coloring and lighting have been done by exploiting fractal algorithms.

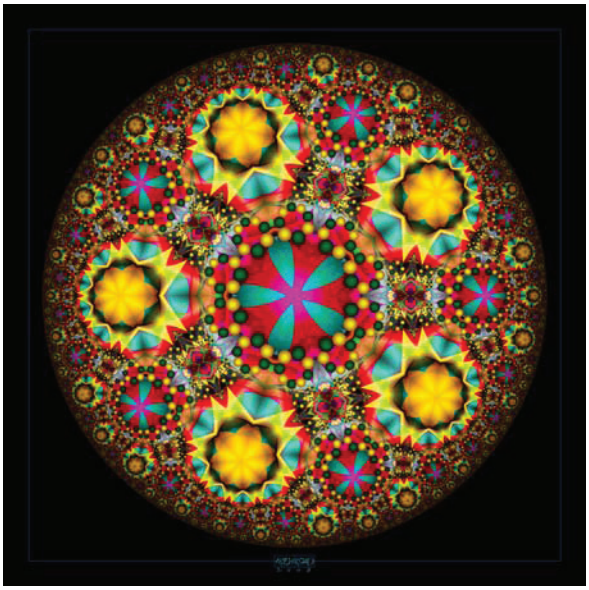

Figure 5: *Indian Globes (2008; © Mehrdad Garousi).*

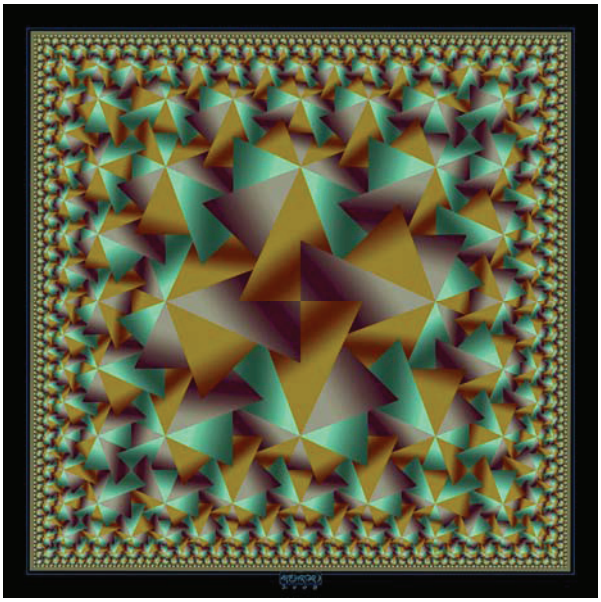

Figure 6: *Paper-folding (2008; © Mehrdad Garousi).*

The *Gestalt* is a nice example of order-7 triakis triangular tiling and a closer look at its details discloses that all the surfaces are covered with fractal forms. Due to the coloring and lighting, the image flips between two views. One view consists of an infinite number of pyramids and another view is a complex set of infinite cubes which are merged in their three sides. Sharing the sides between abutting cubes and the pyramidal form of the tessellation provides a gestalt in this image which makes the viewer confused. By watching it from each point of view you will see a different pattern and by exploring the whole image in one view, you will find different relations between formative triangles which is the generator of the gestalt property.

The *Iron Tortoise* artwork is a kind of hyperbolic tiling with octahedrons. Actually it is a mixture of three similar superimposed and overlapping hyperbolic tessellations: one is composed of eight pointed yellow stars and the woody bridges between them, the next one consists of connected network of pipes around yellow stars, and the last one would be disclosed by connecting black holes.

The special property of *Indian Globes* is something more than the visual complexity resulting from exploiting different geometrical shapes. This tiling is a complex set of pink and yellow globes and at first, both yellow and pink groups of globes follow a pentagonal pattern, but yellow globes have heptagonal forms. Around each yellow globe you can find seven pink globes while around each pink globe there are five yellow ones. Therefore, this tessellation is a mixture of two completely different patterns of the hyperbolic plane.

One of my tessellations is *Paper-folding* (Figure 6) which is created by a kind of paper-folding method. This work of art consists of triangular paper pieces with three different colors. These pieces are repeatedly placed upon and under each other. The most important property of this kind of arrangement is that the central four pointed star, with different colors, is repeated infinitely through diagonals.

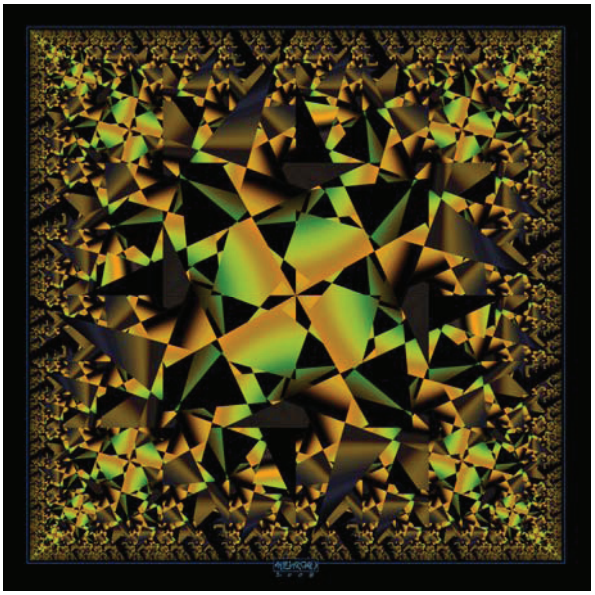

Figure 7: *Tetramerous (2008; © Mehrdad Garousi).*

Tetramerous (Figure 7) is another example of this kind of tiling with papers, but with more complexity and chaos. The tetramerous shape is also repeated diagonally in this image.

Aesthetics in Creating Fractal Images

Mehrdad Garousi
Freelance fractal artist
No. 153, Second floor, Block #14
Maskan Apartments, Kashani Ave Hamadan, Iran
E-mail: mehrdad_fractal@yahoo.com
http://mehrdadart.devianart.com

Saheb Mohamadian Mansoor
Bu-Ali Sina University,
Hamadan, Iran
E-mail: Mansoor@basu.ac.ir

Abstract

Art and mathematics has had a long and intimate relationship. With the introduction of fractal mathematics, “Fractal Art' has emerged as a new genre of mathematical art. In this paper we discuss how to achieve aesthetically pleasing art works utilizing fractal geometry by examining hidden mathematics in some fractal works created by the first author.

Introduction

Art and aesthetics have been considered as ambiguous phenomena far from comprehensive and exclusive definitions. No scientific set of rules can be defined to recognize aesthetic factors in artistic works. Richard Arthur Wollheim [1,2] describes the understanding of art as one of the most tempting and charming ancient questions from human culture. Nature has been glorified in art and sometimes as the assessment factor of artistic degree and representational beauty in artistic works. Nature, itself, presents some criteria judging art works [3].

Mathematics has also emerged from nature. Yet due to enjoying a logical and recurring essence, mathematics is completely different from art. Based on this interaction, art and mathematics throughout history complement each other in various areas such as music, architecture and painting. On the other hand, exploiting art has helped to represent natural phenomena related to a mathematical formulation. Johannes Kepler says [4]: "I believe the geometric proportion served the creator as an idea when He introduced the continuous generation of similar objects from similar objects."

Throughout history, artistic works resulted from combining art and mathematics. Mathematics of Pythagoras was applied in music, the Golden Ration appears in Greek architecture, and geometric perspective was introduced in the Renaissance. Mathematics also yielded new insights concerning the theory of light and the theory of complementary colors [5]. Islamic architecture and design is strongly influenced by geometry [6].

The rapid advancement of technology and the rise of computers and mathematical algorithms in image making led to the formation of many questions in aesthetics concerning works of art. Aesthetics, which was regarded as an immediate bridge between nature, artist and audience was challenged in postmodernism due to the rise of computer technology's role in the process of creating artistic images. In this case mathematics played a leading role in creating the work. This has narrowed the boundary between artist, computer and artistic work.

With the enhancement of complexity in creating computerized works, the acceptance of this fact became easier since the creation of most images could only be done with a computer. The computer allowed the artist to introduce complex mathematical patterns. The computer artist was not influenced by nature but by the relationship between mathematics and art.

In particular, mathematics reached its peak influence with the introduction of fractal mathematics and geometry by Benoit Mandelbrot, which led to geometrically innovative images. Mandelbrot showed how fractals occurred in mathematics and in nature. This led to the formation of complex images which contained

unique innovations. Fractal phenomena consist of factors such as self-similarity, complexity, fractal dimension and the potential for combining regularity and chaos. These factors make images so complex that they were completely different from earlier simple images of computer art. In these images which are direct representations of fractal phenomena, the distance between art and mathematics approaches zero, so that mathematical representations are posed as artistic works and full of artistic aesthetics in direct statements of nature's real behavior. Heidegger believed [7]: "Beauty is one way in which truth occurs as unconcealedness."

Therefore, the simultaneous rise of several properties based on mathematics and complexity leads to mathematical beauty in fractal images. Bertrand Russell said [8]: "Mathematics, rightly viewed, possesses not only truth, but supreme beauty."

Due to exploiting a large amount of fractal concepts and characteristics, these images either have some sort of geometrical aesthetics or motivate the audience's feelings due to their extreme complexity and innovation which cause an aesthetically emotional response. Despite the fact that aesthetics emerges from social, cultural and emotional conditions of specific eras, now the common feeling of audiences toward complex works of art and fractal images results from today's great complexity of human emotions and societies. Peter Halley points out [9]: "Where once geometry provided a sign of stability, order, and proportion, today it offers an array of shifting images of confinement and deterrence."

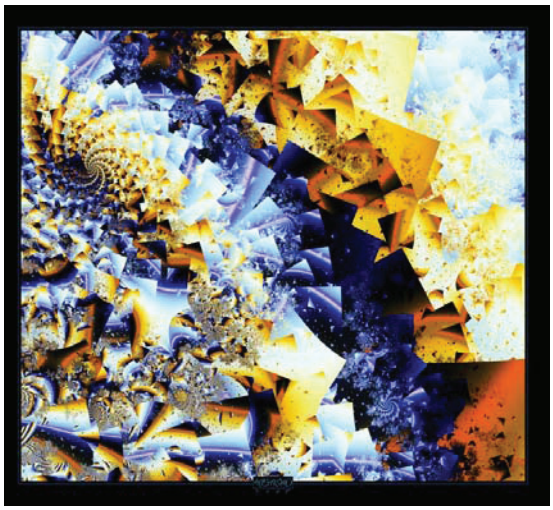

Figure 1: Emotion of Life (2007; © MehrdaFigure 2: Heaven and Hell (2007; © Mehrdad Garousi) Garousi)

Since fractal mathematics calculations are complex and time consuming, most of the mathematical processes of image creation are done by a computer. The artist is playing the role of a creative mind conducting aesthetic decisions concerning these images. The mathematical knowledge required by artists to participate in the creative process is now essentially nil [10].

Therefore, having outlined the general lines of the artistic aesthetics and mathematical relationships, we will now explain the aesthetics appearing in some fractal works and introduce methods to recognize and apply aesthetics in fractal imaging. First, we describe the aesthetics resulted from fractal chaos (section 1). Second, we examine the use of Euclidean traditional geometry in constructing fractal images (section 2). Third, we provide examples of fractal art by introducing images of natural phenomena (section 3).

We will pay attention to the role of geometry in the aesthetics of these images, free from some other artistic factors such as colour, view angle and framing, because the key element of forming fractal images is the mathematics constituting them. The next step concerns colors, framing and other emotional processes related to the artist's aesthetic nature.

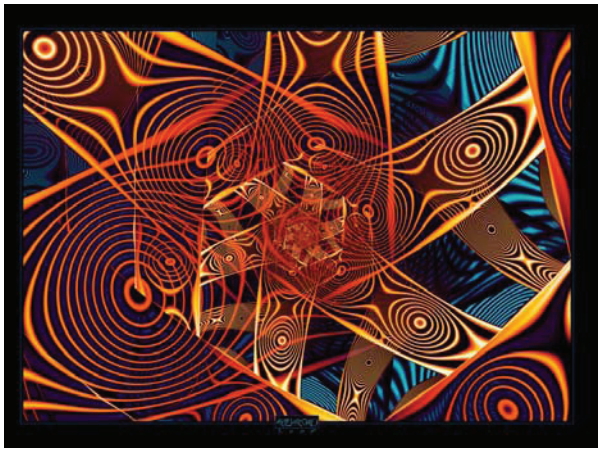

Figure 3: Magnets (2007; © Mehrdad Garousi)

Figure 4: Green Dragon (2007; © Mehrdad Garousi)

Beauty from Chaos

In nature there is the simultaneous existence of order and chaos. In fact, the unique chaos governing all the phenomena in nature follows some sort of mathematical pattern leading to the representation of order. Juxtaposition of these phenomena, while orderly and complementary, has created a wonderful landscape which most artists have failed to represent. Most painters have created numerous drawings from natural scenes including clouds and trees which may seem inaccurate due to leaving out the chaotic fractal component. Artists have painted chaotic details to the extent the materials and conditions have allowed him, while he couldn't have thought of painting a tree with a myriad of leaves, several million pieces of grass of a chaotic lawn in an exact relationship with each other, or clouds with endless borders. In fact, clearly Euclidean geometry is not able to characterize the natural world [11].

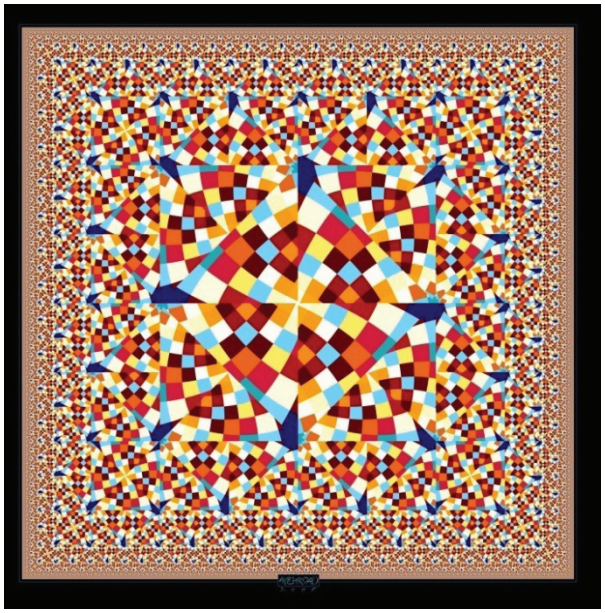

Figure 5: The carpet (2007; © Mehrdad Garousi)

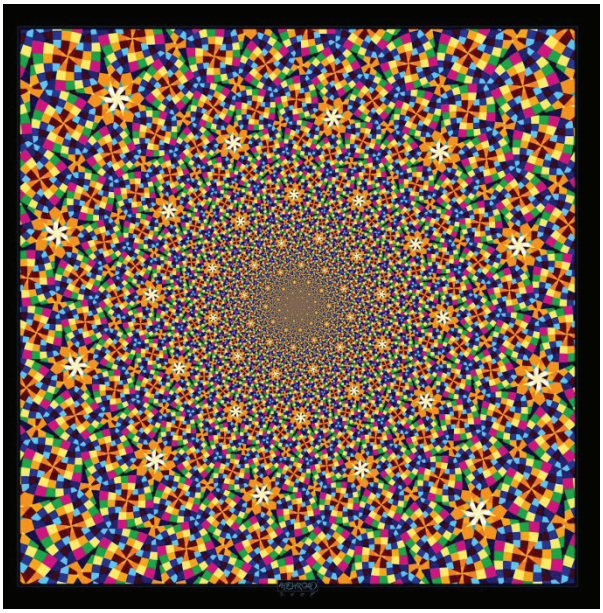

Figure 6: The Dome (2007; © Mehrdad Garousi)

Some samples of fractal patterns have been found in the works of painters such as Leonardo da Vinci, Katsushika Hokusai and Jackson Pollack, showing the effort of these artists to attain fractal patterns, and simultaneous order and chaos governing the phenomena [12]. Fractals, in general, describe the common chaos dominating the totality and particularity of nature but in the language of mathematics. Fractal images translate behavioral characteristics of natural phenomena in the form of geometrical images, amongst which chaos, fractal dimension, complete, rough or statistical existence of self-similarity and simultaneous existence of chaos and order can be mentioned.

Fractal images constitute the mathematical skeleton of some natural activities. In fact, these images bring forth the behavioral dynamism of nature in the form of unifying shapes instead of depicting a fixed landscape of nature. This allows them to have some instinctive characteristic of nature such as aesthetics. *Emotion of Life* (Figure 1) is an obvious example of fractal chaos. This image is the result of several million mathematical calculations based on mathematics of natural behavior, albeit it is chaotic and unusual and we face some orderly patterns of self-similarity and recursiveness. The audience sees the most chaotic possible image at first and then an image pattern with infinite spirals. The work of *Heaven and Hell* (Figure 2) is also a more complex representation of fractal interwoven forms which are not distinguished easily, but the color contrast dominating these forms creates some sort of cosmic space, the details of which are not endless like the real sky.

Magnets (Figure 3) and *Green Dragon* (Figure 4) exploit more clearly some self-similarity, not accessible through anything other than fractal advanced mathematics and computer technology. Therefore, suitable use of chaos and regulation of parameters such as self-similarity, fractal dimension and other mathematical characteristics, let us have a revolution of artistic aesthetics, the secret of which lies in suitable regulation of simultaneous order and chaos to attain a perfect ideal.

Combining Euclidean and Fractal Geometry

Since the fractal images primarily follow relatively similar image patterns, Euclidean geometry can be applied to these patterns to obtain a more tangible beauty. For example, symmetry and tiling are two key Euclidean concepts that can be exploited to obtain aesthetically pleasing art works. In *The Carpet* (Figure 5), the fractal repetition of triangles and squares following Euclidean symmetry and rotation have resulted in a visually rich image. Thus the familiar concepts of symmetry and rotation combined with fractal repetition facilitates the appreciation of the art works.

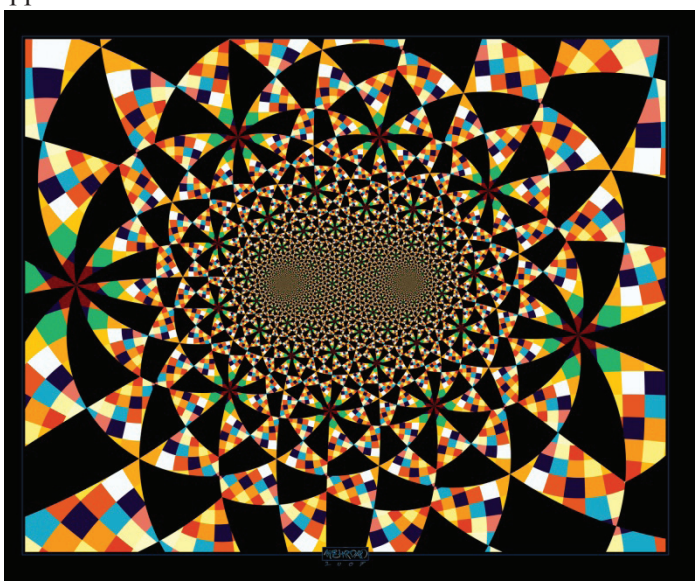

Figure 7: Bicentric Dome (2007; © Mehrdad Garousi)

Figure 8: Blue Sun (2007; © Mehrdad Garousi)

The other vital factor, tiling, due to the infinite dynamism of fractal patterns in these works provides for "a movement to infinity". *The Carpet* (Figure 5) is based on tiling while exploiting geometrical symmetry. *The Dome* (Figure 6) is another example of this technique. At first glance, this work reminds us of the tiling of Islamic mosque domes. In these mosques, tiles and forms on the sides of the dome seem smaller due to the spherical shape and they become much smaller when we approach the center. This image continues this tiling on a flat surface not to a dome center but to infinity. While traveling to the center of the picture, instead of a decrease in the number of tiles, they get smaller in a certain ratio to the previous tiles and keep their coherence and continuity in a certain ratio which is not possible in 3dimensional space but is possible with fractals. It is worth mentioning that color plays a key element in this work of Islamic tiling, increasing clarity of forms like flowers or stars in the tiles. Robert Fathauer's encyclopedia [13] is an illustrative sample of tilings.

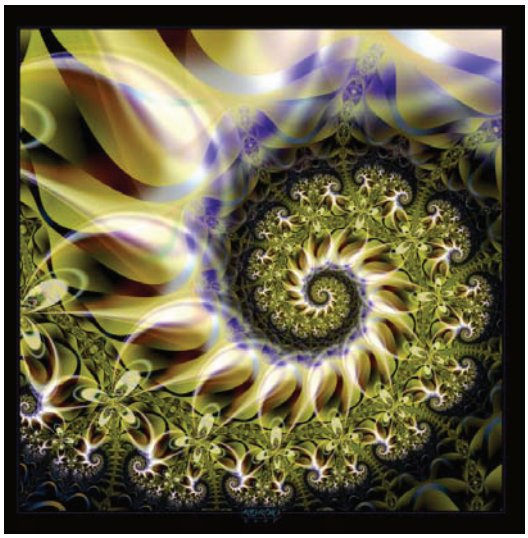

Figure 9: Pistachios.

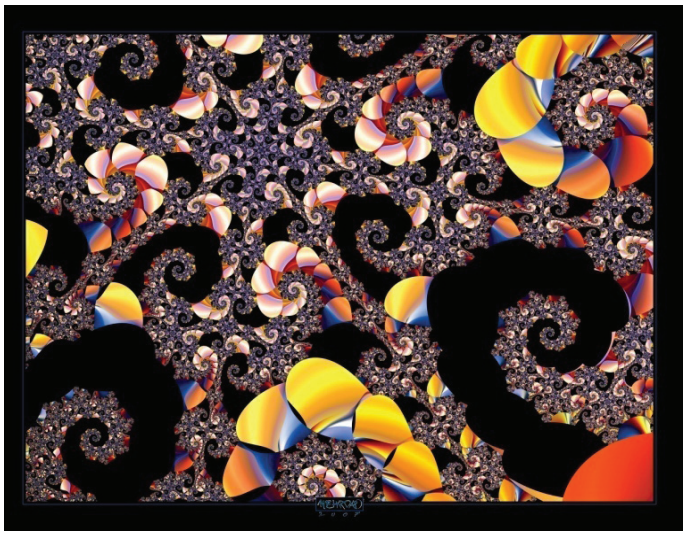

Figure 10: Scorpions.

Bicentric Dome (Figure 7)is concerned with the architectural concept of bicentric domes. The continuity of tiles in the space between the two domes exploits fractal geometry. *Blue Sun* (Figure 8) is a recursive application of symmetrically placed geometrical forms such as octagons, eight edge stars with different angles and lotuses. The fusing of concentric Euclidean forms is also reminiscent of mandalas and Yantric paintings with the difference that the audience is allowed to pass toward the infinite image center according to Yantric traditions.

Natural Forms

Exploiting natural forms is another effective method for obtaining beauty in fractal imaging. Here fractal geometry is combined with natural forms such as flowers and trees which leads to more familiar visual aesthetics.

An example of combining natural forms with fractal geometry is *Pistachios* (Figure 9), which pictures open-mouthed pistachios continuously rotating toward the extreme of the image center. Two other examples are *Scorpions* (Figure 10), which is a representation of the tails of numerous scorpions, and *Daemon's Heart* (Figure 11), which pictures both chambers of the heart, and which endlessly represents continuing heartbeats.

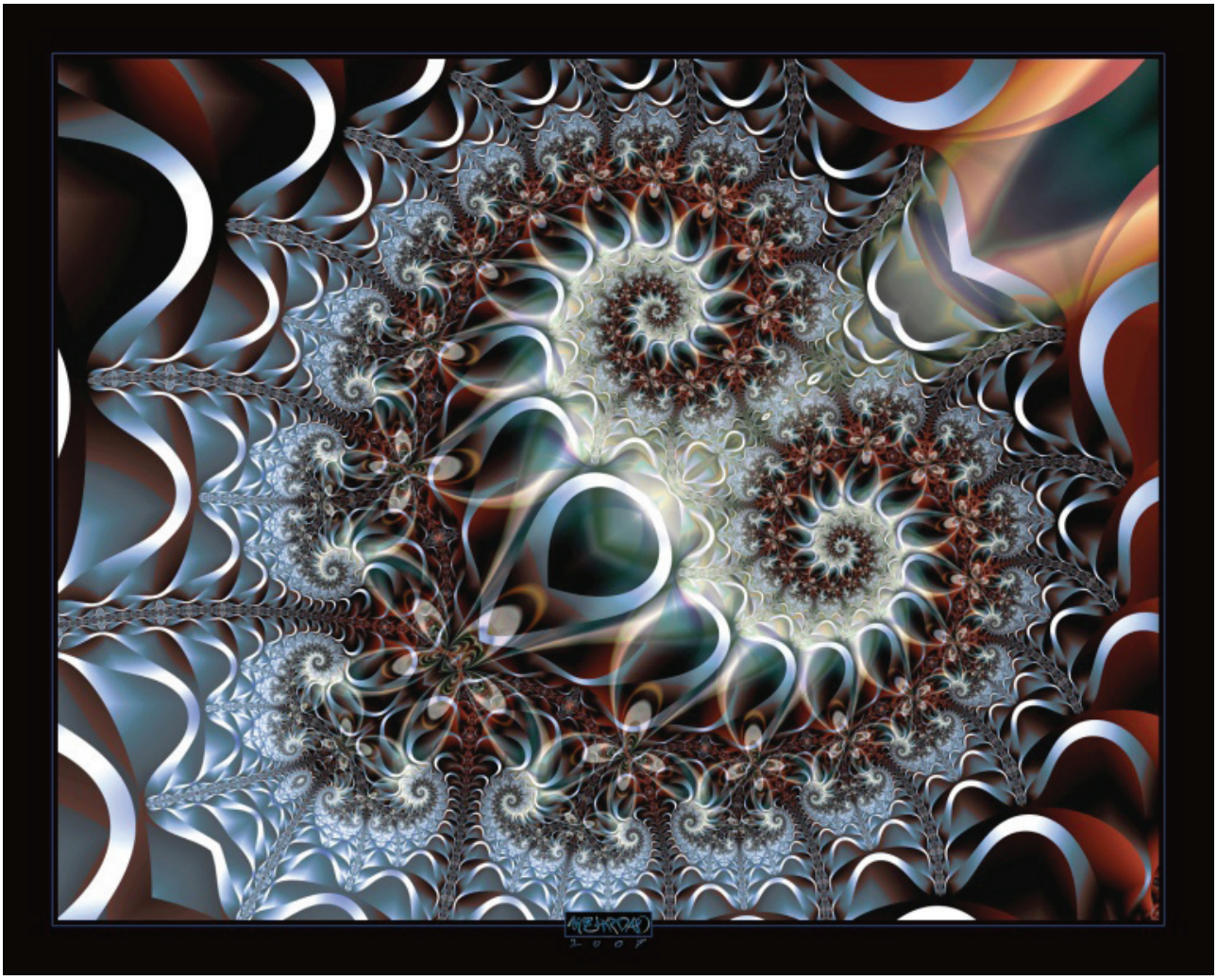

Figure 11: Daemon's heart (2007; © Mehrdad Garousi)

Conclusion

During recent years applying fractal image making has been very prevalent among artists. There are frequent advances due to newer software.

This paper has tried to facilitate the audience's appreciation of fractal artworks by considering three methods for obtaining aesthetically pleasing works. We are also concerned with leading artists to more beautiful and familiar uses of image making by introducing methods that artists can use to exploit fractals, as well as facilitate applications to architecture, sculpture, environmental activities and any other common areas between art and mathematics.

References

[1] Wollheim, R., 1980, *Art and Its Objects*, Cambridge University Press, Cambridge, UK, (Second Edition).

[2] Wollheim, R., 1988, *Painting as an Art*, Princeton University Press, Princeton, NJ.

[3] Goguen, J.A., 2000, *Editorial Introduction to Art and the Brain*, In: Goguen, J.A. and Myin, E. (Ed.), Journal of Consciousness Studies: ART AND THE BRAIN, PART II, 7(8-9), pp. 7-15. Imprint Academic Journals, Exeter, UK.

[4] Pickover, C.A., 2003, *Wonders of Numbers: Adventures in Mathematics, Mind, and Meaning*, pp. 119. Oxford University Press, New York ,NY.

[5] Eskridge, R., *The Enduring Relationship of Science and Art*, The Art Institute of Chicago. Available at http://www.artic.edu/aic/education/sciarttech/2a1.html (accessed 2 July 2008).

[6] Sarhangi, R., 2005, *Mathematical Connections in Art*, In: Ekeland, I. (Ed.), Pi in the Sky Magazine, 9, pp. 9-13. Available at http://www.pims.math.ca/pi/issue9/page09-13.pdf (accessed 2 July 2008).

[7] Moi, S., 2006, *Perplexity and Passion in Heidegger: A Study in the Continuity of his Thought*, In: Desai, D., McCain, K., Tomalty, J. (Ed.), GNOSIS: A Journal of Philosophical Interest, 8(1), pp. 14-24. Concordia University Department of Philosophy, Montreal, Canada. Available at http://philosophy.concordia.ca/gnosis/vol_viii/Moi.pdf (accessed 2 July 2008).

[8] Borwein, J. and Bailey, DH., 2003, *Mathematics by Experiment: Plausible Reasoning in the 21st Century*, p. 84. AK Peters publishing company, Natick, MA.

[9] Halley, P., 1984, *The Crisis in Geometry* In: Arts Magazine, 58(10), pp. 111-115. New York, NY.

[10] Sisson, P.D., 2007, *Fractal art using variations on escape time algorithms in the complex plane*, In: Greenfield, G.R. (Ed.), Journal of Mathematics and the Arts, 1(1), pp. 41-45. Taylor & Francis Group, London, UK.

[11] Russ, J.C., 1994, *Fractal Surfaces*, p.3 , Plenum Press, New York, NY.

[12] Taylor, R., 2006, *Personal reflections on Jackson Pollock's fractal paintings*, In: Benchimol, J.L. (Ed.), Hist. cienc. saude-Manguinhos, 13(1), Rio de Janeiro,RJ. Available at http://www.scielo.br/pdf/hcsm/v13s0/06.pdf (accessed 2 July 2008).

[13] Fathauer, R., *Dr. Fathauer's Encyclopedia of Fractal Tilings*. Available at http://members.cox.net/fractalenc/encyclopedia.html (accessed 2 July 2008).

[14] Bird, R.J., 2003, *Chaos and Life: Complexity and Order in Evolution and Thought*, p.80, Columbia University Press, New York, NY.

Mobius Bands, Braids, and Knots

Nat Friedman
artmath@albany.edu

Abstract

The concept of a Mobius band has generated a variety of mathematical sculptures [1,2]. I will discuss some variations of ceramic Mobius bands. I will also point out that braid forms [3,4] for knots are useful for making knot sculptures. Knots generate totally three-dimensional mathematical sculptures and are perfect for hyperseeing since a knot has no preferred top, bottom, front or back and can look deceptively different from different viewpoints. I will discuss ceramic knots as well as knots made from copper tubing.

Figure 1. Mobius Band, 2005, 12 w x 10 h x 4 d inches, stoneware, private collection.

Figure 2. Mobius Band Curl, 2005, 10 w x 8 h x 4 d inches, stoneware private collection.

Mobius Bands

In 2002 I started taking an evening ceramics course with Regis Brodie at Skidmore College in Saratoga Springs, NY, about a half-hour drive from my home in Albany, NY. I thought I would try slab building, but discovered that clay was a natural material for making Mobius bands. The method is to first roll out a slab of clay of uniform thickness, say ½ inch, and then use a compass and knife to cut out a circular ribbon. The circular ribbon is better for forming a Mobius band than a long strip since it is already curved. The circular ribbon is first cut so it can be manipulated: given a half twist, shaped, and then the two ends are rejoined to obtain a Mobius band. The green (wet) clay is allowed to dry for several days. The green clay is "propped up" with various types of supports such as paper tubes and/or plastic bottles to hold its shape while drying. Anything, even crumpled paper is useful for props. After drying, the fragile unfired band is carefully sanded and then low-fired in a kiln. After low firing, the band is sanded again and then high fired. After high firing, the clay is turned into stone; hence the name stoneware. Thus

in order to obtain a stone Mobius band, one starts with clay, shapes the band, and then turns it into stone by firing. An example is shown below. The propping involved putting a paper tube under the right part of the band to give it a "roundness" and a support on the outside of the left part to keep it up while drying. The finish is natural, no glaze. Another Mobius band is shown in Figure 2. It is a loop with a curl and stands by itself.

By adding another curl around the curl in Figure 2 and then joining, we obtain the double curled Mobius band in Figure 3. It is a version of a trefoil knot. A lot of propping is necessary in order to keep the shape of a knotted band. I also use short round wooden dowels of various diameters for separating the various parts of the knot where it tends to get close to itself.

Figure 3. Mobius Band Double Curl, 2005, 8 w x 8 h x 4 d inches, stoneware, author's collection.

Braid Configuration

In Figure 3, choose a point at the top left of the knot and traverse the knot moving clockwise initially to the right and down. Note that as you traverse the knot, the clockwise direction is maintained. That is, you continue in a circular clockwise motion until you return to the starting point. This is referred to as a *braid form* because if you cut the knot along a radial line from the center of rotation, the knot can be straightened out into a set of three braided strands [3,4]. A braid form is particularly advantageous for shaping a circular band into a knot since one does not have to reverse the direction of curvature of the circular band as you wrap it around to form the knot and then rejoin the two ends.

Two-sided band

A ceramic two-sided band is shown in Figures 4 and 5. This is a particularly nice configuration of two perpendicular arches consisting of a small arch passing under a taller arch.

Figure 4. Double Arches, 2005, 10 w x 5 ½ h x 5 d inches, Stoneware, author's collection.

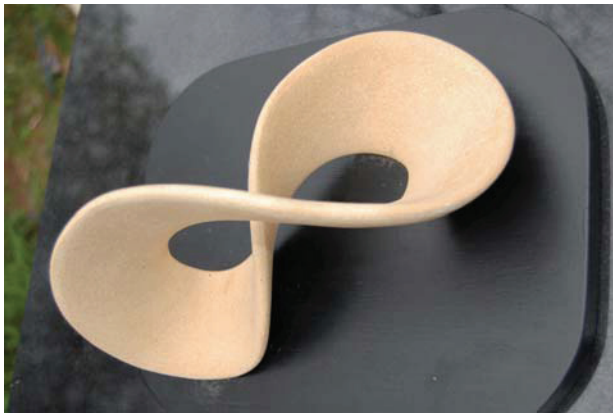

Figure 5. Double Arches, alternate view.

Stoneware Knots

We have already seen an example of a knotted Mobius band in Figure 3, which is in the shape of a trefoil knot. Another example of a trefoil sculpture is shown in Figure 6. One can check that this is a two-sided band. The band width is relatively wide and parts of the band enclose spaces that other parts of the band pass through. For example, on the right, the band encloses a space that another part of the band passes through from back to front. This part of the band continues to the left to enclose a space that another part of the band passes through from horizontal in back to vertical in front. This part of the band can also be thought of as enclosing a space that the vertical middle part of the band passes through.

Figure 6. Trefoil Form and Space I, 2005, 10 w x 6 ½ h x 6 d inches, Stoneware, author's collection.

Figure 7. Trefoil Form and Space II, 2005, 7n1/2 w x 5 h x 5 d, Stoneware, author's collection.

Another two-sided trefoil knot is shown in Figure 7. This configuration is a narrower version of the trefoil configuration in Figure 8. Similar remarks apply to parts of the knot passing through spaces formed by other parts of the knot.

Figure 8. Variety of copper tubing knots, 2009, ACG, Albany, NY.

Copper Tubing Knots

The sculptor Charles Perry told me about the usefulness of flexible copper tubing for forming knots. Copper tubing comes packaged in a circular coil, which is a braid form, and so is all ready to be shaped into a knot that is in braid form. Copper tubing comes in diameters of ¼", 3/8", ½", and larger. It is best to start with ¼", which is easier to bend slowly without "crinking". A variety of knots by the author are shown in Figure 8, at a recent exhibit at the Albany Center Galleries (ACG) in Albany, NY.

Figure 9. 3 crossings, trefoil 3_1.

Figure 10. 4 crossings, switch to 4_1.

A selection of knot images with the number of crossings being 3, 4, 5, 6, and 7 are shown in Figures 9-13, respectively. This is actually the same knot seen from multiple viewpoints; hence an example of hyperseeing a knot. The minimum and maximum dimensions are 6 and 8 inches, respectively.

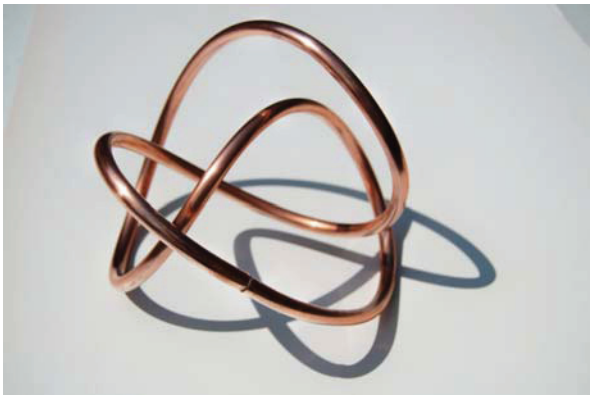

Figure 11. 5 crossings, switch to 5_2.

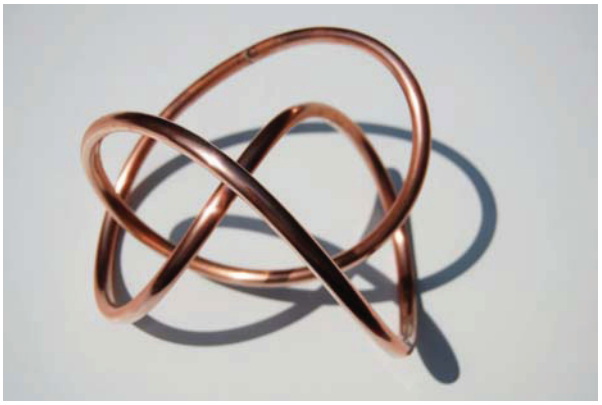

Figure 12. 6 crossings, switch to 6_2.

The knot in Figure 9 is a trefoil knot with three crossings. Starting at a point on the upper left and moving to the right and down: at the first crossing at the top the knot passes **over** itself, then **under** in the middle, and then **over** at the lower crossing. Continuing along the knot, we return to the top crossing moving **under**, then back **over** at the middle crossing, and **under** at the lower crossing before returning to the upper left starting point. Thus the crossings alternate over, under, over, under, over, under. In a standard knot table [3], the trefoil is denoted by 3_1. The 3 denotes the number of crossings and the 1 refers to the fact it is the only knot in the table with 3 crossings.

The image in Figure 10 with 4 crossings is not alternating. However, if certain crossings were switched, by reversing over and under, to make it alternating, then it would be an alternating diagram with 4 crossings and would be knot 4_1 in a knot table. Thus the terminology "switch to 4_1" below Figure 10.

The image in Figure 11 with 5 crossings is not alternating. However, if certain crossings were switched to make it alternating, then it would be an alternating knot with 5 crossings and would be knot 5_2, the second knot with 5 crossings in a knot table.

The image in Figure 12 with 6 crossings is not alternating. However, if certain crossings were switched to make it alternating, then it would be an alternating knot with 6 crossings and would be knot 6_2, the second knot with 6 crossings in a knot table.

The image in Figure 13 with 7 crossings is not alternating. However, if certain crossings were switched to make it alternating, then it would be an alternating knot with 7 crossings and would be knot 7_4, the fourth knot with 7 crossings in a knot table.

Thus by hyperseeing a trefoil knot 3_1 and switching crossings, we can find knots 4_1, 5_2, 6_2, and 7_4. That is, we can find higher order knots in a lower order knot.

References

[1] Nat Friedman, *Keizo Ushio: Mobius Band and Torus Divided*, Hyperseeing, May, 2007, Proceedings of ISAMA 2007, www.isama.org/hyperseeing/.
[2] Nat Friedman, *Larry Frazier: Topological Surfaces*, Hyperseeing, August, 2007, www.isama.org/hyperseeing/.
[3] Colin Adams, *The Knot Book*, W.H. Freeman and Company, New York, 1994, now published by the American Mathematical Society, Providence, Rhode Island.
[4] Colin Adams, *Introduction to Knot theory from the Physical Point of View*, Applications of Knot Theory, Proceedings of Symposia in Applied Mathematics, 66, 2008, American Mathematical Society, Providence, Rhode Island.

Figure 13. 7 crossings, switch to 7_4.

Slot Canyons:
Form, Space, Light, Color

Robert Fathauer and Nat Friedman
tessellations@cox.net and artmath@albany.edu

Abstract

The slot canyons along the border between Arizona and Utah are among the most spectacular natural sculptures. They are formed by the timeless passage of water over stone. These images were taken by Robert Fathauer.

Introduction

The slot canyons are wonderful inter-active form/space natural sculptures that you can enter and have a total experience of being in the spaces as well as viewing the forms. They are a photographer's delight as the range of light and color is dramatic. We also refer the reader to [1].

Image 1.
Here we see the linear horizontal surface marks of the powerful water pressure swirling through the canyon. The narrow vertical spaces and range of light/dark colors is striking. NF.

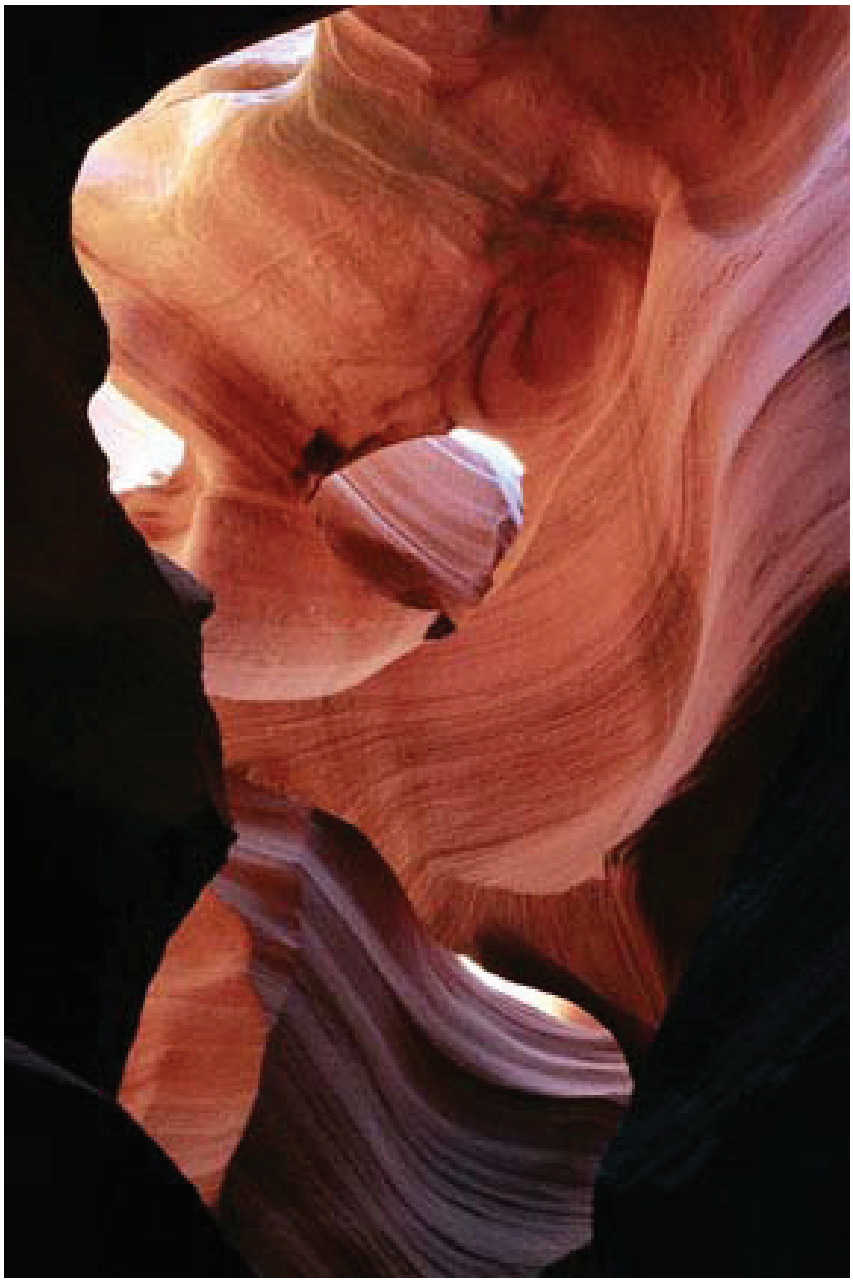

Image 2

This image is quite deceptive. At first I thought the lower central dark portion was coming forward as a positive form. Then I realized it was actually a receding wall passing under the lighter colored central overhang. The five spaces, or“windows”, in the image, including the lower left, allow light to enter from various directions. This is truly a great image. NF

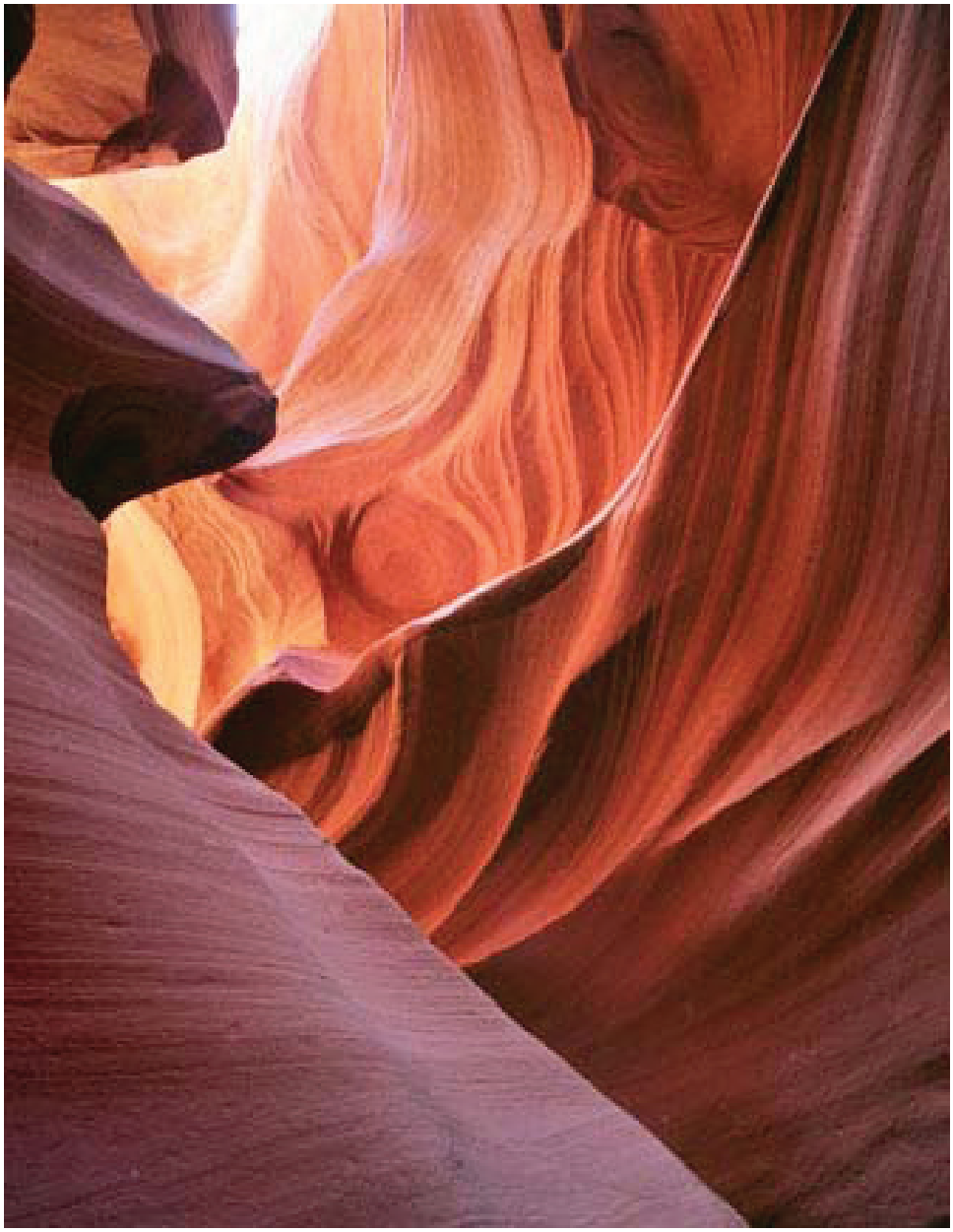

Image 3

Here one can really feel the light coming from the left. It lights up the thin diagonal edge from the upper right. This particularly delicate wisp of a curved line still seems to dominate the view. NF

The variety and complexity of these sandstone forms is a source of endless fascination. RF These slot canyons are dry most of the time. Erosion occurs primarily during flash floods, in which water gathered over a large area is forced into a narrow slot. These are violent events, and the water is carrying sand as well as rocks. The erosion is therefore caused by what is in the water as well as by the water itself. Presumably the scalloped features are due to large chunks of sandstone being broken off by large rocks. The creation of such beauty through acts of violence is a bit paradoxical. These photographs were taken in Lower Antelope Canyon, also known as

The Corkscrew. Eleven tourists were killed here by a flash flood in 1997, reportedly caused by a thunderstorm five miles away.

Image 4

A vertical image catching the curving wave of stone like drapery in the upper center. One can imagine the water hollowing out this space. NF

Image 5

A minimal image accentuating the light/dark contrast. This image seems quiet in relation to some of the more active forms. NF

These photographs were taken with either an Olympus FE-340 compact digital camera or with a Minolta X-700 35-mm film camera. A tripod was used due to the low light levels in these narrow and relatively deep spaces. Some adjustments of levels in the images was performed in PhotoShop. In most of these images, there is neither sky nor directly sunlit rock, only shadow. This allows the subtle colors in the sandstone to come out, as bright areas would make the rest of the image extremely dark.

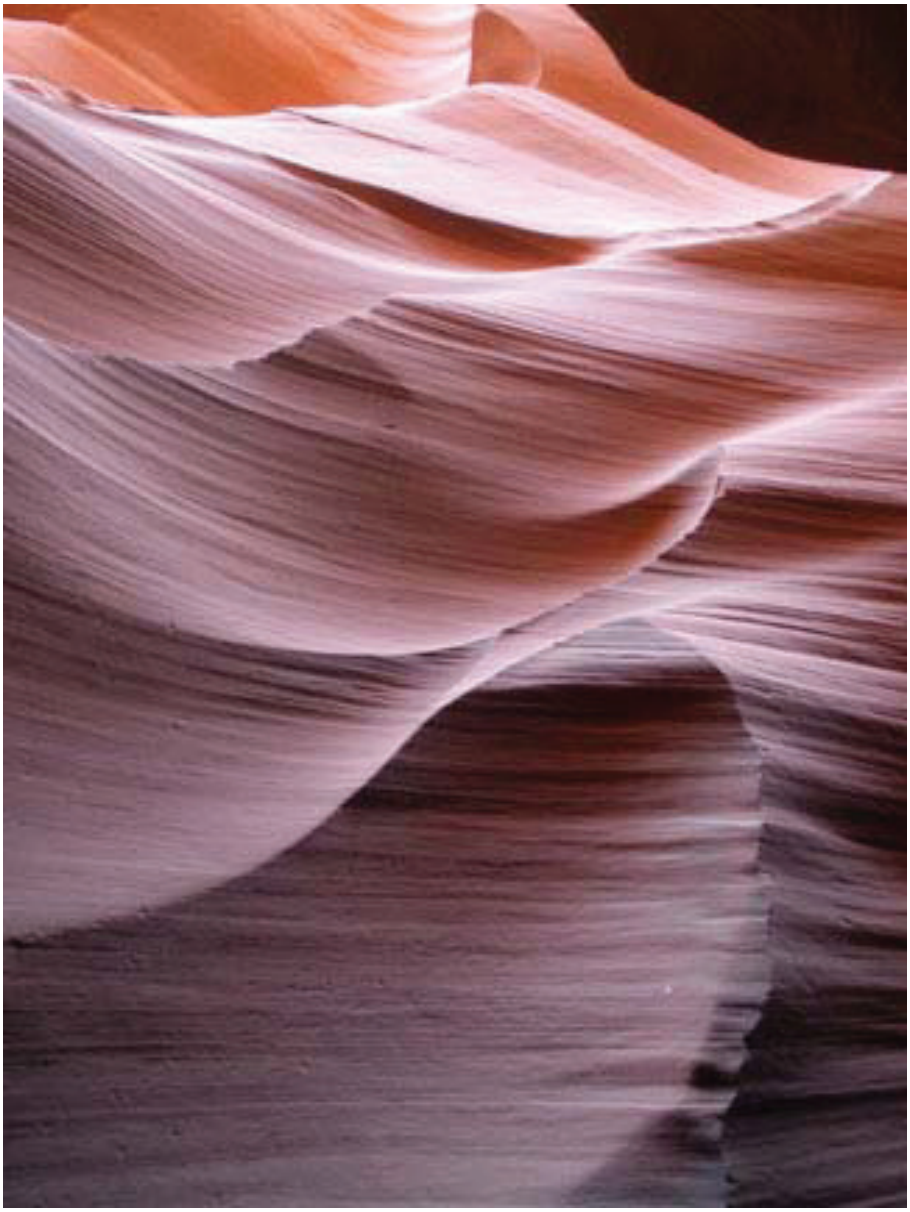

Image 6

Here I am reminded of sand dunes blown by the wind. Thus there is a form equivalence of water on stone and sand on wind. NF

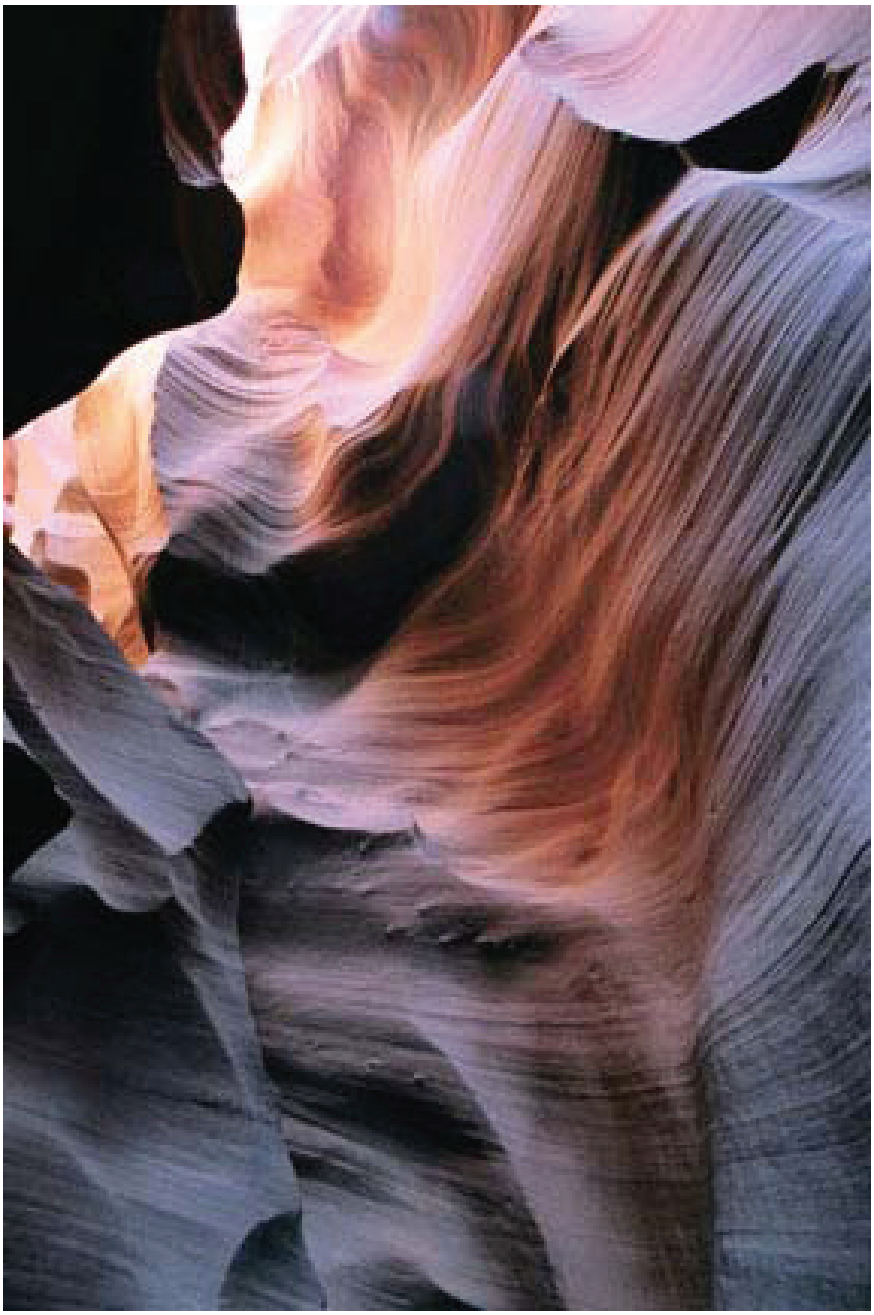

Image 7

The variety of forms in this image reflect parts that have broken off leaving sharp edges, as well as those smoothed by time. Again the surface flow lines are the water's footprints. NF
The turbulent motion in this image is striking. RF

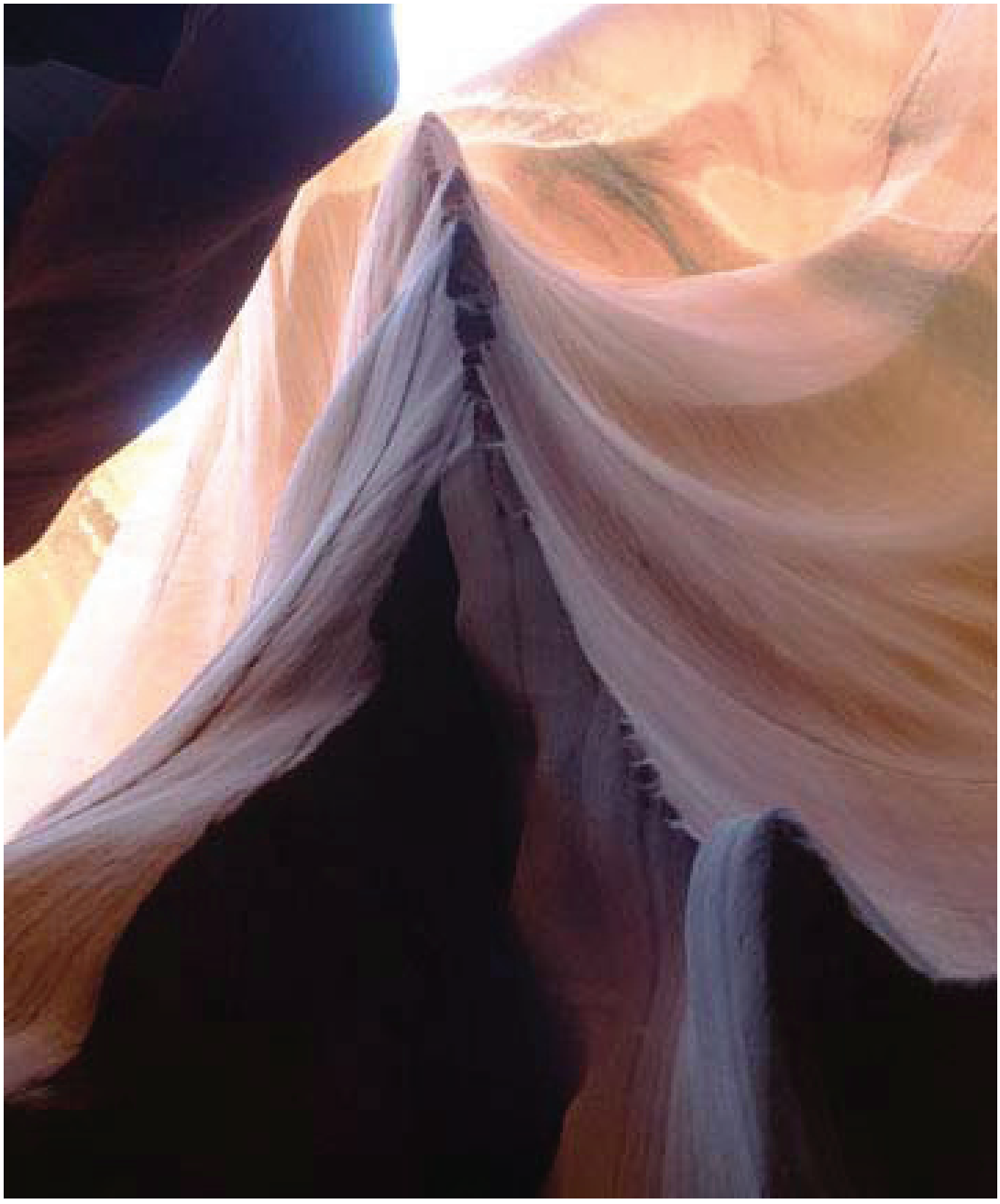

Image 8

A beautiful detail shot of a form that is a sculpture in itself. An example of the photographer high lighting a detail. NF

This powerful upward thrusting form contrasts nicely with the restfulness of image 9. RF

Image 9

Here is a quiet image with a delicate color. This is one of many inspirational images for a stone carver. NF

In this and many of these images, the camera sees more color than the naked eye. However, the experience of walking through these spaces is wonderful for the fact that one is surrounded by three-dimensional forms that are constantly changing. RF

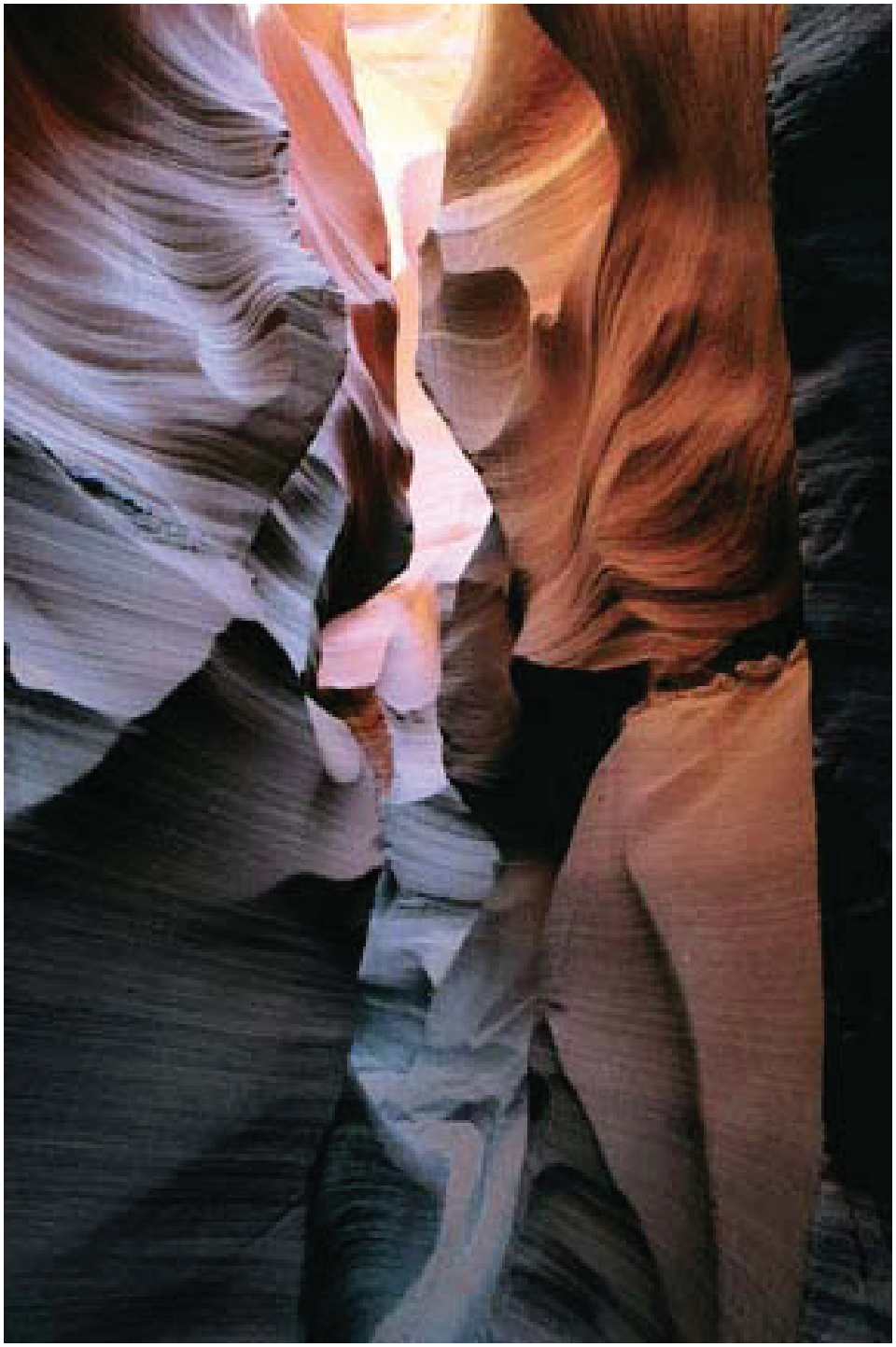

Image 10

A tall narrow space emphasizing the range of light and color. The narrow walking path is visible at the bottom. This is a classic slot canyon image. NF

Image 11

This horizontal image accentuates the feeling of wave forms in stone. A feature I hadn't thought of before. The camera angle changes the vertical wall to a more horizontal wave surface. NF
The amount of movement one feels looking at this image of static stone is remarkable. RF

Reference

[1] Robert Fathauer and Nat Friedman, Water Holes Canyon: Form, Space, Light, and Color, Hyperseeing, March/April 2008, www.isama.org/hyperseeing/